Design of Fixed-Order Feedback Controllers for Mechatronic Systems

Gijs HILHORST

Dissertation presented in partial
fulfillment of the requirements for the
degree of Doctor in Engineering

December 2015

Design of Fixed-Order Feedback Controllers for Mechatronic Systems

Gijs HILHORST

Dankwoord

De afgelopen vier jaren zijn omgevlogen. Het is met geen pen te beschrijven hoe leerzaam en verrijkend deze relatief korte periode voor mij is geweest, op zowel professioneel als persoonlijk vlak. Dit is voornamelijk te danken aan de uiteenlopende aard van alle opgedane ervaringen. Aan een deel van deze ervaringen denk ik nog dagelijks op een positieve manier terug, wat er soms toe leidt dat ik even heel gelukkig en soms wat emotioneel word. Vanzelfsprekend wil ik de mensen die de afgelopen vier jaren een positieve rol in mijn leven hebben gespeeld, onder andere door het bieden van mooie kansen of door me te steunen op moeilijke momenten, heel hartelijk bedanken. Bij deze zal ik uitgebreid van de gelegenheid gebruik maken.

Op de eerste plaats wil ik mijn promotoren Goele, Jan en Wim heel erg bedanken. Bedankt voor het vertrouwen dat jullie ruim vier jaar geleden lieten blijken door me te aanvaarden als doctoraatsstudent. Ik weet nog heel goed hoeveel ik toentertijd twijfelde of ik een doctoraat wel aan zou kunnen, maar niets is minder waar. Bedankt voor jullie steun, geduld en begrip, vooral in tijden dat ik het mentaal moeilijk had. Bedankt voor alle kansen en vrijheid die jullie me hebben gegeven om mezelf verder te ontwikkelen. Met name mijn bezoek aan Brazilië was een onvergetelijke ervaring. Ondanks mijn negatieve ervaringen in dit land, waardoor ik toch wel even diep in de put zat, zou ik deze reis zonder twijfel over doen. Bedankt prof. Karl Meerbergen, prof. Wim Desmet en Wim Symens voor het nalezen van mijn thesis. Onze interessante discussie heeft nieuwe inzichten opgeleverd en zodoende de kwaliteit van mijn werk verbeterd. Bedankt prof. Hugo Hens om de verdediging voor te zitten.

Pedro, quero agradecer-lhe por tudo! Muito obrigado pela sua ajuda na procura de habitação. Muito obrigado pelas noites agradáveis. É extremamente valioso ter um 'pai' se você estiver em um país estrangeiro longe de amigos e familiares.

Ricardo e Cristiano, muito obrigado pelas discussões científicas. Estes me ajudaram muito a progredir com minha pesquisa. Márcio grande e Márcio pequeno, obrigado pela Lacerdar. Isso resultou em muitos momentos hilariantes. Vocês ainda tem que me fazer café um dia.

Quero agradacer meu grande amigo Brasileiro David Ricardo (Johnson). Johnson, muito obrigado pelo cumprimento da tarefa de ser o meu professor de Português, por brincar com os cães, e especialmente por todos os risos. Obrigado por me mostrar as belas lados do Brasil! Jorge, Miguel e Alvaro, muito obrigado caras por serem grandes companhias no Brasil! Aydalith, nosso encontro foi muito especial. Obrigado por abrir meus olhos e ouvir a minha história.

Edson, also you deserve a big thank you wise man. Thank you for showing up in Campinas that morning, telling me about Brazil and taking me to beautiful places. Thank you for your Brazilian hospitality!

Johann, thank you for the enjoyable evenings, for all the interesting discussions and for looking at the people together while having a beer.

Nicholas, bedankt voor de gezelligheid die we de afgelopen jaren hebben beleefd. Een dikke merci ook om uw venster open te laten voor mijn kameraden.

Graag bedank ik ook mijn (ex-)collega's van PMA. Allen bedankt voor de goede sfeer op de afdeling en voor gezellige activiteiten zoals kleurenwiezen, happy hour en conferenties. Bedankt administratief en technisch personeel, voor het regelen van vervoer van en naar conferenties, het boeken van zalen en voorzien van koffie, het beantwoorden van financiële vragen, het lenen van apparatuur, etc.

Meindert, jouw naam hoort ook zeker in dit dankwoord thuis. Bedankt voor de gezelligheid de afgelopen 10 jaren, voor de vele fietstochten samen en voor je steun en begrip. Je bent de eerlijkste en meest betrouwbare kerel die ik ken.

Edwin, allereerst wil ik je bedanken voor je prachtige droge humor. Ik vind het fantastisch dat we, ondanks dat je al jaren aan de andere kant van de wereld woont, nog steeds meerdere malen per week contact hebben. Bedankt ook voor de mooie vakantie in West-Australië.

Uiteraard verdienen de Klein Verzet toppers Martijn, Erwin, Matthijs en Sander ook een bedankje. Bedankt voor jullie gezellige bezoeken aan Leuven, voor het lekkere eten en voor het afzien op de fiets.

Buis, Duijf en overige oud huisgenoten van de Calslaan 5-3 in Enschede met wie ik nog contact heb, bedankt voor jullie gezelligheid de afgelopen jaren. De vele verjaardagen, bezoeken aan Leuven, uitstapjes naar vakantieparken, etc.

hebben mij allen goed gedaan.

Kars, bedankt voor al je tijd en steun na mijn relatiebreuk. Dit is precies wat ik nodig had. Ik vind het geweldig hoe dit ertoe leidde dat onze vriendschap zich na een pauze weer voortzet.

Als laatste wil ik mijn ouders bedanken om er altijd voor me te zijn. Jullie onvoorwaardelijke liefde is niet iets vanzelfsprekend, dat realiseer ik me inmiddels maar al te goed. Hoewel we hier nooit zoveel woorden aan vuil maken, verdient dit om gezegd te worden. Bedankt om mij altijd weer aan de positieve dingen in het leven te herinneren. Bedankt om mij te motiveren om niet op te geven en kansen aan te grijpen. Bedankt om als raadgevers op te treden en me tegelijkertijd vrij te laten in al mijn beslissingen. Bedankt voor alle gezelligheid samen, jullie behoren tot mijn beste vrienden.

Similarities between a PhD, a jigsaw puzzle and a life

- They are most interesting when they get difficult, and boring when they get easy.

- They should be approached step by step, piece by piece, never as a whole.

- They might get more and more complete, more and more structured, while an unexpected blowing wind might destroy part of the structure, requiring a step back and a new start.

- They take time and patience to create and understand.

- They might not make sense in the beginning, but there will be a time they do.

- They cannot be completed without love, passion and mistakes.

- They require hard work, but also allow time for enjoyment.

- They are incredibly interesting.

Abstract

The continuously increasing demands from industry drive research communities to push the limits in the design of accurate and high performance controllers for dynamical systems, such as autonomous vehicles, production machines, etc. Therefore, enhanced controller design procedures are indispensable in this evolution. Typically, first a mathematical model describing the behavior of a dynamical system is derived. Then, a controller using real-time measurements is designed for this model according to the desired performance specifications. For instance, a fast response should be guaranteed while limiting energy consumption. In a last step, the controller is validated in closed loop with the dynamical system.

The complexity of a controller design problem depends on several factors, such as the dynamics of the system to be controlled, the desired controller structure, and the number/type of performance specifications. For linear time-invariant (LTI) dynamics, a wide range of successful controller design approaches have emerged over the last decades. However, several important control problems, such as the design of optimal fixed-order controllers (i.e., controllers with an a priori fixed structure), or optimal controllers satisfying multiple conflicting design objectives, remain unsolved. At the same time, many applications feature dynamics which are dominantly linear, but are affected by time-varying and/or uncertain parameters. In these applications, LTI controllers do not provide the desired accuracy and performance. Therefore, linear parameter-varying (LPV) dynamics have been widely considered as a useful extension, characterized by a linear input-output relation depending on real-time measurable parameters. Accounting for real-time parameter measurements in a controller design, higher closed-loop performance can be achieved compared to an LTI controller. Although modern LPV controller design techniques are very attractive when the system dynamics are affected by real-time measurable parameters, more involved approaches are required to cope with uncertain parameters.

To meet the tightening performance and accuracy demands from industry, this

thesis presents a versatile approach to design high performance fixed-order multi-objective controllers for the general class of linear parameter-dependent (LPD) systems, encompassing LTI, LPV and uncertain linear dynamics. For each of these subclasses, the effectiveness and practical viability of our approach is demonstrated by theoretical proofs of stability and performance, numerical comparisons with existing approaches, and experimental validations. In addition, a novel model order reduction technique is combined with our approach to design fixed-order controllers for continuous-time linear time-delay systems. Finally, a parametric programming approach is presented to design high performance feedback controllers for LTI systems, while simultaneously optimizing structural parameters affecting the system dynamics.

Beknopte samenvatting

De constant groeiende vraag vanuit de industrie naar het verhogen van de efficiëntie van dynamische systemen geeft aanleiding tot het verrichten van grensverleggend onderzoek op het gebied van regelaarontwerp. Denk bijvoorbeeld aan het ontwikkelen van alsmaar betere besturingen voor autonome voertuigen, of het vervaardigen van telkens kleinere computerchips. Daarom zijn geavanceerde regelaarontwerpmethodes van essentieel belang in deze evolutie. Typisch wordt eerst een wiskundig model bepaald welke het dynamisch gedrag van het systeem beschrijft. Vervolgens wordt een regelaar ontworpen welke gebruik maakt van actuele metingen om het systeem aan te sturen en hierbij efficiëntie van het gesloten lus model te garanderen. Denk bijvoorbeeld aan het optimaliseren van de responstijd voor een gegeven beperking op energieverbruik. In een laatste stap wordt de efficiëntie van de regelaar gevalideerd door deze te koppelen aan het dynamische systeem.

De complexiteit van een regelaarontwerp hangt af van verschillende factoren, zoals het dynamisch gedrag van het systeem, de gewenste structuur van de regelaar en het aantal/type specificaties waar het gesloten lus systeem aan moet voldoen. Voor lineaire tijdsinvariante (LTI) dynamica is in de afgelopen decennia een waaier aan regelaarontwerpmethodes ontwikkeld. Verscheidene belangrijke controleproblemen, zoals het ontwerp van optimale regelaars met een van tevoren vastgelegde structuur, of optimale regelaars welke aan meerdere conflicterende specificaties moeten voldoen, blijven echter onopgelost. Tegelijkertijd zijn er veel toepassingen wiens dynamisch gedrag wordt beïnvloed door tijdsvariërende en/of onzekere parameters. Bijgevolg verschaffen LTI regelaars niet de gewenste nauwkeurigheid en efficiëntie. Daarom worden lineaire parameter variërende (LPV) dynamica veelal beschouwd als aantrekkelijke uitbreiding op het LTI raamwerk. Een LPV systeem wordt gekenmerkt door lineaire dynamica welke afhangt van de huidige waarde van tijdsvariërende parameters. Door in een regelaarontwerp rekening te houden met huidige parameterwaarden kan hogere efficiëntie behaald worden vergeleken met een LTI regelaar. Terwijl moderne LPV regelaarontwerpmethodes erg aantrekkelijk zijn

als huidige parameterwaarden beschikbaar zijn, vereisen onzekere parameters ingewikkeldere ontwerpprocedures.

Om aan de steeds strengere industriële eisen te voldoen, presenteert deze thesis een veelzijdige methode om efficiënte regelaars met een vaste structuur te ontwerpen voor de algemene klasse van lineaire parameter-afhankelijke (LPD) systemen. Deze klasse omvat zowel LTI, LPV als onzekere lineaire dynamica. Voor ieder van deze subklasses wordt de doeltreffendheid en praktische uitvoerbaarheid van onze aanpak aangetoond door middel van theoretische bewijzen van stabiliteit en efficiëntie, numerieke vergelijkingen met bestaande aanpakken, en experimentele validaties. Als aanvulling combineren we een nieuwe model orde reductie techniek met onze methode om regelaars te ontwerpen voor continue-tijd lineaire tijdvertraagde systemen. Tenslotte wordt een op parametrisch programmeren gebaseerde aanpak gepresenteerd om efficiënte regelaars te ontwerpen voor LTI systemen, terwijl tegelijkertijd structurele parameters worden geoptimaliseerd welke de systeemdynamica beïnvloeden.

List of abbreviations

BMI	bilinear matrix inequality
FRF	frequency response function
LMI	linear matrix inequality
LPD	linear parameter-dependent
LPV	linear parameter-varying
LTI	linear time-invariant
LTD	linear time-delay
LTV	linear time-varying
MIMO	multiple-input multiple-output
RMS	root mean square

List of symbols

Sets

$\mathbb{R}$	set of real numbers
$\mathbb{R}_+$	set of nonnegative real numbers
$\mathbb{R}^n$	set of real n-dimensional vectors
$\mathbb{N}$	set of natural numbers (including 0)
$\mathbb{N}_+$	set of strictly positive natural numbers
$\mathbb{T}$	generalized time axis: $\mathbb{T} = \mathbb{N}$ in discrete time and $\mathbb{T} = \mathbb{R}_+$ in continuous time
$\mathbb{S}^n$	set of $n \times n$ symmetric matrices
$\mathbb{S}^n_+$	set of $n \times n$ (strictly) positive definite matrices
$\mathcal{C}^1(X, Y)$	space of continuously differentiable functions $f : X \to Y$, where X is (an interval on) the real axis and $Y \subseteq \mathbb{R}^n$
$\mathcal{L}_2(\mathbb{T}, \mathbb{R}^n)$	continuous time: space of square integrable functions

$$\mathcal{L}^2_n(\mathbb{R}_+, \mathbb{R}^n) := \left\{ f : \mathbb{R}_+ \to \mathbb{R}^n \,\bigg|\, \int_0^\infty f(t)' f(t) dt < \infty \right\}$$

discrete time: space of square summable sequences

$$\mathcal{L}^2_n(\mathbb{N}, \mathbb{R}^n) := \left\{ f : \mathbb{N} \to \mathbb{R}^n \,\bigg|\, \sum_{t=0}^\infty f(t)' f(t) < \infty \right\}$$

$\mathcal{S}$	set of performance indices
$\mathcal{S}_{\mathcal{H}_\infty}$	set of $\mathcal{H}_\infty$ performance indices
$\mathcal{S}_{\mathcal{H}_2}$	set of $\mathcal{H}_2$ performance indices
$\mathcal{T}$	set of possible parameter trajectories

Norms

$\| \cdot \|$ vector norm

$\| \cdot \|_2$ in case of a vector $x \in \mathbb{R}^n$:

$$\|x\|_2 = \left(\sum_{k=0}^{n} x_k^2 \right)^{1/2}$$

in case of a continuous-time function $x : \mathbb{R}_+ \to \mathbb{R}^n$:

$$\|x(t)\|_2 = \left(\int_0^\infty x(t)'x(t)dt \right)^{1/2}$$

in case of a discrete-time function $x : \mathbb{N} \to \mathbb{R}^n$:

$$\|x(t)\|_2 = \left(\sum_{t=0}^{\infty} x(t)'x(t) \right)^{1/2}$$

in case of a system: $\mathcal{H}_2$ performance

$\| \cdot \|_{2,[0,T]}$ $\mathcal{L}_2$ norm defined on the finite interval $[0,T]$
in case of a continuous-time function $x : [0,T] \to \mathbb{R}^n$:

$$\|x(t)\|_{2,[0,T]} = \left(\int_0^T x(t)'x(t)dt \right)^{1/2}$$

in case of a discrete-time function $x : \{0, \ldots, T\} \to \mathbb{R}^n$:

$$\|x(t)\|_{2,[0,T]} = \left(\sum_{t=0}^{T} x(t)'x(t) \right)^{1/2}$$

in case of a system: finite horizon $\mathcal{H}_2$ performance

$\| \cdot \|_\infty$ in case of a system: $\mathcal{H}_\infty$ performance

$\| \cdot \|_{X,[0,T]}$ weighted signal norm involving the trace, defined on the finite interval $[0,T]$, defined in continuous time as

$$\|S\|_{X,[0,T]} = \left(\int_0^T \text{Tr}\{S(t)X(t)S(t)'\}dt \right)^{1/2},$$

and in discrete time as

$$\|S\|_{X,[0,T]} = \left(\sum_{t=0}^{T} \text{Tr}\{S(t)X(t)S(t)'\} \right)^{1/2},$$

where $S : \mathbb{T} \to \mathbb{R}^{n \times m}$ and $X : \mathbb{T} \to \mathbb{S}_+^n$.

Operators

sup	supremum: least upper bound
lim sup	limit superior
δ	continuous time: time derivative operator discrete time: forward time shift operator
δ_{ts}	continuous time: Dirac delta

$$\delta_{ts} = \left\{ \begin{array}{ll} 0 & \text{if } t \neq s \\ \infty & \text{if } t = s \end{array} \right.$$

discrete time: Kronecker delta

$$\delta_{ts} = \left\{ \begin{array}{ll} 0 & \text{if } t \neq s \\ 1 & \text{if } t = s \end{array} \right.$$

$\mathbb{E}$	expected value
Tr	trace operator
X'	transpose of a matrix X
X^{-1}	inverse of a matrix X
$X_\perp$	an arbitrary matrix whose columns form a basis for the null space of a matrix X
$\text{He}\{X\}$	shorthand for $X + X'$
$\text{diag}\{X_1, \ldots, X_n\}$	block diagonal matrix with matrices $X_1, \ldots, X_n$ as main diagonal blocks
$\lceil \cdot \rceil$	ceil operator

Miscellaneous

I_n	identity matrix of dimension $n \times n$. The subscript is omitted when the dimension can be inferred from the context.
$0_{m \times n}$	zero matrix of dimension $m \times n$. The subscript is omitted when the dimensions can be inferred from the context.
$\star$	symmetric block in a matrix inequality

Contents

Chapter 1

Introduction

This first chapter introduces and motivates the research subject considered in this thesis, by reviewing the current state of the art and identifying shortcomings and challenges. An overview of the main part of the thesis, describing its specific contributions, is also provided.

1.1 Motivation

The continuously increasing demands from industry drive research communities to keep pushing the limits in the design of accurate and high performance control systems. Typically, first a mathematical model P describing the behavior of a dynamical system is derived. Subsequently, a controller K is designed for this model according to some desired performance specifications, as schematically depicted in Figure 1.1. Based on real-time measurements y from the dynamical system, the controller K generates a control signal u which is in turn applied to the dynamical system, such that the influence of the exogenous (e.g., reference/disturbance) input w on the regulated output z meets the performance requirements.

Obviously, the complexity of a controller design depends on the nature of the dynamical system to be controlled. Under the assumption that the dynamics are linear and time-invariant (LTI), a wide range of successful controller design approaches have emerged over the last decades. Although control design for this restricted class of systems constitutes a mature research field, several important control problems, such as the design of optimal controllers with an a priori fixed
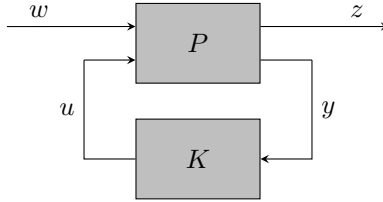
Figure 1.1: General control configuration.

structure, or optimal controllers satisfying multiple conflicting design objectives, remain unsolved [16, 54, 103, 114].

At the same time, many applications feature dynamics which are dominantly linear, but affected by time-varying and/or uncertain parameters. Consequently, LTI techniques are unsatisfactory for providing the desired accuracy and performance, hence more advanced controller design techniques are required. To this end, various extensions of the LTI framework to cope with time-varying and/or uncertain parameters have been developed and applied.

In this context, the framework of linear parameter-varying (LPV) systems has been widely considered as a fruitful extension of LTI dynamics, as discussed in the interesting survey papers [55, 71, 95]. LPV systems are characterized by a linear input-output relation, which is assumed to depend on real-time measurable parameters. Accounting for real-time parameter values in a controller design, higher closed-loop performance can be achieved compared to an LTI controller. The latter is demonstrated in various practical applications, including CD players [33], wafer stages [121], servo systems [122], active noise and vibration control [13], active suspension systems [34], vibroacoustic applications [27], and overhead cranes [52, 127]. In fact, the available LPV controller design approaches are featured by a clear distinction between so-called classical and modern techniques.

The classical approaches, see for instance [85, 90, 127], consist of the following steps. First, the LPV model is evaluated for different fixed parameter values, resulting in so-called local LTI models. Subsequently, using an available LTI technique, an LTI controller is designed for each local model. Finally, the local LTI controllers are interpolated by assuming a specific parameterization (e.g., see [29]), such that an LPV controller is obtained. Although application of these approaches is relatively straightforward, they might be unreliable, since extensive numerical simulations are required to assess stability and performance for time-varying parameters.

In the more elaborate modern LPV synthesis approaches, on the other hand,

an LPV controller is directly designed by solving a sophisticated parameter-dependent optimization problem, see, amongst others, [28, 52, 99, 100]. The main benefit of these approaches is that, in contrast to the classical approaches, they provide a certificate of stability and performance, since they rely on Lyapunov stability theory [74].

Although modern LPV controller design techniques are very attractive when the system dynamics are affected by real-time measurable parameters, more involved approaches are required to cope with uncertain parameters. Fortunately, Lyapunov based conditions are very appealing for the design of robust controllers (i.e., controllers guaranteeing stability and performance despite parametric uncertainty). Specifically for linear systems with parametric (time-varying) uncertainty, various approaches have been presented [3, 5, 31, 53, 88, 102, 105].

Despite the fact that many interesting controller design approaches have been presented for linear parameter-dependent (LPD) systems, improved approaches are indispensable to meet the increasing performance and accuracy demands from the manufacturing industry. Therefore, a general overview addressing the main issues in controller design for LPD systems is provided now.

Generally speaking, the complexity of a controller design for an LPD system depends on several factors, such as the desired controller structure, the presence (and number of) time-varying/uncertain parameters affecting the system dynamics, and the number of performance specifications. The notion of convexity (see, e.g., [19]) plays a crucial role in defining this complexity. Namely, whenever an optimization problem is convex, it has the attractive property that every local optimum is a global optimal solution [18, 19, 105]. Moreover, efficient algorithms have been developed to solve convex optimization problems, such that an optimal controller is readily computed. Although a few important control problems are convex, the industrially most relevant cases are intrinsically nonconvex. The fact that nonconvex problems remain hard to solve motivates the investigation of improvements on available techniques for solving these complex control problems. In addition, even convex optimization problems might be challenging depending on the problem size, which is affected by, amongst others, the number of equations and parameters describing the dynamical system to be controlled. Figure 1.2 characterizes the complexity of a controller design problem in terms of convexity/nonconvexity and problem size. The problem complexity ranges from the design of unstructured controllers for LTI systems satisfying a single performance objective, to the design of structured robust controllers for uncertain linear systems satisfying multiple performance specifications.

convex   large optimization problem

no prefixed controller structure   parameter-dependent
no robustness   systems

                                        multiple (conflicting)
                                        performance objectives

LTI systems   prefixed controller structure
single performance objective   robustness

small optimization problem   nonconvex
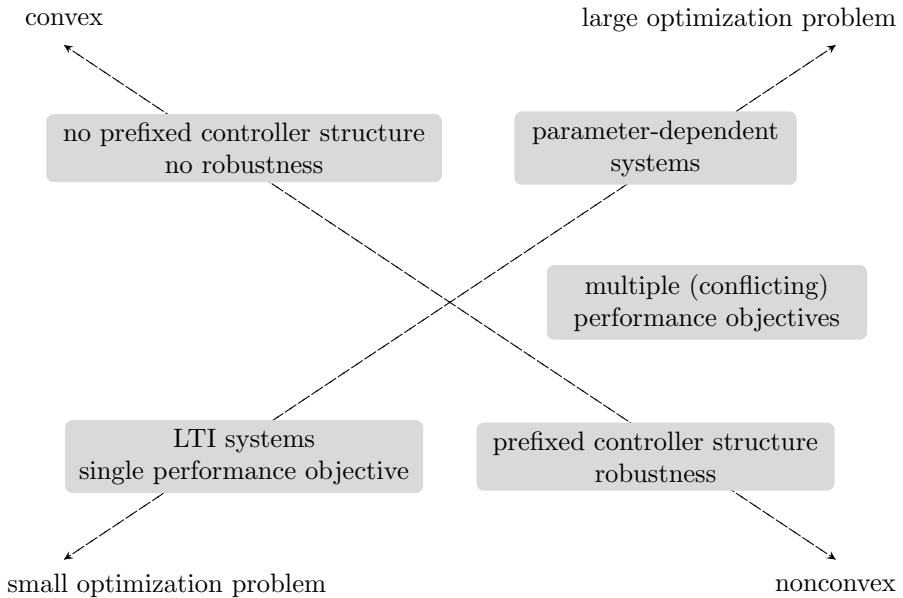
Figure 1.2: General overview characterizing the complexity of various relevant control problems.

1.2 Challenges

Based on the above motivation, the following challenges can be recognized:

Provide improved procedures for the design of high performance controllers

- which are structurally simple, allowing the design of intuitive, reliable and affordable control systems for highly complex industrial applications.

- satisfying multiple (conflicting) design specifications, since it is often complicated to capture all design specifications in a single objective.

- which are robust against (time-varying) model uncertainties, resulting in highly reliable controllers.

- for multiple-input multiple-output (MIMO) systems, since many realistic applications feature multiple inputs and/or multiple outputs.

- for both continuous-time and discrete-time systems. While most applications feature continuous-time dynamics, controllers are nowadays

almost always implemented in a digital environment. Depending on the application, discretization of either the system or the controller might be preferred.

- in a numerically efficient way. Since reductions of conservatism come at the expense of an increase of the numerical burden, clever optimization procedures are indispensable.

- featuring limited conservatism. This is necessary to meet the tightening performance and accuracy demands from the manufacturing industry.

- whose performance is validated experimentally, to demonstrate practical viability.

- requiring limited manual intervention from experts. In other words, the gap between the tuning of simple and highly suboptimal controllers in industry, and the complex design of high performance controllers in academia, should be reduced.

1.3   Overview and contributions

This thesis presents a versatile approach to design high performance controllers for the general class of LPD systems, addressing the challenges listed in Section 1.2.

First, the class of LPD systems is introduced in Chapter 2, together with the notions of stability and two widely used performance measures. Furthermore, mathematical tools from convex optimization are exploited to determine stability and performance of a given LPD system.

The main theoretical contribution of this thesis is presented in Chapter 3, providing a novel framework of convex sufficient conditions to design so-called fixed-order controllers (i.e., controllers described by a fixed number of equations) for LPD systems. Although the proposed framework is subject to conservatism, it applies to MIMO systems, unifies continuous-time and discrete-time, allows multiple performance specifications, and is numerically attractive.

Numerical and experimental validations for several subclasses of LPD systems confirm the potential of the convex framework presented in Chapter 3. Its merits for LTI dynamics are demonstrated in Chapter 4, presenting various numerical comparisons with existing approaches and experimental validations of multi-objective controllers for a lab-scale overhead crane with fixed cable length. Allowing a cable with *varying* length, and considering the cable length

as measurable parameter, results in an LPV system. For the latter system, experimental validations of fixed-order multi-objective controllers are provided in Chapter 5, assessing the practical viability of our controller design approach for LPV systems. In Chapter 6, the controller design framework presented in Chapter 3 is extended with an iterative convex procedure, to design high performance fixed-order robust controllers for LTI systems with parametric uncertainty.

Chapter 7 presents a combined approach to design fixed-order controllers for continuous-time linear time-delay (LTD) systems. This approach relies on the following steps. First, a novel model order reduction technique is exploited to determine a finite-dimensional LTI approximation of the LTD system. Subsequently, the framework of Chapter 3 is applied to design fixed-order controllers for the approximating model. Finally, the controllers are validated on the original LTD system.

Chapter 8 presents a parametric programming approach to design high performance feedback controllers for LTI systems, while simultaneously optimizing structural parameters affecting the system dynamics. The effectiveness of the approach is validated by simultaneously designing a state feedback controller and optimizing structural parameters for earthquake isolation of a civil engineering structure.

Finally, concluding remarks and suggestions for future research are given in Chapter 9.

Chapter 2

Preliminaries

In this first technical chapter, we define the general class of LPD systems in state-space form. This class encompasses a broad range of linear systems, including LPV and uncertain LTI systems. The state-space form is very useful for analysis and controller design purposes, since it allows us to directly derive convex conditions for stability and performance based on Lyapunov's direct method. We define the concept of exponential stability, and derive parameter-dependent LMIs that guarantee exponential stability of an LPD system based on this definition. Subsequently, these parameter-dependent LMIs are extended to incorporate $\mathcal{H}_\infty$ and $\mathcal{H}_2$ performance specifications. We briefly discuss some well-known approaches that, starting from the parameter-dependent LMI conditions for stability and $\mathcal{H}_\infty / \mathcal{H}_2$ analysis, allow the derivation of convex synthesis conditions for full-order LPD controller design. Due to the fact that the LMI constraints should generally hold for an infinite number of parameter values, and since the optimization variables are functions, numerically intractable feasibility or optimization problems result. The latter issue is relieved by imposing a specific parameterization on the optimization variables, allowing the application of relaxations to arrive at a tractable set of sufficient LMIs.

2.1 Linear parameter-dependent systems

The class of LPD systems is defined in this section. Defining a generalized time axis $\mathbb{T}$, which equals $\mathbb{R}_+$ in continuous time and $\mathbb{N}$ in discrete time, we consider the class of finite-dimensional MIMO LPD systems in state-space form

$$H : \begin{cases} \delta x & = & A(\alpha)x & + & B(\alpha)w\,, & x(0) = 0, \\ z & = & C(\alpha)x & + & D(\alpha)w\,, \end{cases} \quad (2.1)$$

with state $x : \mathbb{T} \to \mathbb{R}^{n_x}$, exogenous input $w : \mathbb{T} \to \mathbb{R}^{n_w}$, performance output $z : \mathbb{T} \to \mathbb{R}^{n_z}$ and exogenous parameter $\alpha : \mathbb{T} \to \mathbb{R}^N$. All system matrices are real continuous functions of α, bounded for all $t \in \mathbb{T}$ and have appropriate dimensions. The operator δ denotes the time derivative $\delta x = dx/dt$ in continuous time, and the forward shift operator $\delta x(t) = x(t+1)$ in discrete time. The parameter α takes values in a compact convex polytope $\Lambda \subset \mathbb{R}^N$. That is, Λ is the convex hull of a finite set of points $v_i \in \mathbb{R}^N$, $i = 1, \ldots, M$:

$$\Lambda = \left\{ \sum_{i=1}^{M} \xi_i v_i \ \middle|\ \sum_{i=1}^{M} \xi_i = 1, \ \xi_i \geq 0, \ i = 1, \ldots, M \right\}. \tag{2.2}$$

Moreover, α is assumed to be continuously differentiable in the continuous-time case (i.e., $\alpha \in \mathcal{C}^1(\mathbb{R}_+, \mathbb{R}^N)$). Accordingly, the set of possible parameter trajectories is given by

$$\left\{ \alpha : \mathbb{T} \to \mathbb{R}^N \mid \alpha(t) \in \Lambda, \ \forall t \in \mathbb{T}, \text{ and } \alpha \in \mathcal{C}^1(\mathbb{T}, \mathbb{R}^N) \text{ if } \mathbb{T} = \mathbb{R}_+ \right\}. \tag{2.3}$$

Whenever bounds on the rate of parameter variation are a priori known, they are taken into account by restricting the set (2.3) to

$$\mathcal{T} := \left\{ \alpha : \mathbb{T} \to \mathbb{R}^N \ \middle|\ \begin{bmatrix} \alpha(t) \\ \Delta\alpha(t) \end{bmatrix} \in \Omega, \ \forall t \in \mathbb{T}, \text{ and } \alpha \in \mathcal{C}^1(\mathbb{T}, \mathbb{R}^N) \text{ if } \mathbb{T} = \mathbb{R}_+ \right\}, \tag{2.4}$$

where $\Delta\alpha = \delta\alpha$ in continuous time and $\Delta\alpha = \delta\alpha - \alpha$ in discrete time. The structure of Λ implies that $\Omega \subset \mathbb{R}^{2N}$ is a compact convex polytope whenever the rate of parameter variation is bounded, and equals $\Lambda \times \mathbb{R}^N$ in the unrestricted case. As a result, taking into account known bounds on the rate of parameter variation provides less conservative analysis and synthesis conditions. However, this comes at the expense of an increased number of vertices of the parameter domain, resulting in a higher numerical burden.

Throughout this work, it is assumed that the parameter α is an *exogenous* signal, hence α is independent of the state, input and output of the LPD system (2.1). Under this assumption, subclasses of LPD systems can be identified based on properties of α. Making a distinction between constant and time-varying parameters on the one hand, and a priori known, real-time measurable and uncertain parameters on the other hand, Table 2.1 shows the types of linear systems encompassed by the general framework of LPD systems (2.1). See, for instance, [108] for an interesting comparison of these different types of linear models. The intention is to cover all linear systems summarized in Table 2.1 in a general fashion.

When α is allowed to depend on the state, input or output, system (2.1) attains a so-called quasi-LPV form [55, 70, 71], covering general nonlinear time-varying systems of the form $\delta x = f(t, x, w)$, $z = g(t, x, w)$. However, nonlinear systems are beyond the scope of this thesis.

Table 2.1: The class of LPD systems encompasses a broad range of linear systems, subdivided according to properties of the parameter α.

α	a priori known	real-time measurable	uncertain
constant	LTI	n.a.	uncertain LTI
time-varying	LTV	LPV	uncertain LPV

2.2 Stability and performance of LPD systems

Stability of dynamical systems is the most fundamental and probably the most actively studied concept within systems and control theory. Stability is characterized by the equilibrium points of a dynamical system, which are the points in the state space where the system is at rest. As conceptually stated in [48] (page 135): *"An equilibrium point of a dynamical system is said to be stable if, for sufficiently small values of initial disturbances, the perturbed motion remains in an arbitrarily prescribed small region of the state space."* Without doubt, the most important contributions to stability of dynamical systems are due to the Russian mathematician A. M. Lyapunov, who characterized stability and proposed a powerful mathematical framework to analyze stability of (non)linear dynamical systems in his famous publication [74] (see [75] for the English translation). All the analysis and synthesis conditions that are presented in this thesis are based on Lyapunov's so-called direct method.

The notion of dissipativity is closely related to stability, and is the starting point for characterizing system performance. A classical definition of a dissipative system is provided in [123]: *"A system is dissipative if the increase in storage over a time interval cannot exceed the supply delivered to the system during this time interval."* As discussed in, for example, [105, 123], Lyapunov theory provides a framework to guarantee stability of *closed* systems (i.e. systems isolated from their environment), while dissipativity theory is a natural generalization that allows to study stability and dissipativity of *open* systems (i.e. systems interacting with their environment). The amount of stored energy in an open system is modeled by a so-called *storage function*, which becomes a Lyapunov function when the interaction of the system with its environment is neglected. The interaction of a system with its environment is modeled through inputs and outputs, and the effect of the inputs on the outputs characterizes system performance. While system performance can be quantified in several ways, $\mathcal{H}_\infty$ and $\mathcal{H}_2$ performance are amongst the most widely used types of performance characterizations (see, for instance, [17, 18, 65, 111] and references therein). The $\mathcal{H}_\infty$ performance of a system is defined as the worst-case ratio of the RMS value of the output to the RMS value of the input, where the input signal is

nonzero and has bounded $\mathcal{L}_2$ norm. The $\mathcal{H}_2$ norm may be interpreted as the expected RMS value of the output when the input is a white Gaussian noise process with zero mean and identity covariance matrix.

As will be demonstrated in the following sections, LMIs arise naturally when studying stability and performance of LPD systems.

2.2.1 Stability

Consider the LPD system

$$\delta x = A(\alpha)x\,, \quad x(0) = x_0\,, \tag{2.5}$$

with state $x : \mathbb{T} \to \mathbb{R}^{n_x}$ and parameter $\alpha : \mathbb{T} \to \Lambda$. Note that $x^* = 0$ is an equilibrium point of the LPD system (2.5), since $x = 0$ implies $\delta x = 0$. The equilibrium point $x^* = 0$ is said to be locally exponentially stable if, for any initial condition x_0 close enough to the origin and for all $\alpha \in \mathcal{T}$, the state of (2.5) converges to zero at an exponential rate. $x^* = 0$ is globally exponentially stable if it is locally exponentially stable for all initial conditions $x_0 \in \mathbb{R}^{n_x}$. Since, for linear systems, local and global exponential stability coincide [98], they are simply referred to as exponential stability. Exponential stability of $x^* = 0$ implies that the origin is the only equilibrium point, therefore we say that the LPD system (2.5) is exponentially stable whenever the origin is an exponentially stable equilibrium point. The concept of exponential stability is formalized in a definition (see, for instance, [48, 61, 98]).

Definition 1 (Exponential stability)**.** *The LPD system* (2.5) *is exponentially stable if there exist scalars $a, b > 0$ such that*

$$\|x(t)\| \leq a\|x_0\|f(t)$$

where $f(t) = e^{-bt}$ in continuous time, and $f(t) = (b+1)^{-t}$ in discrete time, for all $x_0 \in \mathbb{R}^{n_x}$ and for all parameter trajectories $\alpha \in \mathcal{T}$, $t \in \mathbb{T}$.

Using Lyapunov's direct method, exponential stability of the LPD system (2.5) can be analyzed. Namely, whenever a positive definite scalar function depending on the system state (with a unique minimum in the origin) can be found, which strictly decreases along trajectories of the state at an exponential rate, then the LPD system (2.5) is exponentially stable. Such a positive definite scalar function is a so-called Lyapunov function for the LPD system (2.5) whenever it proves stability. This idea is illustrated in Figure 2.1, showing a typical Lyapunov function. Sufficient conditions for exponential stability of the LPD system (2.5), based on Lyapunov's direct method, are presented in the following theorem.
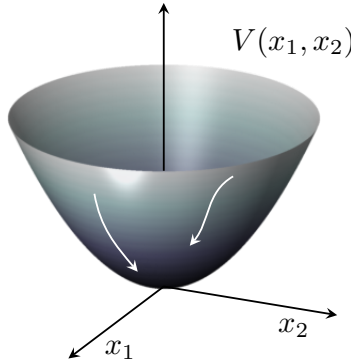
Figure 2.1: A typical quadratic Lyapunov function. If V strictly decreases along trajectories of the state $x = [\, x_1 \quad x_2 \,]'$, then the state converges to zero.

Theorem 1 (Exponential stability, Lyapunov). *If there exists a continuously differentiable/continuous (continuous time/discrete time) function $V : \mathbb{R}^N \times \mathbb{R}^{n_x} \to \mathbb{R}$ and scalars $a, b, c > 0$ and $d \geq 1$, such that*

$$a\|x\|^d \leq V(\alpha, x) \leq b\|x\|^d \,, \tag{2.6a}$$

$$\Delta V(\alpha, x) \leq -c\|x\|^d \,, \tag{2.6b}$$

for all $\alpha \in \mathcal{T}$ and all possible trajectories $x : \mathbb{T} \to \mathbb{R}^{n_x}$ of (2.5), then the LPD system (2.5) is exponentially stable. The operator Δ is defined as $\Delta V(\alpha, x) := \delta V(\alpha, x)$ in continuous time and $\Delta V(\alpha, x) := V(\delta\alpha, \delta x) - V(\alpha, x)$ in discrete time.

Proof. See Appendix A.1. □

By explicitly incorporating the (time-varying) parameter α, Theorem 1 is a straightforward extension of the theorems presented in [48] for nonlinear time-varying systems (see page 229 and page 785 for the continuous-time, respectively, discrete-time case). Theorem 1 is very powerful, since conclusions about exponential stability of the LPD system (2.5) can be drawn without explicit computation of state trajectories. Obviously, the main difficulty is to find a Lyapunov function, and unfortunately no general technique exists to construct one. However, for LPD systems, a very common approach is to search for a parameter-dependent Lyapunov function that is quadratic in the state:

$$V(\alpha, x) = x' P(\alpha) x \,, \tag{2.7}$$

where $P(\alpha)$ is a bounded positive definite matrix for all $\alpha \in \mathcal{T}$. Using the quadratic form (2.7), the conditions of Theorem 1 reduce to a set of parameter-dependent sufficient LMIs. This is the context of the following theorem, whose presentation is facilitated by defining the parameter-dependent matrices

$$\Phi_c(\alpha) := \begin{bmatrix} \delta P(\alpha) & P(\alpha) \\ P(\alpha) & 0 \end{bmatrix}, \quad \Phi_d(\alpha) := \begin{bmatrix} -P(\alpha) & 0 \\ 0 & P(\delta\alpha) \end{bmatrix}.$$

Theorem 2 (Exponential stability, Lyapunov)**.** *If there exists a bounded matrix* $P(\alpha(t)) \in \mathbb{S}_+^{n_x}$, *for all* $\alpha \in \mathcal{T}$, $t \in \mathbb{T}$, *such that*

$$\begin{bmatrix} I \\ A(\alpha(t)) \end{bmatrix}' \Phi(\alpha(t)) \begin{bmatrix} I \\ A(\alpha(t)) \end{bmatrix} \prec 0 \tag{2.8}$$

for all $\alpha \in \mathcal{T}$, $t \in \mathbb{T}$, *where* $\Phi = \Phi_c$ *in continuous time and* $\Phi = \Phi_d$ *in discrete time, then the LPD system* (2.5) *is exponentially stable.*

Proof. See Appendix A.2. $\qquad\qquad\qquad\qquad\qquad\qquad\qquad\qquad\qquad$ $\square$

While the parameter-dependent LMI (2.8) is only a sufficient condition in general, it is necessary and sufficient when considering time-invariant parameters. Specifically, a necessary and sufficient condition for exponential stability of LTI systems results when the parameter-dependency in (2.8) is dropped. Moreover, the existence of a Lyapunov function (2.7) (without imposing any structure on $P(\alpha)$) is necessary and sufficient for stability of an uncertain LTI system [87].

2.2.2 $\mathcal{H}_\infty$ performance

The $\mathcal{H}_\infty$ performance is defined similar as in [15] (see also [28]).

Definition 2 ($\mathcal{H}_\infty$ performance)**.** *Let the LPD system* (2.1) *be exponentially stable, and assume that* $w(t) \in \mathcal{L}_2(\mathbb{T}, \mathbb{R}^{n_w})$. *Then, the* $\mathcal{H}_\infty$ *performance of* (2.1) *is defined as*

$$\|H\|_\infty := \sup_{\alpha \in \mathcal{T}} \sup_{w(t) \neq 0} \frac{\|z(t)\|_2}{\|w(t)\|_2}.$$

The following theorem provides an LMI characterization for an upper bound on the $\mathcal{H}_\infty$ performance of the LPD system (2.1), which is based on the bounded real lemma (see, for example, [18, 105]).

Theorem 3 ($\mathcal{H}_\infty$ performance). *If there exists a bounded matrix $P(\alpha(t)) \in \mathbb{S}_+^{n_x}$, for $\alpha \in \mathcal{T}$, $t \in \mathbb{T}$, and a bounded scalar $\gamma > 0$, such that the LMI*

$$\begin{bmatrix} I & 0 \\ A(\alpha(t)) & B(\alpha(t)) \\ 0 & I \\ C(\alpha(t)) & D(\alpha(t)) \end{bmatrix}' \begin{bmatrix} \Phi(\alpha(t)) & 0 & 0 \\ 0 & -\gamma I & 0 \\ 0 & 0 & I \end{bmatrix} \begin{bmatrix} I & 0 \\ A(\alpha(t)) & B(\alpha(t)) \\ 0 & I \\ C(\alpha(t)) & D(\alpha(t)) \end{bmatrix} \prec 0 \quad (2.9)$$

is feasible for all $\alpha \in \mathcal{T}$, $t \in \mathbb{T}$, where $\Phi = \Phi_c$ in continuous time and $\Phi = \Phi_d$ in discrete time, then the LPD system (2.1) is exponentially stable and satisfies the $\mathcal{H}_\infty$ performance bound $\|H\|_\infty < \sqrt{\gamma}$.

Proof. See Appendix A.3. □

2.2.3 $\mathcal{H}_2$ performance

The following definition of $\mathcal{H}_2$ performance is adopted from [14, 27, 43, 112].

Definition 3 ($\mathcal{H}_2$ performance). *Let the LPD system (2.1) be exponentially stable, and assume that $D(\alpha) = 0$ for all $\alpha \in \mathcal{T}$ and $x(0) = 0$. Then, the $\mathcal{H}_2$ performance of (2.1) is defined as*

$$\|H\|_2^2 := \sup_{\alpha \in \mathcal{T}} \limsup_{T \to \infty} \mathbb{E} \left\{ \frac{1}{T} \|z(t)\|_{2,[0,T]}^2 \right\},$$

when $w(t)$ is a white Gaussian noise process with zero mean and covariance matrix

$$\mathbb{E}[w(t)w(s)'] = \delta_{ts} I_{n_w},$$

where δ_{ts} represents the Dirac/Kronecker delta (continuous time/discrete time).

A characterization for $\mathcal{H}_2$ performance of the LPD system (2.1) in terms of its state-space matrices is presented in the following lemma, which is a straightforward extension of the characterizations presented in [14, 43] for LTV systems.

Lemma 1 ($\mathcal{H}_2$ performance). *Let the LPD system (2.1) be exponentially stable, and assume that $D(\alpha) = 0$ for all $\alpha \in \mathcal{T}$. Then, the $\mathcal{H}_2$ performance of (2.1) is given by*

$$\|H\|_2^2 = \sup_{\alpha \in \mathcal{T}} \limsup_{T \to \infty} \frac{1}{T} \|C(\alpha)\|_{\bar{Q}(\alpha),[0,T]}^2,$$

with $\bar{Q}(\alpha)$ satisfying

$$\delta \bar{Q}(\alpha) = A(\alpha)\bar{Q}(\alpha) + \bar{Q}(\alpha)A(\alpha)' + B(\alpha)B(\alpha)', \quad \bar{Q}(\alpha(0)) = 0 \quad (2.10)$$

in continuous time, and

$$\bar{Q}(\delta\alpha) = A(\alpha)\bar{Q}(\alpha)A(\alpha)' + B(\alpha)B(\alpha)', \quad \bar{Q}(\alpha(0)) = 0 \qquad (2.11)$$

in discrete time.

LMIs characterizing an upper bound on the $\mathcal{H}_2$ performance are obtained by relaxing the conditions of Lemma 1, which is the context of the next theorem. It is worth emphasizing that these LMIs rely on the Lyapunov function $V_Q(\alpha, x) = x'Q(\alpha)^{-1}x$, such that a unified presentation is facilitated by defining the following matrices

$$\Gamma_{\mathrm{c}}(\alpha) = \begin{bmatrix} -\delta Q(\alpha) & Q(\alpha) \\ Q(\alpha) & 0 \end{bmatrix}, \quad \Gamma_{\mathrm{d}}(\alpha) = \begin{bmatrix} -Q(\delta\alpha) & 0 \\ 0 & Q(\alpha) \end{bmatrix}.$$

Theorem 4 ($\mathcal{H}_2$ performance). *Consider the LPD system* (2.1), *and assume that* $D(\alpha) = 0$ *for all* $\alpha \in \mathcal{T}$. *If there exist bounded matrices* $Q(\alpha(t)) \in \mathbb{S}_+^{n_x}$ *and* $W(\alpha(t)) \in \mathbb{S}_+^{n_z}$ *for* $\alpha \in \mathcal{T}$, $t \in \mathbb{T}$, *such that the LMIs*

$$\begin{bmatrix} I & A(\alpha(t)) \end{bmatrix} \Gamma(\alpha(t)) \begin{bmatrix} I & A(\alpha(t)) \end{bmatrix}' + B(\alpha(t))B(\alpha(t))' \prec 0, \qquad (2.12\mathrm{a})$$

$$C(\alpha(t))Q(\alpha(t))C(\alpha(t))' \prec W(\alpha(t)), \qquad (2.12\mathrm{b})$$

are feasible for all $\alpha \in \mathcal{T}$, $t \in \mathbb{T}$, *where* $\Gamma = \Gamma_{\mathrm{c}}$ *in continuous time and* $\Gamma = \Gamma_{\mathrm{d}}$ *in discrete time, then the LPD system* (2.1) *is exponentially stable and satisfies the* $\mathcal{H}_2$ *performance bound*

$$\|H\|_2^2 < \sup_{\alpha \in \mathcal{T}} \limsup_{T \to \infty} \frac{1}{T} \|I_{n_z}\|_{W(\alpha),[0,T]}^2. \qquad (2.13)$$

Proof. See Appendix A.4. □

Elaborating on the LMIs (2.12), the following set of equivalent LMIs relying on the Lyapunov function (2.7) is derived.

Theorem 5 ($\mathcal{H}_2$ performance). *Consider the LPD system* (2.1), *and assume that* $D(\alpha) = 0$ *for all* $\alpha \in \mathcal{T}$. *If there exist bounded matrices* $P(\alpha(t)) \in \mathbb{S}_+^{n_x}$ *and* $W(\alpha(t)) \in \mathbb{S}_+^{n_z}$ *for* $\alpha \in \mathcal{T}$, $t \in \mathbb{T}$, *such that the LMIs*

$$\begin{bmatrix} I & 0 \\ A(\alpha(t)) & B(\alpha(t)) \\ 0 & I \end{bmatrix}' \begin{bmatrix} \Phi(\alpha(t)) & 0 \\ 0 & -I \end{bmatrix} \begin{bmatrix} I & 0 \\ A(\alpha(t)) & B(\alpha(t)) \\ 0 & I \end{bmatrix} \prec 0 \qquad (2.14\mathrm{a})$$

and

$$\begin{bmatrix} W(\alpha(t)) & C(\alpha(t)) \\ C(\alpha(t))' & P(\alpha(t)) \end{bmatrix} \succ 0 \qquad (2.14\mathrm{b})$$

are feasible for all $\alpha \in \mathcal{T}$, $t \in \mathbb{T}$, where $\Phi = \Phi_c$ in continuous time and $\Phi = \Phi_d$ in discrete time, then the LPD system (2.1) is exponentially stable and satisfies the $\mathcal{H}_2$ performance bound (2.13).

Proof. See Appendix A.5. □

Remark 1. *For continuous-time LPD systems, the $\mathcal{H}_2$ performance is finite if and only if $D(\alpha) = 0$ (see [43], page 93). However, in case of a discrete-time LPD system that is not strictly proper (i.e., $D(\alpha) \neq 0$), the $\mathcal{H}_2$ performance can be finite, and the LMI (2.14b) should be replaced with*

$$\begin{bmatrix} W(\alpha) - D(\alpha)D(\alpha)' & C(\alpha) \\ C(\alpha)' & P(\alpha) \end{bmatrix} \succ 0.$$

Similar as for the stability case (see Theorem 2), Theorem 3 and Theorem 5 are generally conservative, thus providing upper bounds on the $\mathcal{H}_\infty$, respectively, $\mathcal{H}_2$ performance of the LPD system (2.1). However, the LMIs (2.9) and (2.14) become necessary and sufficient when restricted to time-invariant parameters, theoretically resulting in the optimal (worst-case) $\mathcal{H}_\infty$ and $\mathcal{H}_2$ performance.

The LMI conditions presented in Theorem 5 rely on the so-called controllability Gramians, which are, for a given parameter trajectory, the unique bounded solutions $\bar{Q}(\alpha)$ of (2.10) and (2.11) [112]. In a similar fashion, LMI conditions based on the observability Gramians can be derived, which generally provide a different $\mathcal{H}_2$ performance bound than the LMIs (2.14). The latter conditions are omitted for reasons of conciseness.

It should be emphasized that the presented LMI characterizations for exponential stability, $\mathcal{H}_\infty$ performance, and $\mathcal{H}_2$ performance should hold for all parameter trajectories $\alpha \in \mathcal{T}$ and for all time instants $t \in \mathbb{T}$, implying infinitely many LMI constraints. Moreover, the fact that the associated optimization variables are *functions* results in infinite-dimensional LMI problems. Therefore, the LMIs (2.8), (2.9) and (2.14) are numerically intractable. However, a finite set of LMIs that guarantees feasibility of (2.8), (2.9) and (2.14) can be derived by imposing a parameterization on the optimization variables and subsequently applying so-called relaxations. Before discussing the latter in Section 2.4, the derivation of convex conditions for full-order LPD controller synthesis is discussed in the next section.

2.3   Full-order controller design for LPD systems

This section reviews the currently available convex approaches to design full-order $\mathcal{H}_\infty$ and $\mathcal{H}_2$ LPD controllers for the LPD system

$$P : \begin{cases} \delta x &=& A(\alpha)x &+& B_w(\alpha)w &+& B_u(\alpha)u, \\ z &=& C_z(\alpha)x &+& D_{zw}(\alpha)w &+& D_{zu}(\alpha)u, \\ y &=& C_y(\alpha)x &+& D_{yw}(\alpha)w \end{cases}$$

with state $x : \mathbb{T} \to \mathbb{R}^{n_x}$, exogenous input $w : \mathbb{T} \to \mathbb{R}^{n_w}$, control input $u : \mathbb{T} \to \mathbb{R}^{n_u}$, regulated output $z : \mathbb{T} \to \mathbb{R}^{n_z}$ and measured output $y : \mathbb{T} \to \mathbb{R}^{n_y}$. It is assumed that all system matrices are real continuous functions of the exogenous parameter $\alpha : \mathbb{T} \to \mathbb{R}^N$, bounded for all $t \in \mathbb{T}$ and have appropriate dimensions. The direct feedthrough matrix from u to y is set to zero without loss of generality [58]. The aim is to design a full-order LPD controller, which is a dynamic output feedback controller of the form

$$K : \begin{cases} \delta x_c &=& A_c(\alpha)x_c &+& B_c(\alpha)y, \\ u &=& C_c(\alpha)x_c &+& D_c(\alpha)y, \end{cases} \qquad (2.15)$$

with the same number of states as the plant to be controlled (i.e., $x_c(t) \in \mathbb{R}^{n_x}$), such that the closed-loop system

$$H : \begin{cases} \delta x_{cl} &=& \mathcal{A}(\alpha)x_{cl} &+& \mathcal{B}(\alpha)w, \\ z &=& \mathcal{C}(\alpha)x_{cl} &+& \mathcal{D}(\alpha)w, \end{cases} \qquad (2.16)$$

with $x_{cl}(t) = \begin{bmatrix} x(t)' & x_c(t)' \end{bmatrix}' \in \mathbb{R}^{2n_x}$ and system matrices

$$\mathcal{A}(\alpha) = \begin{bmatrix} A(\alpha) + B_u(\alpha)D_c(\alpha)C_y(\alpha) & B_u(\alpha)C_c(\alpha) \\ B_c(\alpha)C_y(\alpha) & A_c(\alpha) \end{bmatrix},$$

$$\mathcal{B}(\alpha) = \begin{bmatrix} B_w(\alpha) + B_u(\alpha)D_c(\alpha)D_{yw}(\alpha) \\ B_c(\alpha)D_{yw}(\alpha) \end{bmatrix},$$

$$\mathcal{C}(\alpha) = \begin{bmatrix} C_z(\alpha) + D_{zu}(\alpha)D_c(\alpha)C_y(\alpha) & D_{zu}(\alpha)C_c(\alpha) \end{bmatrix},$$

$$\mathcal{D}(\alpha) = D_{zw}(\alpha) + D_{zu}(\alpha)D_c(\alpha)D_{yw}(\alpha).$$

is exponentially stable and meets an $\mathcal{H}_\infty$ or $\mathcal{H}_2$ performance specification for all $\alpha \in \mathcal{T}$. See Figure 2.2 on page 17 for a schematic representation. It is obvious that the controller matrices should be constant (i.e., independent of α) in case α is uncertain, while the general form (2.15) applies when α is a priori known or real-time measurable.
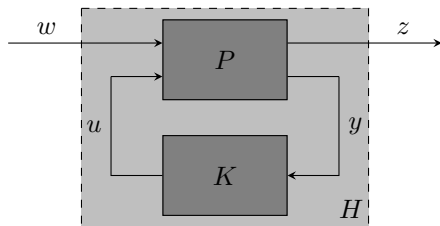
Figure 2.2: The objective is to design a controller K that exponentially stabilizes the system P, such that an $\mathcal{H}_\infty$ or $\mathcal{H}_2$ performance specification from w to z is satisfied.

Using Theorem 2, the closed-loop system (2.16) is exponentially stable if there exists a bounded matrix $P(\alpha(t)) \in \mathbb{S}_+^{2n_x}$, $\alpha \in \mathcal{T}$, $t \in \mathbb{T}$, such that

$$\begin{bmatrix} I \\ \mathcal{A}(\alpha(t)) \end{bmatrix}' \Phi(\alpha(t)) \begin{bmatrix} I \\ \mathcal{A}(\alpha(t)) \end{bmatrix} \prec 0 \tag{2.17}$$

is feasible for all $\alpha \in \mathcal{T}$, $t \in \mathbb{T}$. Since the closed-loop matrix $\mathcal{A}(\alpha)$ depends on the controller matrices, it is clear that (2.17) is a nonlinear matrix inequality, and thus yields a nonconvex problem. A similar reasoning applies to the $\mathcal{H}_\infty$ and $\mathcal{H}_2$ controller synthesis problems (see Theorem 3 on page 13 and Theorem 5 on page 14).

To circumvent this issue, several approaches for full-order $\mathcal{H}_\infty$ and $\mathcal{H}_2$ controller design have been proposed over the last decades. For LTI systems, the corresponding nonlinear matrix inequalities can be reformulated into equivalent LMIs by a nonlinear change of variables [76, 103], elimination of the controller variables [41, 58], or a combination of the two aforementioned approaches [5]. In other words, the full-order $\mathcal{H}_\infty$ and $\mathcal{H}_2$ control problems for LTI systems are convex.

The above approaches for LTI systems are extendable to LTV and LPV dynamics. However, structural constraints need to be imposed on LMI variables to obtain *practical* controllers (i.e., controllers independent of derivatives or future parameter values) [5, 28], introducing conservatism.

The full-order synthesis problem for uncertain linear systems remains a very hard problem, which is mainly due to structural constraints on the controller. The nonlinear change of variables can no longer be applied, since the reconstructed controller depends on the parameter-dependent matrices of the open-loop system. A possible conservative approach is to reformulate the full-order synthesis problem as a static output feedback problem, and subsequently apply a conservative approach for robust static output feedback synthesis. See for instance [23, 64, 107].

2.3.1   Multi-objective control

As it is often complicated to capture all design specifications in a single objective, several extensions to multi-objective controller design have been developed [32, 62, 76, 103, 126], allowing the incorporation of various performance specifications (i.e., $\mathcal{H}_\infty$, $\mathcal{H}_2$, amongst others). Specifically, the design of full-order multi-objective LTI controllers gives rise to a nonconvex problem, and conservatism is introduced to derive convex sufficient conditions.

Applying the nonlinear transformation of controller variables that is presented in [76, 103], sufficient LMIs result when selecting a single Lyapunov matrix for all performance specifications. This conservative procedure is named the Lyapunov shaping paradigm. A less conservative approach is proposed in [32] for the discrete-time case, relying on the introduction of an additional matrix variable G. Products between the closed-loop matrices and G appear in the resulting LMIs, while the closed-loop matrices and the Lyapunov matrices are decoupled. Selecting a constant matrix G in the latter synthesis method, which is referred to as the G shaping paradigm, allows the use of a different Lyapunov matrix for each performance specification while convexity is retained.

Both the Lyapunov and the G shaping paradigm are extendable to LTV and LPV dynamics [28]. In fact, more general full-order synthesis LMIs (featuring additional slack variables and scalar parameters) can be derived using the projection lemma [83, 94], but are out of scope here.

2.4   Relaxations

Since all the previously presented LMI conditions feature infinite-dimensional optimization variables and infinitely many constraints, they are numerically intractable. Therefore, this section discusses how tractable convex conditions are derived whose feasibility implies feasibility of such an intractable LMI. The latter is incredibly powerful, since it enables to guarantee stability and performance of an LPD system by solving a numerically tractable optimization problem. The derivation of numerically tractable conditions is performed in two steps. First, a parameterization is imposed on the LMI variables, resulting in a finite number of optimization variables. Subsequently, so-called relaxations are applied, which boils down to replacing the infinite set of constraints by a more restrictive finite (i.e., conservative) set of constraints. The following section provides a brief overview of the most common parameterizations. Subsequently, it is demonstrated how the structure of these parameterizations is exploited in

conjunction with positivity of basis functions to derive a finite set of sufficient LMIs.

2.4.1 Parameterizations

In this section, the most widely used parameterizations for relaxing intractable LMIs are listed, and ordered according to their generality.

Affine parameterization   A matrix $A(\alpha)$ has an affine dependency on an N-dimensional parameter α if

$$A(\alpha) = A_0 + \sum_{k=1}^{N} \alpha_k A_k \,,$$

where $A_k\,, \quad k = 0, \ldots, N$ are constant matrices.

Multi-affine parameterization   A matrix $A(\alpha)$ has a multi-affine dependency on an N-dimensional parameter α if

$$A(\alpha) = \sum_{k_1=0}^{1} \sum_{k_2=0}^{1} \cdots \sum_{k_N=0}^{1} \alpha_1^{k_1} \alpha_2^{k_2} \cdots \alpha_N^{k_N} A_{k_1,k_2,\cdots,k_N} \,,$$

where $A_{k_1,k_2,\cdots,k_N}\,, \quad k_i = 0, 1\,, \quad i = 1, \ldots, N$ are constant matrices. An affine parameterization is recovered as a special case, by only allowing $(k_1, \ldots, k_N) = 0$ and the combinations $k_i = 1$ and $k_j = 0$ for $j \neq i\,, \quad i = 1, \ldots, N$.

Univariate polynomial parameterization   A matrix $A(\alpha)$ has an polynomial dependency of degree g on a scalar parameter α if

$$A(\alpha) = \sum_{k=0}^{g} \alpha^k A_k \,,$$

where $A_k\,, \quad k = 0, \ldots, g$ are constant matrices.

Multivariate polynomial parameterization   A matrix $A(\alpha)$ has an polynomial dependency of degree $(g_1, g_2, \cdots, g_N)$ on an N-dimensional parameter α if

$$A(\alpha) = \sum_{k_1=0}^{g_1} \sum_{k_2=0}^{g_2} \cdots \sum_{k_N=0}^{g_N} \alpha_1^{k_1} \alpha_2^{k_2} \cdots \alpha_N^{k_N} A_{k_1,k_2,\cdots,k_N} \,,$$

where $A_{k_1,k_2,\cdots,k_N}$, $k_i = 1,\ldots,g_i$, $i = 1,\ldots,N$ are constant matrices. This parameterization encompasses the multi-affine parameterization, which is seen by selecting $g_i = 1$, $i = 1,\ldots,N$.

Example 1. *The matrix*

$$A(\alpha) = \begin{bmatrix} \alpha_1^3(1-\alpha_2) & \pi \\ \sqrt{2}+\alpha_1 & 5\alpha_2^2 \end{bmatrix}$$

has a polynomial parameter dependency of degree $g = (3,2)$ on the 2-dimensional parameter $\alpha = (\alpha_1, \alpha_2)$.

Univariate polynomial spline parameterization Consider a scalar parameter α on a closed and bounded interval $[\underline{\alpha}, \overline{\alpha}] \subset \mathbb{R}$, and let $\xi = (\xi_0, \ldots, \xi_{l+1})$ be a sequence of points satisfying

$$\underline{\alpha} = \xi_0 < \xi_1 < \cdots < \xi_l < \xi_{l+1} = \overline{\alpha}.$$

Then, a matrix $A(\alpha)$ is a polynomial spline (i.e. piecewise polynomial) of degree g with internal break points $\xi_1, \ldots, \xi_l$ and continuity conditions $\nu_1, \ldots, \nu_l$ if there exist polynomial matrices $P_0(\alpha), \ldots, P_l(\alpha)$ of degree g such that

$$A(\alpha) = P_i(\alpha), \quad \text{for } \alpha \in [\xi_i, \xi_{i+1}), \quad i = 0, \ldots, l-1,$$

$$A(\alpha) = P_l(\alpha), \quad \text{for } \alpha \in [\xi_l, \xi_{l+1}],$$

and

$$\left.\frac{d^{j-1}P_{i-1}}{d\alpha^{j-1}}\right|_{\alpha=\xi_i} = \left.\frac{d^{j-1}P_i}{d\alpha^{j-1}}\right|_{\alpha=\xi_i}, \quad \text{for } j = 1,\ldots,\nu_i, \quad i = 1,\ldots,l.$$

This parameterization is a generalization of the univariate polynomial parameterization when restricted to a bounded interval, which is immediate from selecting $l = 0$ (i.e., no internal break points).

Tensor product polynomial spline parameterization So-called tensor product polynomial splines are considered, constituting a particular multivariate extension of univariate polynomial splines. Consider a N-dimensional parameter $\alpha = (\alpha_1, \ldots, \alpha_N)$ defined on the Cartesian product of closed and bounded intervals:

$$[\underline{\alpha}_1, \overline{\alpha}_1] \times \cdots \times [\underline{\alpha}_N, \overline{\alpha}_N] \subset \mathbb{R}^N.$$

Then, in a similar fashion as multivariate polynomials follow from the univariate case, tensor product polynomial splines follow as a straightforward extension
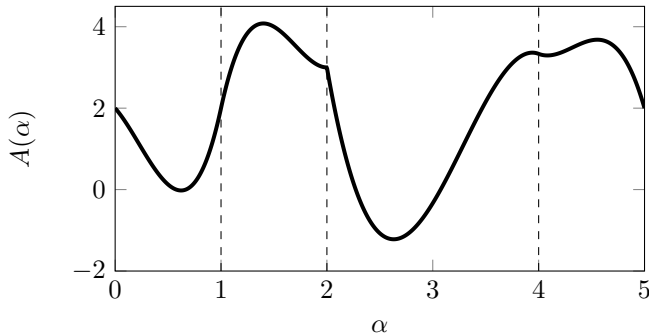
Figure 2.3: A polynomial spline is a piecewise polynomial with continuity requirements. A scalar univariate polynomial spline $A : [0, 5] \to \mathbb{R}$ of degree 3 with internal break points $(\xi_1, \xi_2, \xi_3) = (1, 2, 4)$ and continuity requirements $(\nu_1, \nu_2, \nu_3) = (2, 1, 2)$ is shown.

from univariate polynomial splines. Namely, by defining a break point sequence $(\xi_{k,0}, \xi_{k,1}, \ldots, \xi_{k,l_k}, \xi_{k,l_k+1})$ and continuity conditions vector $(\nu_{k,1}, \ldots, \nu_{k,l_k})$ for each α_k, $k = 1, \ldots, N$. This parameterization is a generalization of the multivariate polynomial parameterization when restricted to a Cartesian product of bounded intervals, which follows from choosing $l_k = 0$, $k = 1, \ldots, N$.

Note that, since α assumes values in a Cartesian product of intervals, $\alpha_1, \ldots, \alpha_N$ are considered to be mutually independent. If $\alpha_1, \ldots, \alpha_N$ are allowed to be mutually dependent, a more general spline parameterization is required. However, a general treatment of multivariate polynomial splines is out of scope here, and the interested reader is referred to [25, 106].

To simplify terminology, tensor product (polynomial) splines are named (polynomial) splines in the remainder of this thesis.

2.4.2   Deriving a finite set of sufficient LMIs

Various approaches have been developed to derive a numerically tractable set of LMIs that guarantee feasibility of a semi-infinite LMI problem. Most of these approaches rely on expressing a parameter-dependent matrix in terms of positive basis functions, such that positivity of each coefficient implies positivity of the parameter-dependent matrix for all parameters in a certain set. For instance, positive definiteness of a parameter-dependent matrix can be checked using an extension of Pólya's theorem to the case of matrix-valued coefficients [87, 88], or by decomposing it as a sum-of-squares [56, 102]. The former approach is briefly discussed for polynomially parameter-dependent LMIs. Subsequently,

using so-called B-splines as basis functions, relaxations are derived for LMIs with a polynomial spline dependency. It is worth mentioning that specific rational parameter dependencies can be handled using the descriptor form, see for instance [21]. The approach presented in [102], see also [100], handles general rational parameter dependencies.

Polynomials

Consider the parameter-dependent LMI

$$P(\alpha) \succ 0,$$

with a polynomial dependency (of arbitrary finite degree) on the N-dimensional parameter $\alpha \in \Lambda$, where $\Lambda \subset \mathbb{R}^N$ is a compact convex polytope.

First, the parameter α is expressed as a convex combination of the vertices f_i, $i = 1, \ldots, M$ of Λ:

$$\alpha = \sum_{i=1}^{M} f_i \beta_i = F\beta, \tag{2.18}$$

where the ith column of F corresponds to vertex f_i, and β takes values in the unit simplex of dimension M. That is, $\sum_{i=1}^{M} \beta_i = 1$, and $\beta_i \geq 0$, $i = 1, \ldots, M$. Using the linear relation (2.18), P is expressed as a function of β as follows:

$$\widehat{P}(\beta) := P(F\beta) = P(\alpha),$$

where the polynomial coefficients of $\widehat{P}$ can always be determined for a given set of vertices.

Next, so-called homogenization is applied to express $\widehat{P}$ in terms of monomial basis functions having the same degree. The latter is achieved by exploiting that β takes values in the unit simplex. Consequently, the relaxation step is to impose positivity on all the coefficients of $\widehat{P}$, since this implies that $\widehat{P}(\beta) \succ 0$ for all β in the unit simplex. In turn, $P(\alpha) \succ 0$ for all $\alpha \in \Lambda$, and thus $P(\alpha(t)) \succ 0$ for all $\alpha : \mathbb{T} \to \Lambda$, $t \in \mathbb{T}$.

Example 2 (Homogenization)**.** *The concept of homogenization is illustrated in this example. Consider the polynomially parameter-dependent matrix*

$$\widehat{P}(\beta_1, \beta_2) = \beta_1^3 \widehat{P}_1 + \beta_1 \beta_2 \widehat{P}_2 + \widehat{P}_3,$$

where $\widehat{P}_j$, $j = 1, \ldots, 3$ are given constant matrices and β is in the unit simplex of dimension 2. To homogenize $\widehat{P}$, note that $\beta_1 + \beta_2 = 1$, such that

$$\widehat{P}(\beta_1, \beta_2) = \beta_1^3 \widehat{P}_1 + (\beta_1 + \beta_2)\beta_1\beta_2\widehat{P}_2 + (\beta_1 + \beta_2)^3\widehat{P}_3$$

$$= \beta_1^3(\widehat{P}_1 + \widehat{P}_3) + \beta_1^2\beta_2(\widehat{P}_2 + 3\widehat{P}_3) + \beta_1\beta_2^2(\widehat{P}_2 + 3\widehat{P}_3) + \beta_2^3\widehat{P}_3 \ .$$

Starting from a homogeneous polynomially parameter-dependent LMI $\widehat{P}(\beta) \succ 0$, degree elevation can be applied to obtain less conservative relaxations, relying on the following relation (see [87]):

$$\widehat{P}(\beta) \succ 0 \Leftrightarrow \left(\sum_{i=1}^{M} \beta_i\right)^d \widehat{P}(\beta) \succ 0, \tag{2.19}$$

for any $d \in \mathbb{N}$.

Example 3 (Degree elevation)**.** *This example, which is borrowed from [26], illustrates the concept of degree elevation for homogeneous polynomially parameter-dependent LMIs. Consider the homogeneous polynomially parameter-dependent matrix*

$$\widehat{P}(\beta_1, \beta_2) = \beta_1^2 \widehat{P}_1 + \beta_1\beta_2\widehat{P}_2 + \beta_2^2\widehat{P}_3,$$

where $\widehat{P}_j$, $j = 1, \ldots, 3$ are given constant matrices and β is in the unit simplex of dimension 2. A set of sufficient conditions for positive definiteness of $\widehat{P}$ is

$$\widehat{P}_1 \succ 0, \quad \widehat{P}_2 \succ 0, \quad \widehat{P}_3 \succ 0. \tag{2.20}$$

Selecting $d = 1$ in (2.19),

$$\widehat{P}(\beta_1, \beta_2) = (\beta_1 + \beta_2)\widehat{P}(\beta_1, \beta_2)$$

$$= \beta_1^3 \widehat{P}_1 + \beta_1^2\beta_2(\widehat{P}_1 + \widehat{P}_2) + \beta_1\beta_2^2(\widehat{P}_2 + \widehat{P}_3) + \beta_2^3\widehat{P}_3,$$

such that a corresponding set of sufficient conditions is

$$\widehat{P}_1 \succ 0, \quad \widehat{P}_1 + \widehat{P}_2 \succ 0, \quad \widehat{P}_2 + \widehat{P}_3 \succ 0, \quad \widehat{P}_3 \succ 0,$$

which is less conservative than (2.20). Hence, conservatism is reduced at the expense of an increase in the number of sufficient LMIs. Generally speaking, higher values of d correspond to less conservative relaxations and a higher number of sufficient LMIs.

It is worth to emphasize that, in fact, for any positive definite polynomial $\widehat{P}(\beta)$ depending on β in the unit simplex, there exists a *finite* value of $d \in \mathbb{N}$ such that all the coefficients of

$$\left(\sum_{i=1}^{M} \beta_i\right)^d \widehat{P}(\beta) \succ 0$$

are positive (see [87] and references therein). Hence, a tractable necessary and sufficient condition for positivity results.

The above relaxation technique is extendable to incorporate bounds on the rate of parameter variation by applying the approaches discussed in [86] (continuous time) or [28, 88] (discrete time). An extension of these approaches, exploiting subdivision of the parameter domain, is presented in Chapter 5 (page 65).

Polynomial splines

Consider the parameter-dependent LMI

$$P(\alpha) \succ 0,$$

with a polynomial spline dependency on the scalar parameter $\alpha \in \Lambda$, where $\Lambda \subset \mathbb{R}$ is a closed and bounded interval.

First, $P(\alpha)$ is expressed in terms of particular normalized (scalar) B-spline basis functions, defined as in [25] (page 87). This is always possible by virtue of the Curry-Schoenberg theorem [25], by considering the knot sequence

$$\lambda = (\underbrace{\xi_0, \ldots, \xi_0}_{g+1}, \underbrace{\xi_1, \ldots, \xi_1}_{g+1-\nu_1}, \ldots, \underbrace{\xi_l, \ldots, \xi_l}_{g+1-\nu_l}, \underbrace{\xi_{l+1}, \ldots, \xi_{l+1}}_{g+1}) \in \mathbb{R}^{n_\lambda}.$$

Denoting the ith normalized B-spline basis function of degree g for the knot sequence λ by $B_{i,g,\lambda}(\alpha)$, the parameter-dependent matrix $P(\alpha)$ is expressed as

$$P(\alpha) = \sum_{i=1}^{n_\lambda - g - 1} C_i B_{i,g,\lambda}(\alpha), \qquad (2.21)$$

where C_i, $i = 1, \ldots, n_\lambda - g - 1$ are matrix-valued coefficients.

B-splines are commonly used as basis functions for polynomial splines, since they possess various useful properties [25, 106]. The following two properties are exploited to derive relaxations:

- Positivity:

$$B_{i,g,\lambda}(\alpha) \geq 0, \quad \forall \alpha \in \Lambda, \quad i = 1, \ldots, n_\lambda - g - 1.$$

- Partition of unity:

$$\sum_{i=1}^{n_\lambda - g - 1} B_{i,g,\lambda}(\alpha) = 1, \quad \forall \alpha \in \Lambda.$$

Namely, combining these properties reveals that

$$C_i \succ 0, \quad i = 1, \ldots, n_\lambda - g - 1 \quad \Rightarrow \quad P(\alpha) \succ 0, \quad \forall \alpha \in \Lambda.$$

Hence, imposing positivity on B-spline coefficients of a polynomial spline is a sufficient condition for positivity of the polynomial spline itself.

In a similar way as for the polynomial case, degree elevation can be applied to obtain less conservative relaxations.

Degree elevation   Increasing the degree of $P(\alpha)$ by one on each subinterval $[\xi_i, \xi_{i+1})$ yields an expression of the form

$$P(\alpha) = \sum_{i=1}^{n_{\tilde{\lambda}}+l+1-g} \tilde{C}_i B_{i,g+1,\tilde{\lambda}}(\alpha),$$

where $\tilde{\lambda}$ is the knot sequence

$$\tilde{\lambda} = (\underbrace{\xi_0, \ldots, \xi_0}_{g+2}, \underbrace{\xi_1, \ldots, \xi_1}_{g+2-\nu_1}, \ldots, \underbrace{\xi_l, \ldots, \xi_l}_{g+2-\nu_l}, \underbrace{\xi_{l+1}, \ldots, \xi_{l+1}}_{g+2}) \in \mathbb{R}^{n_{\tilde{\lambda}}},$$

with $n_{\tilde{\lambda}} = n_\lambda + l + 2$. Requiring $\tilde{C}_i \succ 0$, $i = 1, \ldots, n_{\tilde{\lambda}} - g - 1$ is less conservative than the conditions $C_i \succ 0, i = 1, \ldots, n_\lambda - g - 1$, which comes at the expense of an increased number of sufficient LMIs (similar as in Example 3).

While degree elevation is the only option to reduce conservatism in a polynomially parameter-dependent LMI, knot insertion provides an alternative to obtain less conservative relaxations for LMIs with a polynomial spline dependency. As a matter of fact, applying knot insertion to relax a set of sufficient LMIs is relatively straightforward.

Knot insertion   Let $\hat{\lambda}$ be constructed from λ by inserting a single knot λ_{add} between λ_j and λ_{j+1}. Then, the B-spline coefficients of

$$P(\alpha) = \sum_{i=1}^{n_{\hat{\lambda}}-g-1} \hat{C}_i B_{i,g,\hat{\lambda}}(\alpha),$$

(with $n_{\hat{\lambda}} = n_\lambda + 1$) are related to the original coefficients C_i, $i = 1, \ldots, n_\lambda - g - 1$ of (2.21) as follows [25]:

$$\hat{C}_i = (1 - \beta_{i,g}(\lambda_{\mathrm{add}}))C_{i-1} + \beta_{i,g}(\lambda_{\mathrm{add}})C_i,$$

where the function $\beta_{i,g}$ is defined by

$$\beta_{i,g}(x) = \left\{ \begin{array}{ll} 0 & \text{if} \quad x \leq \lambda_i, \\ \frac{x - \lambda_i}{\lambda_{i+g} - \lambda_i} & \text{if} \quad \lambda_i < x < \lambda_{i+g}, \\ 1 & \text{if} \quad \lambda_{i+g} \leq x. \end{array} \right.$$

The extension to tensor product polynomial spline parameterizations is obvious and therefore omitted.

2.5   Summary

In this chapter, the general class of LPD systems in state space form has been defined. For this class of systems, sufficient parameter-dependent LMI characterizations for exponential stability and $\mathcal{H}_\infty$ and $\mathcal{H}_2$ performance were derived. Subsequently, we discussed how these characterizations can be adapted to derive full-order (multi-objective) $\mathcal{H}_\infty$ and $\mathcal{H}_2$ synthesis LMIs for particular subclasses of LPD systems. The corresponding parameter-dependent LMIs are numerically intractable, since they feature infinite-dimensional optimization variables and infinitely many constraints. To relieve the latter issue, it was shown how to derive numerically tractable conditions whose feasibility guarantees feasibility of a numerically intractable LMI, by imposing a polynomial (spline) parameterization on the LMI variables and subsequently applying relaxations. The resulting tractable conditions are incredibly powerful, since they enable us to guarantee stability and $\mathcal{H}_\infty/\mathcal{H}_2$ performance of an LPD system by solving a numerically tractable optimization problem.

Based on the mathematical notions and techniques discussed in this chapter, a unifying framework to design fixed-order controllers for LPD systems is presented next.

Recapitulation

- The general class of LPD systems encompasses a broad range of linear systems, including (uncertain) LTI and LPV systems.

- Exponential stability and $\mathcal{H}_\infty$ and $\mathcal{H}_2$ performance of an LPD system are characterized in terms of parameter-dependent LMIs, featuring infinite-dimensional optimization variables and infinitely many constraints.

- The full-order $\mathcal{H}_\infty$ and $\mathcal{H}_2$ synthesis problem is convex for LTI dynamics.

- The full-order $\mathcal{H}_\infty$ and $\mathcal{H}_2$ synthesis LMIs for LTI systems are extendable to LTV and LPV dynamics, but structural constraints need to be imposed on LMI variables to obtain practical controllers.

- The full-order control problem for uncertain linear systems remains very hard (nonconvex), which is mainly due to structural constraints on the controller.

- The full-order multi-objective control problem is nonconvex, even for LTI systems, and conservatism needs to be introduced to derive convex (sufficient) conditions.

- A tractable set of convex conditions, whose feasibility implies feasibility of a parameter-dependent LMI with infinite-dimensional optimization variables and infinitely many constraints, is derived as follows. A polynomial (spline) parameterization is imposed on the LMI variables, and then relaxations are applied.

Chapter 3

A unifying framework to design fixed-order controllers for LPD systems

This theoretical chapter presents a novel projection lemma based LMI framework to design fixed-order multi-objective $\mathcal{H}_\infty/\mathcal{H}_2$ controllers for LPD systems. This framework relies on a set of a priori computed full-order LPD controllers that stabilize the LPD system for all possible parameter trajectories, which are used as parameters in sufficient LMIs for the fixed-order controller design. In these sufficient LMIs, continuous-time and discrete-time controller designs are treated in a unified fashion, and the controller complexity, which is completely characterized by the number of states and the parameter-dependency of the controller, is fixed in advance.

3.1 Introduction

The fixed-order controller design problem is amongst the most relevant problems in control theory, and remains an open problem to date even for LTI systems [16, 114]. In words, the fixed-order controller design problem for LPD systems is stated as follows: given an LPD system, find a fixed-order dynamic output feedback controller (i.e., a controller with an a priori fixed number of states and parameter dependency) such that the closed-loop system satisfies some desirable stability and performance specifications, or show that such a feedback controller does not exist. The fixed-order controller design problem has received

substantial attention in the last decades, since it is of paramount importance for realistic control applications. Especially for high-order systems, low-order controllers are desirable due to reliability requirements and implementation cost constraints. A detailed literature overview related to fixed-order controller design is provided independently for several considered subclasses of LPD systems in Chapters 4 to 6.

This chapter presents a unifying convex framework to design fixed-order multi-objective $\mathcal{H}_\infty/\mathcal{H}_2$ controllers for the general class of LPD systems. Since this class encompasses a broad range of linear systems (as shown in Table 2.1 on page 9), the proposed controller design framework is suitable for many different applications. Starting from a high-level mathematical problem description (Section 3.2), novel extended LMI conditions for closed-loop $\mathcal{H}_\infty/\mathcal{H}_2$ performance analysis of a given fixed-order controller are derived in Section 3.3, by expressing the closed-loop matrices as a function of an arbitrary full-order controller for the same system. By imposing structural constraints on the variables in these extended analysis LMIs, sufficient LMIs for fixed-order $\mathcal{H}_\infty$ and $\mathcal{H}_2$ controller synthesis are derived in Section 3.4, which require an a priori computed stabilizing full-order controller. Since practical applications often desire multiple design objectives, the fixed-order synthesis conditions are extended to handle multi-objective control problems in Section 3.4.3, requiring a full-order controller for each performance specification.

3.2   Problem formulation

Consider the finite-dimensional LPD state-space representation

$$
\begin{cases}
\delta x &=& A(\alpha)x &+& B_w(\alpha)w &+& B_u(\alpha)u, \\
z &=& C_z(\alpha)x &+& D_{zw}(\alpha)w &+& D_{zu}(\alpha)u, \\
y &=& C_y(\alpha)x &+& D_{yw}(\alpha)w
\end{cases}
\tag{3.1}
$$

with state $x : \mathbb{T} \to \mathbb{R}^{n_x}$, exogenous input $w : \mathbb{T} \to \mathbb{R}^{n_w}$, control input $u : \mathbb{T} \to \mathbb{R}^{n_u}$, regulated output $z : \mathbb{T} \to \mathbb{R}^{n_z}$ and measured output $y : \mathbb{T} \to \mathbb{R}^{n_y}$. It is assumed that all system matrices are real continuous functions of the exogenous parameter $\alpha : \mathbb{T} \to \mathbb{R}^N$, bounded for all $t \in \mathbb{T}$, and have appropriate dimensions.

The objective is to design fixed-order dynamic output feedback controllers

$$
\begin{cases}
\delta x_c &=& A_c(\alpha)x_c &+& B_c(\alpha)y, \\
u &=& C_c(\alpha)x_c &+& D_c(\alpha)y,
\end{cases}
\tag{3.2}
$$

with $x_c(t) \in \mathbb{R}^q$, $q \le n_x$, that exponentially stabilize the LPD system (3.1) and satisfy multiple closed-loop $\mathcal{H}_\infty$ and/or $\mathcal{H}_2$ performance specifications for all

$\alpha \in \mathcal{T}$. Obviously, the state-space matrices of (3.2) are taken constant when α is uncertain, while the more general form (3.2) is assumed when α is either a priori known or real-time measurable.

Grouping the controller matrices of (3.2) as

$$\Theta(\alpha) := \begin{bmatrix} A_\mathrm{c}(\alpha) & B_\mathrm{c}(\alpha) \\ C_\mathrm{c}(\alpha) & D_\mathrm{c}(\alpha) \end{bmatrix}, \tag{3.3}$$

the closed-loop interconnection of the LPD system (3.1) with the LPD controller (3.2) is indicated as

$$H_\Theta : \begin{cases} \delta x_\mathrm{cl} & = & \mathcal{A}_\Theta(\alpha) x_\mathrm{cl} & + & \mathcal{B}_\Theta(\alpha) w, \\ z & = & \mathcal{C}_\Theta(\alpha) x_\mathrm{cl} & + & \mathcal{D}_\Theta(\alpha) w, \end{cases} \tag{3.4}$$

where $x_\mathrm{cl}(t) = \begin{bmatrix} x(t)' & x_\mathrm{c}(t)' \end{bmatrix}' \in \mathbb{R}^{n_x + q}$ is a closed-loop state vector. Moreover, defining the matrices

$$\begin{bmatrix} \tilde{A}(\alpha) & \tilde{B}_w(\alpha) & \tilde{B}_u(\alpha) \\ \tilde{C}_z(\alpha) & \tilde{D}_{zw}(\alpha) & \tilde{D}_{zu}(\alpha) \\ \tilde{C}_y(\alpha) & \tilde{D}_{yw}(\alpha) & 0 \end{bmatrix} := \left[\begin{array}{cc|c|cc} A(\alpha) & 0 & B_w(\alpha) & 0 & B_u(\alpha) \\ 0 & 0 & 0 & I_q & 0 \\ \hline C_z(\alpha) & 0 & D_{zw}(\alpha) & 0 & D_{zu}(\alpha) \\ \hline 0 & I_q & 0 & 0 & 0 \\ C_y(\alpha) & 0 & D_{yw}(\alpha) & 0 & 0 \end{array} \right], \tag{3.5}$$

the affine dependency of the closed-loop matrices in (3.4) on $\Theta(\alpha)$ is expressed as

$$\begin{bmatrix} \mathcal{A}_\Theta(\alpha) & \mathcal{B}_\Theta(\alpha) \\ \mathcal{C}_\Theta(\alpha) & \mathcal{D}_\Theta(\alpha) \end{bmatrix} = \begin{bmatrix} \tilde{A}(\alpha) & \tilde{B}_w(\alpha) \\ \tilde{C}_z(\alpha) & \tilde{D}_{zw}(\alpha) \end{bmatrix} + \begin{bmatrix} \tilde{B}_u(\alpha) \\ \tilde{D}_{zu}(\alpha) \end{bmatrix} \Theta(\alpha) \begin{bmatrix} \tilde{C}_y(\alpha) & \tilde{D}_{yw}(\alpha) \end{bmatrix}. \tag{3.6}$$

Remark 2. *In what follows, the matrix $\Theta(\alpha)$ defined in (3.3) is often referred to as a controller, by which a controller of the form (3.2) is meant.*

3.3 Extended analysis conditions

This section presents novel extended parameter-dependent LMIs for $\mathcal{H}_\infty$ and $\mathcal{H}_2$ performance analysis of the LPD system (3.1) in closed loop with a given controller $\Theta(\alpha)$, defined in (3.3). These parameter-dependent LMIs are constructed by linking $\Theta(\alpha)$ to a (possibly unstable/destabilizing) full-order LPD controller $\Psi(\alpha)$ of dimension $(n_x + n_u) \times (n_x + n_y)$, which is defined as in (3.3). The controller $\Theta(\alpha)$ is augmented with exponentially stable unobservable and/or uncontrollable dynamics to form a so-called augmented controller $\Theta_\mathrm{a}(\alpha)$
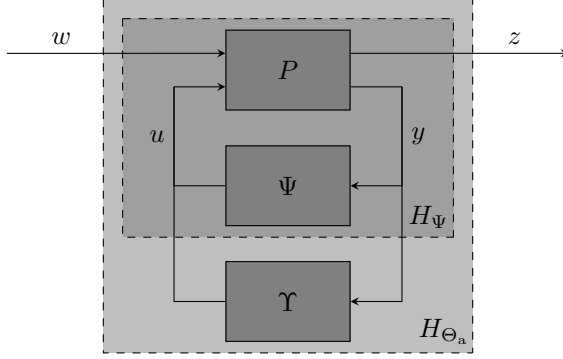
Figure 3.1: Novel extended LMI characterizations for $\mathcal{H}_\infty$ and $\mathcal{H}_2$ performance of H_Θ are derived by expressing H_{Θ_a} in terms of H_Ψ and the difference $\Upsilon = \Theta_a - \Psi$.

with the same dimensions as $\Psi(\alpha)$. We assume that the augmented controller matrix attains a so-called Kalman canonical form [124]:

$$\Theta_a(\alpha) = \left[\begin{array}{cc|c} A_c(\alpha) & A_{12}(\alpha) & B_c(\alpha) \\ 0 & A_{22}(\alpha) & 0 \\ \hline C_c(\alpha) & C_2(\alpha) & D_c(\alpha) \end{array}\right], \tag{3.7}$$

where $A_{22}(\alpha)$ corresponds to exponentially stable dynamics. Subsequently, since H_Θ and H_{Θ_a} share the same stability and performance properties, stability and performance of H_Θ is characterized in terms of H_Ψ. Namely, defining the difference

$$\Upsilon(\alpha) := \Theta_a(\alpha) - \Psi(\alpha),$$

note that (3.6) implies

$$\begin{bmatrix} \mathcal{A}_{\Theta_a}(\alpha) & \mathcal{B}_{\Theta_a}(\alpha) \\ \mathcal{C}_{\Theta_a}(\alpha) & \mathcal{D}_{\Theta_a}(\alpha) \end{bmatrix} = \begin{bmatrix} \mathcal{A}_\Psi(\alpha) & \mathcal{B}_\Psi(\alpha) \\ \mathcal{C}_\Psi(\alpha) & \mathcal{D}_\Psi(\alpha) \end{bmatrix} + \begin{bmatrix} \tilde{B}_u(\alpha) \\ \tilde{D}_{zu}(\alpha) \end{bmatrix} \Upsilon(\alpha) \begin{bmatrix} \tilde{C}_y(\alpha) & \tilde{D}_{yw}(\alpha) \end{bmatrix}, \tag{3.8}$$

which is schematically shown in Figure 3.1.

Based on relation (3.8) and the specific form (3.7), extended parameter-dependent LMI characterizations for $\mathcal{H}_\infty$ and $\mathcal{H}_2$ performance of the LPD system (3.4) are presented next. The following parameter-dependent matrices are defined to facilitate the presentation of these characterizations:

$$R_{\Psi,\infty}(\alpha) := \left[\begin{array}{cc|c} I & 0 & 0 \\ \mathcal{A}_\Psi(\alpha) & \mathcal{B}_\Psi(\alpha) & \tilde{B}_u(\alpha) \\ 0 & I & 0 \\ \mathcal{C}_\Psi(\alpha) & \mathcal{D}_\Psi(\alpha) & \tilde{D}_{zu}(\alpha) \end{array}\right],$$

$$R_{\Psi,2}(\alpha) := \left[\begin{array}{cc|c} I & 0 & 0 \\ \mathcal{A}_\Psi(\alpha) & \mathcal{B}_\Psi(\alpha) & \tilde{B}_u(\alpha) \\ 0 & I & 0 \end{array} \right].$$

3.3.1 $\mathcal{H}_\infty$ performance

The following theorem provides a novel extended $\mathcal{H}_\infty$ performance characterization for the LPD system (3.1) in closed-loop with a given fixed-order controller (3.2).

Theorem 6 (Extended $\mathcal{H}_\infty$ performance)**.** *Let $\Psi(\alpha(t)) \in \mathbb{R}^{(n_x+n_u)\times(n_x+n_y)}$ be an arbitrary bounded matrix for all $\alpha \in \mathcal{T}$, $t \in \mathbb{T}$, and let $\Theta_{\mathrm{a}}(\alpha(t)) \in \mathbb{R}^{(n_x+n_u)\times(n_x+n_y)}$ be constructed from $\Theta(\alpha(t)) \in \mathbb{R}^{(q+n_u)\times(q+n_y)}$ by adding exponentially stable uncontrollable and/or unobservable dynamics. Then, the closed-loop system H_Θ, defined as in (3.4), is exponentially stable and $\|H_\Theta\|_\infty < \sqrt{\gamma}$ if there exist bounded matrices*

$$P(\alpha(t)) \in \mathbb{S}_+^{2n_x} \qquad\qquad X_1(\alpha(t)) \in \mathbb{R}^{2n_x \times (n_x+n_u)}$$

$$X_2(\alpha(t)) \in \mathbb{R}^{n_w \times (n_x+n_u)} \qquad\qquad X_3(\alpha(t)) \in \mathbb{R}^{(n_x+n_u)\times(n_x+n_u)}$$

for all $\alpha \in \mathcal{T}$, $t \in \mathbb{T}$, such that the parameter-dependent LMI

$$R_{\Psi,\infty}(\alpha(t))' \begin{bmatrix} \Phi(\alpha(t)) & 0 & 0 \\ 0 & -\gamma I & 0 \\ 0 & 0 & I \end{bmatrix} R_{\Psi,\infty}(\alpha(t)) +$$

$$\mathrm{He}\left\{ \begin{bmatrix} X_1(\alpha(t)) \\ X_2(\alpha(t)) \\ X_3(\alpha(t)) \end{bmatrix} \begin{bmatrix} \Upsilon(\alpha(t))\tilde{C}_y(\alpha(t)) & \Upsilon(\alpha(t))\tilde{D}_{yw}(\alpha(t)) & -I \end{bmatrix} \right\} \prec 0 \quad (3.9)$$

is feasible for all $\alpha \in \mathcal{T}$, $t \in \mathbb{T}$, where $\Phi = \Phi_{\mathrm{c}}$ in continuous time and $\Phi = \Phi_{\mathrm{d}}$ in discrete time.

Proof. See Appendix A.6. □

3.3.2 $\mathcal{H}_2$ performance

A novel extended $\mathcal{H}_2$ performance characterization for the LPD system (3.1) in closed-loop with a given fixed-order controller (3.2) is presented now.

Theorem 7 (Extended $\mathcal{H}_2$ performance). *Let $\Psi(\alpha(t)) \in \mathbb{R}^{(n_x+n_u)\times(n_x+n_y)}$ be an arbitrary bounded matrix for all $\alpha \in \mathcal{T}$, $t \in \mathbb{T}$, and let $\Theta_{\mathrm{a}}(\alpha(t)) \in \mathbb{R}^{(n_x+n_u)\times(n_x+n_y)}$ be constructed from $\Theta(\alpha) \in \mathbb{R}^{(q+n_u)\times(q+n_y)}$ by adding exponentially stable uncontrollable and/or unobservable dynamics. Furthermore, assume that $\mathcal{D}_\Theta(\alpha) = 0$ for all $\alpha \in \mathcal{T}$. Then, the closed-loop system H_Θ, defined as in (3.4), is exponentially stable and*

$$\|H_\Theta\|_2^2 < \sup_{\alpha \in \mathcal{T}} \limsup_{T \to \infty} \frac{1}{T}\|I_{n_z}\|_{W(\alpha),[0,T]}^2 \qquad (3.10)$$

if there exist bounded matrices

$$P(\alpha(t)) \in \mathbb{S}_+^{2n_x} \qquad\qquad W(\alpha(t)) \in \mathbb{S}_+^{n_z}$$

$$X_1(\alpha(t)) \in \mathbb{R}^{2n_x \times (n_x+n_u)} \qquad X_2(\alpha(t)) \in \mathbb{R}^{n_w \times (n_x+n_u)}$$

$$X_3(\alpha(t)) \in \mathbb{R}^{(n_x+n_u)\times(n_x+n_u)} \qquad X_4(\alpha(t)) \in \mathbb{R}^{n_z \times (n_x+n_u)}$$

$$X_5(\alpha(t)) \in \mathbb{R}^{2n_x \times (n_x+n_u)} \qquad X_6(\alpha(t)) \in \mathbb{R}^{n_w \times (n_x+n_u)}$$

for all $\alpha \in \mathcal{T}$, $t \in \mathbb{T}$, such that the parameter-dependent LMIs

$$R_{\Psi,2}(\alpha(t))' \begin{bmatrix} \Phi(\alpha(t)) & 0 \\ 0 & -I \end{bmatrix} R_{\Psi,2}(\alpha(t)) +$$

$$\mathrm{He}\left\{ \begin{bmatrix} X_1(\alpha(t)) \\ X_2(\alpha(t)) \\ X_3(\alpha(t)) \end{bmatrix} \begin{bmatrix} \Upsilon(\alpha(t))\tilde{C}_y(\alpha(t)) & \Upsilon(\alpha(t))\tilde{D}_{yw}(\alpha(t)) & -I \end{bmatrix} \right\} \prec 0 \quad (3.11a)$$

$$\begin{bmatrix} W(\alpha(t)) & \mathcal{C}_\Psi(\alpha(t)) & \tilde{D}_{zu}(\alpha(t)) \\ \star & P(\alpha(t)) & 0 \\ \star & \star & 0 \end{bmatrix} +$$

$$\mathrm{He}\left\{ \begin{bmatrix} X_4(\alpha(t)) \\ X_5(\alpha(t)) \\ X_6(\alpha(t)) \end{bmatrix} \begin{bmatrix} 0 & \Upsilon(\alpha(t))\tilde{C}_y(\alpha(t)) & -I \end{bmatrix} \right\} \succ 0 \quad (3.11b)$$

are feasible for all $\alpha \in \mathcal{T}$, $t \in \mathbb{T}$, where $\Phi = \Phi_{\mathrm{c}}$ in continuous time and $\Phi = \Phi_{\mathrm{d}}$ in discrete time.

Proof. See Appendix A.7. $\qquad\qquad\qquad\qquad\qquad\qquad\qquad\qquad\qquad\qquad$ $\square$

The following remark provides an extension of Theorem 7, incorporating discrete-time LPD systems that are not strictly proper (see also Remark 1 on page 15).

Remark 3. *In case of a discrete-time LPD system H_Θ (see (3.4) on page 31) that is not strictly proper (i.e., $\mathcal{D}_\Theta(\alpha) \neq 0$), the LMI (3.11b) should be replaced with*

$$\begin{bmatrix} W(\alpha) & \mathcal{C}_\Psi(\alpha) & \mathcal{D}_\Psi(\alpha) & \tilde{D}_{zu}(\alpha) \\ \star & P(\alpha) & 0 & 0 \\ \star & \star & I & 0 \\ \star & \star & 0 & 0 \end{bmatrix} +$$

$$\mathrm{He}\left\{ \begin{bmatrix} X_4(\alpha) \\ X_5(\alpha) \\ X_6(\alpha) \\ X_7(\alpha) \end{bmatrix} \begin{bmatrix} 0 & \Upsilon(\alpha)\tilde{C}_y(\alpha) & \Upsilon(\alpha)\tilde{D}_{yw}(\alpha) & -I \end{bmatrix} \right\} \succ 0 \,,$$

which, after elimination of $X_4(\alpha), \ldots, X_7(\alpha)$ using the projection lemma (see Appendix B.2), and subsequent application of the Schur complement (see Appendix B.1), is equivalent to

$$\begin{bmatrix} W(\alpha) - \mathcal{D}_\Theta(\alpha)\mathcal{D}_\Theta(\alpha)' & \mathcal{C}_\Theta(\alpha) \\ \star & P(\alpha) \end{bmatrix} \succ 0 \,.$$

The latter matrix inequality is similar to the LMI presented in Remark 1 on page 15.

Briefly speaking, Theorem 6 and Theorem 7 provide parameter-dependent sufficient LMIs for $\mathcal{H}_\infty$, respectively, $\mathcal{H}_2$ performance analysis of the LPD system (2.1) in closed loop with a given fixed-order LPD controller (3.2). In fact, these analysis LMIs are equivalent to the analysis conditions presented in Theorem 3, respectively, Theorem 5, applied to a given closed-loop LPD system (3.4). This is seen by applying the projection lemma (see Appendix B.2) to eliminate the slack variables $X_j(\alpha)$ in the LMIs (3.9) and (3.11). It is worth to emphasize that the choice of $\Psi(\alpha)$ is irrelevant in the analysis LMIs (3.9) and (3.11). However, the synthesis LMIs that are presented next require a *stabilizing* controller $\Psi(\alpha)$, see the discussion below Theorem 9 on page 37.

3.4   Fixed-order synthesis conditions

This section presents a novel framework of parameter-dependent sufficient LMIs to design fixed-order controllers of the form (3.2) for the LPD system (3.1),

such that the closed-loop system is exponentially stable and satisfies one or more $\mathcal{H}_\infty$ and/or $\mathcal{H}_2$ performance specifications for all parameter trajectories $\alpha \in \mathcal{T}$, $t \in \mathbb{T}$. This approach is based on the extended $\mathcal{H}_\infty$ and $\mathcal{H}_2$ performance characterizations derived in the previous section, and requires a set of *stabilizing* full-order controllers

$$\Psi_j(\alpha(t)) \in \mathbb{R}^{(n_x+n_u)\times(n_x+n_y)}, \quad \alpha \in \mathcal{T},\ t \in \mathbb{T},\ j \in \mathcal{S},$$

defined as in (3.3), where each index j corresponds to a performance specification and $\mathcal{S} \subset \mathbb{N}_+$ denotes the set of performance indices. The full-order controllers $\Psi_j(\alpha)$ should be computed a priori using, for instance, the convex approaches discussed in [7, 28, 32, 41, 103] (see Section 2.3 on page 16).

After presenting parameter-dependent sufficient LMIs for single-objective fixed-order $\mathcal{H}_\infty$ and $\mathcal{H}_2$ synthesis in Section 3.4.1, respectively, Section 3.4.2, the extension to multi-objective fixed-order control problems is provided in Section 3.4.3.

3.4.1 $\mathcal{H}_\infty$ performance

The following theorem presents a parameter-dependent sufficient LMI to design fixed-order $\mathcal{H}_\infty$ controllers (3.2) for the LPD system (3.1). Hence, feasibility of this parameter-dependent LMI guarantees that the closed-loop system (3.4) is exponentially stable and satisfies an upper bound on the closed-loop $\mathcal{H}_\infty$ performance for all parameter trajectories $\alpha \in \mathcal{T}$, $t \in \mathbb{T}$.

Theorem 8 (Fixed-order $\mathcal{H}_\infty$ synthesis)**.** *Let* $\Psi(\alpha(t)) \in \mathbb{R}^{(n_x+n_u)\times(n_x+n_y)}$, *defined as in* (3.3), *parameterize a stabilizing full-order controller for the LPD system* (3.1), *and let* $\mathcal{A}_\Psi(\alpha)$, $\mathcal{B}_\Psi(\alpha)$, $\mathcal{C}_\Psi(\alpha)$ *and* $\mathcal{D}_\Psi(\alpha)$ *denote the corresponding closed-loop matrices, as in* (3.4)*. For a predefined controller order* q $(0 \leq q \leq n_x)$, *let* $A_{22}(\alpha(t)) \in \mathbb{R}^{(n_x-q)\times(n_x-q)}$ *correspond to exponentially stable dynamics. If there exist bounded matrices*

$$P(\alpha(t)) \in \mathbb{S}_+^{2n_x},$$

$$\bar{\Theta}(\alpha) = \begin{bmatrix} \bar{\Theta}_{11}(\alpha) & \bar{\Theta}_{12}(\alpha) & \bar{\Theta}_{13}(\alpha) \\ 0 & 0_{(n_x-q)\times(n_x-q)} & 0 \\ \bar{\Theta}_{21}(\alpha) & \bar{\Theta}_{22}(\alpha) & \bar{\Theta}_{23}(\alpha) \end{bmatrix} \tag{3.12}$$

with $\bar{\Theta}_{11}(\alpha(t)) \in \mathbb{R}^{q\times q}$, $\bar{\Theta}_{12}(\alpha(t)) \in \mathbb{R}^{q\times(n_x-q)}$, *and* $\bar{\Theta}_{23}(\alpha(t)) \in \mathbb{R}^{n_u\times n_y}$, *and*

$$Y(\alpha) = \begin{bmatrix} Y_{11}(\alpha) & Y_{12}(\alpha) & Y_{13}(\alpha) \\ 0 & Y_{22}(\alpha) & 0 \\ Y_{31}(\alpha) & Y_{32}(\alpha) & Y_{33}(\alpha) \end{bmatrix} \tag{3.13}$$

with $Y_{11}(\alpha(t)) \in \mathbb{R}^{q \times q}$, $Y_{22}(\alpha(t)) \in \mathbb{R}^{(n_x - q) \times (n_x - q)}$, and $Y_{33}(\alpha(t)) \in \mathbb{R}^{n_u \times n_u}$, for all $\alpha \in \mathcal{T}$, $t \in \mathbb{T}$, such that the parameter-dependent LMI

$$R_{\Psi,\infty}(\alpha(t))' \begin{bmatrix} \Phi(\alpha(t)) & 0 & 0 \\ 0 & -\gamma I & 0 \\ 0 & 0 & I \end{bmatrix} R_{\Psi,\infty}(\alpha(t)) +$$

$$\mathrm{He} \left\{ \begin{bmatrix} 0 \\ 0 \\ I \end{bmatrix} \begin{bmatrix} Z(\alpha(t))\tilde{C}_y(\alpha(t)) & Z(\alpha(t))\tilde{D}_{yw}(\alpha(t)) & -Y(\alpha(t)) \end{bmatrix} \right\} \prec 0 \quad (3.14)$$

is feasible for all $\alpha \in \mathcal{T}$, $t \in \mathbb{T}$, with

$$Z(\alpha) := \bar{\Theta}(\alpha) + Y(\alpha) \left(\begin{bmatrix} 0_{q \times q} & 0 & 0 \\ 0 & A_{22}(\alpha) & 0 \\ 0 & 0 & 0_{n_u \times n_y} \end{bmatrix} - \Psi(\alpha) \right), \quad (3.15)$$

where $\Phi = \Phi_\mathrm{c}$ in continuous time and $\Phi = \Phi_\mathrm{d}$ in discrete time, then the fixed-order controller parameterized by

$$\Theta(\alpha) = \begin{bmatrix} Y_{11}(\alpha) & Y_{13}(\alpha) \\ Y_{31}(\alpha) & Y_{33}(\alpha) \end{bmatrix}^{-1} \begin{bmatrix} \bar{\Theta}_{11}(\alpha) & \bar{\Theta}_{13}(\alpha) \\ \bar{\Theta}_{21}(\alpha) & \bar{\Theta}_{23}(\alpha) \end{bmatrix} \quad (3.16)$$

stabilizes the LPD system (3.1) with a guaranteed bound $\|H_\Theta\|_\infty < \sqrt{\gamma}$ on the closed-loop $\mathcal{H}_\infty$ performance.

Proof. See Appendix A.8. □

3.4.2 $\mathcal{H}_2$ performance

Parameter-dependent sufficient LMIs to design fixed-order $\mathcal{H}_2$ controllers (3.2) for the LPD system (3.1) are presented next. Thus, whenever these parameter-dependent LMIs are feasible, the closed-loop system (3.4) is exponentially stable and satisfies an upper bound on the closed-loop $\mathcal{H}_2$ performance for all parameter trajectories $\alpha \in \mathcal{T}$, $t \in \mathbb{T}$.

Theorem 9 (Fixed-order $\mathcal{H}_2$ synthesis). *Consider the LPD system (3.1), and assume that $D_{zw}(\alpha) = 0$, and that $D_{zu}(\alpha) = 0$ or $D_{yw}(\alpha) = 0$, for all $\alpha \in \mathcal{T}$. Let $\Psi(\alpha(t)) \in \mathbb{R}^{(n_x + n_u) \times (n_x + n_y)}$, defined as in (3.3), parameterize a stabilizing full-order controller for the LPD system (3.1), and let $\mathcal{A}_\Psi(\alpha)$, $\mathcal{B}_\Psi(\alpha)$, $\mathcal{C}_\Psi(\alpha)$ and $\mathcal{D}_\Psi(\alpha)$ denote the corresponding closed-loop matrices, as in (3.4). For*

a predefined controller order q $(0 \leq q \leq n_x)$, let $A_{22}(\alpha(t)) \in \mathbb{R}^{(n_x-q) \times (n_x-q)}$ correspond to exponentially stable dynamics. If there exist bounded matrices

$$P(\alpha(t)) \in \mathbb{S}^{2n_x}_+ \qquad\qquad W(\alpha(t)) \in \mathbb{S}^{n_z}_+$$

$$\bar{\Theta}(\alpha(t)) \in \mathbb{R}^{(q+n_u) \times (n_x+n_y)} \qquad Y(\alpha(t)) \in \mathbb{R}^{(n_x+n_u) \times (n_x+n_u)}$$

for all $\alpha \in \mathcal{T}$, $t \in \mathbb{T}$, where $\bar{\Theta}(\alpha)$ and $Y(\alpha)$ are as in (3.12), respectively, (3.13), such that the parameter-dependent LMIs

$$R_{\Psi,2}(\alpha(t))' \begin{bmatrix} \Phi(\alpha(t)) & 0 & 0 \\ 0 & -\gamma I & 0 \\ 0 & 0 & I \end{bmatrix} R_{\Psi,2}(\alpha(t)) +$$

$$\mathrm{He}\left\{ \begin{bmatrix} 0 \\ 0 \\ I \end{bmatrix} \begin{bmatrix} Z(\alpha(t))\tilde{C}_y(\alpha(t)) & Z(\alpha(t))\tilde{D}_{yw}(\alpha(t)) & -Y(\alpha(t)) \end{bmatrix} \right\} \prec 0 \quad (3.17a)$$

$$\begin{bmatrix} W(\alpha(t)) & \mathcal{C}_\Psi(\alpha(t)) & \tilde{D}_{zu}(\alpha(t)) \\ \star & P(\alpha(t)) & 0 \\ \star & \star & 0 \end{bmatrix} +$$

$$\mathrm{He}\left\{ \begin{bmatrix} 0 \\ 0 \\ I \end{bmatrix} \begin{bmatrix} 0 & -Z(\alpha(t))\tilde{C}_y(\alpha(t)) & Y(\alpha(t)) \end{bmatrix} \right\} \succ 0 \quad (3.17b)$$

are feasible for all $\alpha \in \mathcal{T}$, $t \in \mathbb{T}$, with $Z(\alpha)$ as in (3.15), where $\Phi = \Phi_c$ in continuous time and $\Phi = \Phi_d$ in discrete time, then the fixed-order controller parameterized by (3.16) stabilizes the LPD system (3.1) with a guaranteed bound

$$\|H_\Theta\|_2^2 < \sup_{\alpha \in \mathcal{T}} \limsup_{T \to \infty} \frac{1}{T} \|I_{n_z}\|_{W(\alpha),[0,T]}^2$$

on the closed-loop $\mathcal{H}_2$ performance.

Proof. See Appendix A.9. □

The fixed-order $\mathcal{H}_2$ synthesis conditions presented in Theorem 9 can be adapted to take into account nonzero feedthrough matrices, as discussed in the following remark.

Remark 4 (Nonzero feedthrough matrices). *The assumptions $D_{zw}(\alpha) = 0$, and $D_{zu}(\alpha) = 0$ or $D_{yw}(\alpha) = 0$, assure a finite $\mathcal{H}_2$ norm of the closed-loop system in the continuous-time case. While, in continuous time, the fixed-order $\mathcal{H}_2$ synthesis LMIs (3.17) require $D_{zw}(\alpha) = 0$, the case $D_{zu}(\alpha) \neq 0$ and $D_{yw}(\alpha) \neq 0$ is handled as follows:*

1. *Design a strictly proper stabilizing full-order controller (i.e., $D_c(\alpha) = 0$), using, for instance, one of the convex approaches [7, 28, 32, 41, 103].*

2. *Impose the following constraints on the LMI variables (3.12) and (3.13):*

$$\bar{\Theta}_{23}(\alpha) = 0, \quad Y_{31}(\alpha) = 0.$$

To see this, note that according to (3.16) we have

$$\bar{\Theta}_{23}(\alpha) = Y_{31}(\alpha)B_c(\alpha) + Y_{33}(\alpha)D_c(\alpha).$$

Consequently, the above constraints imply that $Y_{33}(\alpha)D_c(\alpha) = 0$. Finally, positive definiteness of $\mathrm{He}\{Y_{33}(\alpha)\}$ results in $D_c(\alpha) = 0$ whenever the LMIs (3.17) are feasible for all $\alpha \in \mathcal{T}$, $t \in \mathbb{T}$, such that from (3.6) and $D_{zw}(\alpha) = 0$ we obtain $\mathcal{D}_\Theta(\alpha) = 0$.

In the discrete-time case, $D_{zw}(\alpha)$, $D_{zu}(\alpha)$ and $D_{yw}(\alpha)$ are all allowed to be nonzero. Then, the LMI (3.17b) should be replaced with

$$\begin{bmatrix} W(\alpha) & \mathcal{C}_\Psi(\alpha) & \mathcal{D}_\Psi(\alpha) & \tilde{D}_{zu}(\alpha) \\ \star & P(\alpha) & 0 & 0 \\ \star & \star & I & 0 \\ \star & \star & \star & 0 \end{bmatrix} +$$

$$\mathrm{He}\left\{ \begin{bmatrix} 0 \\ 0 \\ I \end{bmatrix} \begin{bmatrix} 0 & -Z(\alpha)\tilde{C}_y(\alpha) & -Z(\alpha)\tilde{D}_{yw}(\alpha) & Y(\alpha) \end{bmatrix} \right\} \succ 0.$$

The synthesis conditions (3.14) and (3.17) feature additional conservatism compared to the analysis conditions (3.9) and (3.11), respectively. Namely, structural constraints are imposed on the slack variables $X_j(\alpha)$ in (3.9) and (3.11) to arrive at convex synthesis conditions, which is made more precise in the following remark.

Remark 5 (Structural constraints synthesis LMIs). *The derivation of the fixed-order $\mathcal{H}_\infty$ synthesis LMI (3.14) relies on the specific selections*

$$X_1(\alpha) = 0, \qquad X_2(\alpha) = 0, \qquad X_3(\alpha) = Y(\alpha)$$

in the analysis condition (3.9)*. Similarly,*

$$X_1(\alpha) = 0, \qquad X_2(\alpha) = 0, \qquad X_3(\alpha) = Y(\alpha)$$

$$X_4(\alpha) = 0, \qquad X_5(\alpha) = 0, \qquad X_6(\alpha) = -Y(\alpha)$$

are selected in the analysis conditions (3.11) *to arrive at the fixed-order* $\mathcal{H}_2$ *synthesis LMIs* (3.17)*. Using* (3.7) *and imposing the specific structure* (3.13) *on* $Y(\alpha)$*, these particular choices allow the reconstruction of a fixed-order LPD controller through the nonlinear transformation* (3.16)*.*

By making the specific choices as discussed in Remark 5, feasibility of the parameter-dependent LMI (3.14) (LMIs (3.17)) for all $\alpha \in \mathcal{T}$, $t \in \mathbb{T}$, implies that the closed-loop system H_Ψ is exponentially stable and satisfies the $\mathcal{H}_\infty$ performance bound $\|H_\Psi\|_\infty < \sqrt{\gamma}$ (the $\mathcal{H}_2$ performance bound (3.10)). This is seen by eliminating $Y(\alpha)$ using the projection lemma. Hence, a stabilizing controller $\Psi(\alpha)$ is required to compute a stabilizing fixed-order LPD controller, as illustrated in Figure 3.3 on page 43. Furthermore, note that a full-order controller $\Psi(\alpha)$ with a good closed-loop $\mathcal{H}_\infty$ ($\mathcal{H}_2$) performance should be selected in the fixed-order synthesis LMI (3.14) (LMIs (3.17)) to obtain a fixed-order controller with a good $\mathcal{H}_\infty$ ($\mathcal{H}_2$) performance *bound*. At the same time, it should be emphasized that the fixed-order synthesis conditions potentially result in a fixed-order LPD controller with an *actual* performance which is potentially better than the performance of $\Psi(\alpha)$, see Section 4.4.2.

Controller parameterization It is remarked that all the optimization variables in (3.14) and (3.17) are allowed to be parameter-dependent. Therefore, by imposing a specific parameterization on the LMI variables

$$\bar{\Theta}_{11}(\alpha), \quad \bar{\Theta}_{13}(\alpha), \quad \bar{\Theta}_{21}(\alpha), \quad \bar{\Theta}_{23}(\alpha), \tag{3.18a}$$

$$Y_{11}(\alpha), \quad Y_{13}(\alpha), \quad Y_{31}(\alpha), \quad Y_{33}(\alpha), \tag{3.18b}$$

it is clear from (3.16) that any desired parameterization of the fixed-order controller can be freely selected. For example, a polynomial parameter dependency is enforced on the fixed-order LPD controller when the LMI variables (3.18a) are chosen polynomially parameter-dependent and (3.18b) are taken constant.

Two extensions of the fixed-order synthesis LMIs are discussed now, demonstrating their flexibility and generality.

Strictly proper fixed-order controller design The fixed-order $\mathcal{H}_\infty$ and $\mathcal{H}_2$ synthesis LMIs (3.14) and (3.17) allow the design of strictly proper fixed-order
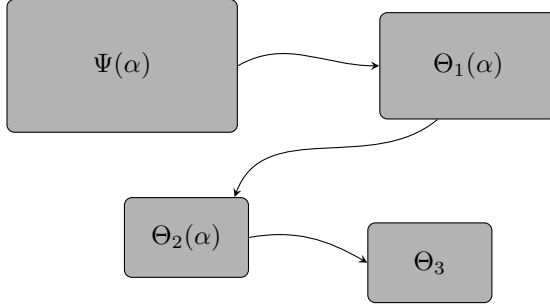
Figure 3.2: Starting from a stabilizing full-order LPD controller $\Psi(\alpha)$, the fixed-order synthesis LMIs can be iteratively applied to gradually decrease the controller order. For example, the figure indicates how a fixed-order robust controller Θ_3 can be computed in 3 steps. Namely, by first reducing the number of controller states twice, and subsequently simplifying the controller parameter dependency once.

controllers (i.e. $D_{\mathrm{c}}(\alpha) = 0$), by imposing structural constraints on some of the LMI variables. Namely, imposing the constraints $\bar{\Theta}_{23}(\alpha) = 0$ and $Y_{31}(\alpha) = 0$ in Theorem 8 and Theorem 9, a strictly proper fixed-order controller results whenever the corresponding parameter-dependent LMIs are feasible. See also Remark 4 on page 39.

Iterative controller order reduction Theorem 8 and Theorem 9 can be generalized in the following way. Given a set of fixed-order controllers

$$\Psi_j(\alpha(t)) \in \mathbb{R}^{(p+n_u) \times (p+n_y)}, \quad \alpha \in \mathcal{T}, \ t \in \mathbb{T}, \ j \in \mathcal{S},$$

where $0 \leq p \leq n_x$, corresponding to controllers of order p, a controller of order q $(0 \leq q < p)$ can be designed. The dimensions of the LMI parameters/variables generalize as follows:

$$P(\alpha(t)) \in \mathbb{S}^{n_x+p}, \quad \bar{\Theta}_{12}(\alpha(t)) \in \mathbb{R}^{q \times (p-q)}, \quad Y_{22}(\alpha(t)) \in \mathbb{R}^{(p-q) \times (p-q)},$$

and $A_{22}(\alpha(t)) \in \mathbb{R}^{(p-q) \times (p-q)}$. This generalization therefore allows iterative application of Theorem 8 and Theorem 9 for fixed-order controller design, such that both the number of controller states and the complexity of the controller parameterization can be gradually reduced. Figure 3.2 illustrates this concept of iterative controller order reduction.

3.4.3 Multi-objective control

For many practical applications, imposing multiple (usually conflicting) control design objectives is desired. Therefore, this section explains how the synthesis conditions (3.14) and (3.17) are adapted to handle multi-objective $\mathcal{H}_\infty/\mathcal{H}_2$ control problems. Such problems include, for instance, the minimization of an $\mathcal{H}_\infty$ performance bound subject to an $\mathcal{H}_2$ performance bound, or minimization of a weighted combination of different performance bounds.

Each performance specification is labeled by an index $j \in \mathcal{S}$, where $\mathcal{S} \subset \mathbb{N}_+$ is the set containing the indices of all performance specifications. Similarly, $\mathcal{S}_{\mathcal{H}_\infty}$ and $\mathcal{S}_{\mathcal{H}_2}$ denote the sets of indices associated with $\mathcal{H}_\infty$, respectively, $\mathcal{H}_2$ performance specifications. Each performance specification $j \in \mathcal{S}$ is imposed by appropriately defining selection matrices L_j and R_j and selecting an input-output channel $w_j \to z_j$ of the LPD system (3.1) as follows

$$\begin{cases} \delta x &=& A(\alpha)x &+& B_w(\alpha)w_j &+& B_u(\alpha)u, \\ z_j &=& L_j C_z(\alpha)x &+& L_j D_w(\alpha)w_j &+& L_j D_u(\alpha)u, \\ y &=& C_y(\alpha)x &+& D_y(\alpha)w_j \end{cases}$$

where $w_j := R_j w$ and $z_j := L_j z$. Denoting the closed-loop system corresponding to performance channel $j \in \mathcal{S}$ by

$$H_{\Theta,j} : \begin{cases} \delta x_{\mathrm{cl}} &=& \mathcal{A}_\Theta(\alpha)x_{\mathrm{cl}} &+& \mathcal{B}_{\Theta,j}(\alpha)w_j, \\ z_j &=& \mathcal{C}_{\Theta,j}(\alpha)x_{\mathrm{cl}} &+& \mathcal{D}_{\Theta,j}(\alpha)w_j, \end{cases} \tag{3.19}$$

with $\mathcal{B}_{\Theta,j}(\alpha) = \mathcal{B}_\Theta(\alpha)R_j$, $\mathcal{C}_{\Theta,j}(\alpha) = L_j \mathcal{C}_\Theta(\alpha)$, and $\mathcal{D}_{\Theta,j}(\alpha) = L_j \mathcal{D}_\Theta(\alpha)R_j$, the synthesis conditions (3.14) (for $j \in \mathcal{S}_{\mathcal{H}_\infty}$) and (3.17) (for $j \in \mathcal{S}_{\mathcal{H}_2}$) are imposed for each of the LPD systems (3.19), $j \in \mathcal{S}$. The performance bounds are accordingly denoted by γ_j, $j \in \mathcal{S}_{\mathcal{H}_\infty}$ and μ_j, $j \in \mathcal{S}_{\mathcal{H}_2}$.

Since the reconstructed multi-objective controller depends on the LMI variables (3.18) (see (3.16)), these optimization variables are chosen identical for all $j \in \mathcal{S}$, introducing additional conservatism with respect to single-objective synthesis. However, the remaining variables are chosen differently for each performance specification. That is, we define the parameter-dependent matrices

$$P_j(\alpha), \quad \bar{\Theta}_{12,j}(\alpha), \quad \bar{\Theta}_{22,j}(\alpha), \quad Y_{12,j}(\alpha), \quad Y_{22,j}(\alpha), \quad Y_{32,j}(\alpha)$$

for $j \in \mathcal{S}$, and moreover $W_j(\alpha)$ for $j \in \mathcal{S}_{\mathcal{H}_2}$, since convexity is then retained while keeping conservatism to a minimum. It is clear that the presented convex framework for fixed-order controller synthesis also allows a different initial controller $\Psi_j(\alpha)$ for each $j \in \mathcal{S}$ (see page 36). This concept is illustrated in Figure 3.3, showing how two full-order LPD controllers are combined to compute a multi-objective fixed-order LPD controller.

$\mathcal{H}_\infty$ performance $\mathcal{H}_2$ performance

full-order
controller design

$\Psi_1(\alpha)$

$\Psi_2(\alpha)$

fixed-order
controller design

$\Theta(\alpha)$
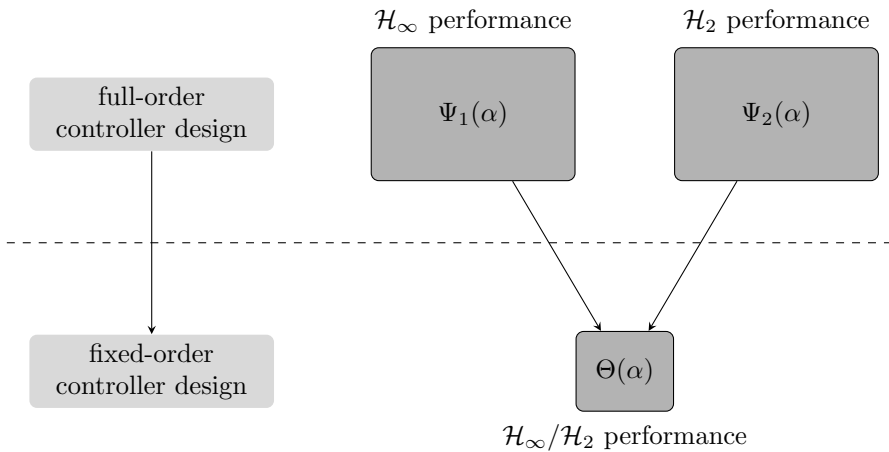
$\mathcal{H}_\infty/\mathcal{H}_2$ performance

Figure 3.3: The fixed-order synthesis conditions require a stabilizing full-order LPD controller for each performance specification. For example, to compute a fixed-order controller with a guaranteed closed-loop $\mathcal{H}_\infty/\mathcal{H}_2$ performance, the set of full-order controllers should be composed of two full-order controllers satisfying an $\mathcal{H}_\infty$, respectively, $\mathcal{H}_2$ performance.

3.5   Summary

This chapter has presented a projection lemma based framework of sufficient LMIs to design fixed-order multi-objective controllers for the general class of LPD systems. Starting from novel extended $\mathcal{H}_\infty$ and $\mathcal{H}_2$ analysis LMIs, that rely on linking the fixed-order controller to an arbitrary full-order controller for the same system, sufficient LMIs for fixed-order synthesis were derived. These synthesis conditions require an a priori computed stabilizing full-order controller for each performance specification (see Figure 3.3 on page 43), and thus allow the design of fixed-order multi-objective $\mathcal{H}_\infty/\mathcal{H}_2$ controllers. Various extensions of the synthesis conditions were proposed, such as the design of strictly proper controllers and an iterative approach to gradually decrease the controller order (see Figure 3.2 on page 41), demonstrating their generality and flexibility.

The potential of the fixed-order controller design approach for different subclasses of LPD systems (see Table 2.1 on page 9 for an overview) is confirmed by numerical and experimental validations in the following chapters.

RECAPITULATION

- The fixed-order controller synthesis problem is nonconvex, even for LTI systems.

- Using the projection lemma, extended LMIs for closed-loop $\mathcal{H}_\infty$ and $\mathcal{H}_2$ performance analysis of a given fixed-order controller are derived, by expressing the closed-loop matrices as a function of an arbitrary full-order controller for the same system.

- By imposing structural constraints on the variables in the extended analysis LMIs, sufficient LMIs are derived to design fixed-order (multi-objective) $\mathcal{H}_\infty/\mathcal{H}_2$ controllers for LPD systems, requiring an a priori computed stabilizing full-order controller for each performance specification.

- The fixed-order synthesis LMIs allow the design of strictly proper controllers.

- Iterative application of the fixed-order synthesis LMIs is possible, such that the controller order can be gradually decreased.

Chapter 4

Fixed-order controller design for LTI systems

Focusing on LTI dynamics, this chapter presents numerical and experimental validations of the fixed-order controller design approach presented in Chapter 3. The existence of a convex reformulation of the fixed-order $\mathcal{H}_\infty/\mathcal{H}_2$ controller design problem for LTI systems is unknown, even when only one performance specification is imposed. Despite this fact, it is demonstrated that our approach allows the computation of fixed-order $\mathcal{H}_\infty$ and $\mathcal{H}_2$ controllers featuring similar closed-loop performance as an optimal full-order $\mathcal{H}_\infty$ or $\mathcal{H}_2$ controller. For the multi-objective case, it is shown how fixed-order $\mathcal{H}_\infty/\mathcal{H}_2$ controllers are computed which are less conservative than full-order designs resulting from well-known LMI approaches. The latter is achieved by exploiting the freedom to use a different full-order controller for each performance specification in our fixed-order LMI framework. Various comparisons with existing fixed-order controller design approaches illustrate the potential of our framework of sufficient LMIs applied to LTI systems.

4.1   Introduction

The existence of a convex reformulation of the fixed-order $\mathcal{H}_\infty/\mathcal{H}_2$ controller design problem for LTI systems is unknown, even when only one performance specification is imposed [97, 103, 116]. Despite the lack of such a convex condition, several approaches have been developed for reduced-order controller design [50]. Those include solving the nonconvex problem directly [116], solving

a nonconvex reformulation in terms of an LMI plus a rank constraint [40, 44, 89], or setting up convex sufficient conditions [3, 51, 77, 118].

The approach presented in Chapter 3 belongs to the last category, and is inspired by the works [1–3], where an LMI procedure consisting of two stages is proposed to design fixed-order controllers satisfying one or more closed-loop $\mathcal{H}_\infty/\mathcal{H}_2$ performance specifications. In this procedure, a stabilizing state feedback for an augmented system is designed first, and subsequently used as a parameter in a sufficient LMI condition for fixed-order controller design. A fixed-order controller results whenever the LMI optimization problem is feasible. However, the state feedback design in the first step has infinitely many solutions, and the particular solution selected strongly affects the subsequent fixed-order controller design step. In fact, structural constraints need to be imposed on the LMI variables in the state-feedback design step to avoid synthesis of a fixed-order controller that is reducible to a static output feedback [3].

As selecting an appropriate state feedback (in the first step) to obtain high performance fixed-order controllers in the second step is not trivial, we apply the novel approach presented in Chapter 3, starting from a set of full-order $\mathcal{H}_2/\mathcal{H}_\infty$ controllers (for the original system), and explain how to intuitively select this set of full-order controllers. Given such a set of feedback controllers, it is numerically demonstrated how to compute high performance fixed-order $\mathcal{H}_\infty/\mathcal{H}_2$ controllers. As illustrated for a fixed-order $\mathcal{H}_\infty$ control example in Section 4.3, the computation of a fixed-order controller can either be performed in one step or by successive reduction of the controller order (see page 41 and Figure 3.2 on page 41).

Since the Lyapunov and G shaping paradigms for full-order multi-objective controller design correspond to sufficient conditions (see Section 2.3.1 on page 18), a reduction of conservatism for these designs using the proposed fixed-order synthesis LMIs is investigated in Section 4.4. Numerical comparisons show that, by exploiting the freedom to use a different full-order controller parameter for each performance specification, fixed-order multi-objective controllers are computed which are less conservative than full-order Lyapunov shaping (continuous time) and G shaping (discrete time) designs.

The practical viability of the fixed-order controller design approach is confirmed by experimental validations on a lab-scale overhead crane with a fixed cable length, presented in Section 4.5.

4.2 Problem formulation

Consider the finite-dimensional LPD state-space model (3.1) (see page 30), and assume that the parameter α is a priori known and constant. In other words, the system dynamics are unaffected by parameters. Then, the dynamics under consideration are LTI (see Table 2.1 on page 9), and hence take the form

$$
\left\{
\begin{array}{rcccccc}
\delta x & = & Ax & + & B_w w & + & B_u u, \\
z & = & C_z x & + & D_{zw} w & + & D_{zu} u, \\
y & = & C_y x & + & D_{yw} w & &
\end{array}
\right.
\tag{4.1}
$$

with state $x : \mathbb{T} \to \mathbb{R}^{n_x}$, exogenous input $w : \mathbb{T} \to \mathbb{R}^{n_w}$, control input $u : \mathbb{T} \to \mathbb{R}^{n_u}$, regulated output $z : \mathbb{T} \to \mathbb{R}^{n_z}$ and measured output $y : \mathbb{T} \to \mathbb{R}^{n_y}$, where all system matrices are real, constant, and have appropriate dimensions.

The aim is to design fixed-order dynamic output feedback LTI controllers

$$
\left\{
\begin{array}{rcccc}
\delta x_c & = & A_c x_c & + & B_c y, \\
u & = & C_c x_c & + & D_c y,
\end{array}
\right.
\tag{4.2}
$$

with $x_c \in \mathbb{R}^q$, $q < n_x$, exponentially stabilizing the LTI system (4.1) such that one ore more closed-loop performance specifications are guaranteed. Note that, in contrast to general LPD controllers (3.2) (see page 30), the controller order is now completely characterized by the dimension of the state x_c.

It is emphasized that, since the system (4.1) is unaffected by parameters, the corresponding LMIs for fixed-order $\mathcal{H}_\infty / \mathcal{H}_2$ controller synthesis simplify to parameter-independent conditions. Consequently, the latter conditions are no longer semi-infinite and infinite dimensional, and are thus directly implemented and solved using available software.

4.3 Fixed-order $\mathcal{H}_\infty$ control

In this section, the *AC7* aircraft model from the COMPl$_e$ib library [68, 69] is considered. This 9th order LTI model is discretized using zero-order hold at a sampling period of $0.01s$, which is sufficiently small to capture the system dynamics. The objective is to design fixed-order controllers for the discretized LTI system, optimizing the $\mathcal{H}_\infty$ performance on the input-output channel $w \to z$.

First an optimal full-order $\mathcal{H}_\infty$ controller (4.2) is computed with the approach [103], resulting in the optimal closed-loop $\mathcal{H}_\infty$ norm $4.0 \cdot 10^{-2}$. This full-order $\mathcal{H}_\infty$ controller is substituted for Ψ in the LMI (3.14), for $q = 0, \ldots, 8$, which is

Table 4.1: A comparison between direct/iterative application of Theorem 8 (T8) and the approaches [3, 8, 47] confirms the potential of our approach. For each approach and each controller order q, the bound $\sqrt{\gamma}$ ($\mathcal{H}_\infty$ performance) multiplied by a factor 10^2 is shown. The approach [8, 47] only returns the actual $\mathcal{H}_\infty$ performance.

q	T8 direct	T8 iterative	[3]	[8, 47]
8	4.0 (4.0)	4.0 (4.0)	5.8 (4.3)	4.0
7	4.1 (4.0)	4.1 (4.0)	6.5 (4.7)	4.0
6	4.1 (4.0)	4.1 (4.0)	7.8 (6.5)	4.0
5	5.0 (5.0)	4.1 (4.0)	11.5 (6.5)	4.0
4	5.1 (5.0)	5.0 (5.0)	11.9 (6.5)	4.0
3	5.0 (4.7)	5.5 (5.3)	13.4 (7.4)	5.2
2	11.1 (5.9)	10.4 (6.8)	14.0 (6.7)	4.0
1	8.0 (6.8)	8.7 (6.4)	15.4 (7.1)	6.5
0	43.0 (6.8)	9.6 (6.9)	10.2 (6.6)	6.5

schematically conceptualized in Figure 4.1a on page 49. Subsequently, selecting $A_{22} = 0$ (see Remark 6 on page 53) and minimizing the bound γ yields controllers of order $q = 2, \ldots, 8$, while the LMI (3.14) is infeasible for $q = 0, 1$. However, a feasible solution might be obtained for $q = 0, 1$ by replacing Ψ with a *suboptimal* full-order controller in the LMI (3.14). Therefore, a suboptimal full-order controller is computed by fixing the $\mathcal{H}_\infty$ bound $\sqrt{\gamma}$ in the full-order synthesis LMI to the suboptimal value 0.3 and solving the corresponding feasibility problem, resulting in a closed-loop $\mathcal{H}_\infty$ norm of $6.4 \cdot 10^{-2}$. Substituting this full-order controller for Ψ in the LMI (3.14) for $q = 0, 1$, feasible solutions are obtained. The results are summarized in Table 4.1, showing the controller order in the first column and the bounds $\sqrt{\gamma}$ (closed-loop $\mathcal{H}_\infty$ norms) in the second column. Note that optimal $\mathcal{H}_\infty$ controllers are obtained for $q \geq 6$, since these controllers yield the same closed-loop performance as the optimal full-order $\mathcal{H}_\infty$ controller.

Now fixed-order controllers are computed by iterative application of Theorem 8, see page 41 and Figure 3.2 on page 41. Specifically, starting from a full-order controller Ψ, controllers of order q are computed by substituting the controller of order $q + 1$ in the LMI (3.14) for $q = n_x - 1, \ldots, 0$. The latter approach is visualized in Figure 4.1b. The corresponding results are given in the third column of Table 4.1. It is remarkable that an optimal controller of order 5 is computed, and that the bound corresponding to the design of a static output feedback controller ($q = 0$) significantly improved compared to direct application of Theorem 8 (see Figure 4.1a).

The discrete-time counterpart of the approach discussed in [3], see also [1, 2],

(a) Direct approach   (b) Iterative approach
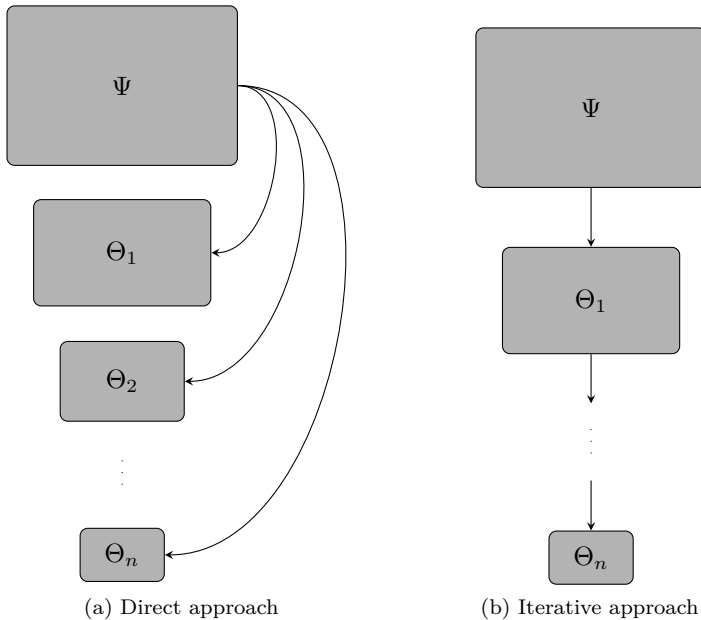
Figure 4.1: Direct (Figure 4.1a) versus iterative (Figure 4.1b) application of the fixed-order synthesis LMI presented in Theorem 8 to compute fixed-order controllers $\Theta_1, \ldots, \Theta_n$ with a guaranteed $\mathcal{H}_\infty$ performance from a full-order $\mathcal{H}_\infty$ controller Ψ.

is applied now. This approach relies on the computation of a state feedback controller for an augmented system, which is subsequently used as a parameter in a sufficient LMI for fixed-order $\mathcal{H}_\infty$ controller design. It is worth to emphasize that a different state feedback controller is required for the computation of controllers of different orders q, whereas our approach allows the use of a single full-order controller to compute fixed-order controllers of different orders. Starting from an optimal $\mathcal{H}_\infty$ state feedback, the approach from [3] returns infeasibility for all orders $q = 0, \ldots, 8$. Therefore, the bound $\sqrt{\gamma} = 4.0 \cdot 10^{-2}$, corresponding to the performance of an optimal full-order controller, is fixed in the LMI for state feedback design, resulting in suboptimal state feedback controllers. The latter controllers are subsequently used for fixed-order controller design. The results are shown in row 4 of Table 4.1. A comparison reveals that, except for $q = 0$, direct and iterative application of Theorem 8 yields controllers with better $\mathcal{H}_\infty$ performance.

The last row of Table 4.1 summarizes the results of the HIFOO package [8, 47]. Since HIFOO can only handle continuous-time models, the continuous-time $AC7$ model is used. Two randomly generated starting points are used, and the

Table 4.2: A comparison between computation times (in seconds) corresponding to Theorem 8 (T8) and HIFOO [8, 47] demonstrates that the former approach is numerically more attractive.

$q:$	8	7	6	5	4	3	2	1	0
T8 direct :	1.00	0.72	0.69	0.78	0.75	0.63	0.39	0.48	0.36
T8 iterative :	0.99	0.75	0.46	0.32	0.34	0.26	0.15	0.17	0.14
[8, 47] :	102	73.0	89.1	59.6	47.2	65.9	43.3	1.56	0.72

option to restrict to the BFGS phase is selected. While HIFOO yields better $\mathcal{H}_\infty$ performance in some cases, our approach provides better results than HIFOO for $q = 3$, and similar results are obtained for $q = 1$ and $q = 5, \ldots, 8$. It should be emphasized that our approach is considerably faster than HIFOO, as Table 4.2 indicates. For each order q specified in the first row, the second row indicates the computation times corresponding to direct application of Theorem 8 (see Figure 4.1a). Note that the time to compute a full-order controller, which is $0.55s$ for the optimal $\mathcal{H}_\infty$ controller, should be added to obtain the total computation time. The third row shows the computation times resulting from iterative application of Theorem 8 (see Figure 4.1b), which are lower for lower controller orders due to fewer LMI rows and variables. In this case, the total computation time follows by adding the computation times of all higher order controllers. It is clear from the last row that, compared to the aforementioned approaches, the computation times of HIFOO are similar for low order controller design, but substantially higher for computation of high order controllers.

4.4 Fixed-order $\mathcal{H}_\infty/\mathcal{H}_2$ control

Two multi-objective fixed-order control problems (continuous and discrete time) are considered next, illustrating how fixed-order controllers can be computed which are less conservative than full-order designs resulting from well-known LMI approaches.

4.4.1 Continuous time academic example

Consider the $AC3$ model from the COMPl$_e$ib library [68, 69]. The aim is to design a fixed-order multi-objective controller for this 5th order aircraft model. Denoting the exogenous input and the regulated output of the $AC3$ model by w and z, respectively, the following performance channels are considered:

$w_1 = w_2 = w$ and $z_1 = z_2 = z$, with $\mathcal{S}_{\mathcal{H}_\infty} = \{1\}$ and $\mathcal{S}_{\mathcal{H}_2} = \{2\}$. The $\mathcal{H}_2$ performance is minimized subject to a bound on the $\mathcal{H}_\infty$ performance.

First, the Lyapunov shaping paradigm (see [103]) is applied to design a full-order controller Ψ, by imposing the $\mathcal{H}_\infty$ performance bound $\|H_{\Psi,1}\|_\infty < b = 3.4$. The obtained controller yields a closed-loop $\mathcal{H}_2$ performance $\|H_{\Psi,2}\|_2 = 5.60$. Subsequently, $\Psi_1 = \Psi_2 = \Psi$, $q = 1$ and $A_{22} = -I$ are selected in the LMIs (3.14) and (3.17) to design a controller Θ of order 1, by minimizing the $\mathcal{H}_2$ bound μ_2 subject to the $\mathcal{H}_\infty$ bound $\sqrt{\gamma_1} < b$. The solution is promising, since the resulting $\mathcal{H}_2$ bound is tight, resulting in similar performance compared to the full-order controller: $\sqrt{\mu_2} = 5.60$ and $\|H_{\Theta,2}\|_2 = 5.60$.

However, by exploiting the freedom of using two different full-order controller parameters Ψ_j, $j = 1, 2$ (see Figure 3.3 on page 43), potentially less conservative fixed-order controllers can be computed. Therefore, the Lyapunov shaping design $\Psi_1 = \Psi$ is substituted in the LMI (3.14) to guarantee the constraint $\sqrt{\gamma_1} < b$, and a second full-order controller Ψ_2 is designed by selecting a higher value for b in the Lyapunov shaping design step, such that better closed-loop $\mathcal{H}_2$ performance compared to Ψ_1 is achieved: $\|H_{\Psi_2,2}\|_2 < \|H_{\Psi_1,2}\|_2$. As a consequence, substitution of Ψ_2 in the $\mathcal{H}_2$ synthesis LMIs (3.17) allows a lower $\mathcal{H}_2$ performance bound in the fixed-order controller design step.

The left part of Figure 4.2 shows the $\mathcal{H}_2$ bound $\sqrt{\mu_2}$ and $\mathcal{H}_2$ performance $\|H_{\Theta,2}\|_2$ for different values of $\|H_{\Psi_2,2}\|_2$. The rightmost point of the subfigures corresponds to the choice $\Psi_2 = \Psi_1 = \Psi$. Gradually improving the closed-loop $\mathcal{H}_2$ performance of Ψ_2 completes the left part of Figure 4.2, revealing that using a controller Ψ_2 with a closed-loop performance $\|H_{\Psi_2,2}\|_2 \approx 4.9$ is optimal in this case: $\|H_{\Theta,2}\|_2 = 5.22$. This corresponds to an improvement of almost 7% in performance compared to the full-order Lyapunov shaping design. Selecting, for example, $\|H_{\Psi_2,2}\|_2 = 5.2$ results in an improvement both in terms of the $\mathcal{H}_2$ bound and the closed-loop $\mathcal{H}_2$ performance: $\sqrt{\mu_2} = 5.48$ and $\|H_{\Theta,2}\|_2 = 5.27$. As can be inferred from the right part of Figure 4.2, the improvement in $\mathcal{H}_2$ performance results in a slight increase of the closed-loop $\mathcal{H}_\infty$ norm.

Figure 4.2: Using different Lyapunov shaping controllers Ψ_j, $j \in \mathcal{S}$, allows the design of fixed-order controllers which are less conservative than a Lyapunov shaping design.

4.4.2 Discrete time academic example

Consider the following LTI system (see Example 4 from [32]):

$$
\begin{aligned}
x(t+1) &= \begin{bmatrix} 2 & 0 & 1 \\ 1 & 0.5 & 0 \\ 0 & 1 & -0.5 \end{bmatrix} x(t) + \begin{bmatrix} 1 & 0 & 0 \\ 0 & 0 & 1 \\ 0 & 0 & 0 \end{bmatrix} w(t) + \begin{bmatrix} 1 \\ 0 \\ 0 \end{bmatrix} u(t), \\
z(t) &= \begin{bmatrix} 1 & 0 & 0 \\ 0 & 1 & 0 \\ 0 & 0 & 1 \\ 0 & 0 & 0 \end{bmatrix} x(t) + \begin{bmatrix} 0 \\ 0 \\ 0 \\ 1 \end{bmatrix} u(t), \\
y(t) &= \begin{bmatrix} 0 & 1 & 0 \end{bmatrix} x(t) + \begin{bmatrix} 0 & 1 & 0 \end{bmatrix} w(t).
\end{aligned}
\tag{4.3}
$$

with $\mathcal{S}_{\mathcal{H}_\infty} = \{1, 2, 3\}$, $\mathcal{S}_{\mathcal{H}_2} = \{4\}$, and input/output selection matrices

$$
R_1 = \begin{bmatrix} 1 & 0 & 0 \end{bmatrix}', \quad R_2 = \begin{bmatrix} 1 & 0 & 0 \end{bmatrix}', \quad R_3 = \begin{bmatrix} 0 & 1 & 0 \end{bmatrix}', \quad R_4 = \begin{bmatrix} 0 & 0 & 1 \\ 0 & 1 & 0 \end{bmatrix}',
$$

$$
L_1 = \begin{bmatrix} 1 & 0 & 0 & 0 \end{bmatrix}, \quad L_2 = \begin{bmatrix} 0 & 0 & 0 & 1 \end{bmatrix}, \quad L_3 = \begin{bmatrix} 0 & 1 & 0 & 0 \end{bmatrix}, \quad L_4 = I_4.
$$

We are interested in the computation of a fixed-order dynamic output feedback controller Θ, such that

$$
\|H_{\Theta,j}\|_\infty < b, \quad j \in \mathcal{S}_{\mathcal{H}_\infty}
\tag{4.4}
$$

for some predefined fixed value of $b > 0$, and moreover the closed-loop $\mathcal{H}_2$ performance $\|H_{\Theta,4}\|_2$ is minimized. The bound $b = 7.4$ is selected.

First a full-order controller Ψ is computed using the G shaping paradigm [32], where a bound on $\|H_{\Psi,4}\|_2$ is minimized subject to the constraints $\|H_{\Psi,j}\|_\infty < b$, $j \in \mathcal{S}_{\mathcal{H}_\infty}$. The resulting closed-loop $\mathcal{H}_2$ norm equals $\|H_{\Psi,4}\|_2 = 16.11$. Selecting $q = 2$, $\Psi_j = \Psi$ for $j \in \mathcal{S}$ and $A_{22} = 0$ in the LMIs (3.14) and (3.17), minimization of μ_4 subject to the constraints (4.4) yields $\sqrt{\mu_4} = 16.11$ and $\|H_{\Theta,4}\|_2 = 15.63$. The bound $\sqrt{\mu_4}$ is equal to $\|H_{\Psi,4}\|_2$, which is theoretically the best achievable according to the discussion below Remark 5 on page 39. However, note that the closed-loop $\mathcal{H}_2$ performance corresponding to the fixed-order controller Θ is better compared to the full-order G shaping design.

However, fixed-order controllers with even better closed-loop $\mathcal{H}_2$ performance might result by selecting different full-order controllers for the different performance specifications in the fixed-order synthesis LMIs. Therefore, a different controller Ψ_4 is designed using the G shaping paradigm, by imposing a bound $b > 7.4$ on the $\mathcal{H}_\infty$ performances. In this way, the $\mathcal{H}_\infty$ constraints are relaxed, such that $\|H_{\Psi_4,4}\|_2 < \|H_{\Psi,4}\|_2$. Hence, a fixed-order controller satisfying the constraints (4.4) that achieves a better $\mathcal{H}_2$ performance potentially results when Ψ_4 instead of Ψ is substituted in the $\mathcal{H}_2$ synthesis LMIs (3.17).

Figure 4.3 shows the bound $\sqrt{\mu_4}$ and $\mathcal{H}_2$ performance $\|H_{\Theta,4}\|_2$ (left), and the maximum of the bounds γ_j and $\mathcal{H}_\infty$ performances $\|H_{\Theta,j}\|_\infty$, $j \in \mathcal{S}_{\mathcal{H}_\infty}$ (right), corresponding to the fixed-order design as a function of $\|H_{\Psi_4,4}\|_2$. The rightmost point of the subfigures corresponds to the choice $\Psi_j = \Psi$, $j \in \mathcal{S}$, and Figure 4.3 is completed by gradually improving the $\mathcal{H}_2$ performance corresponding to Ψ_4. The left part of Figure 4.3 implies that selecting a controller Ψ_4 with a slightly better closed-loop $\mathcal{H}_2$ performance than Ψ (i.e., $\|H_{\Psi_4,4}\|_2 < \|H_{\Psi,4}\|_2$) causes a decrease of the bound μ_4 and a better $\mathcal{H}_2$ performance. For example, taking $b = 7.9$ yields $\|H_{\Psi_4,4}\|_2 = 15.4$, resulting in $\sqrt{\mu_4} = 15.6$ and $\|H_{\Theta,4}\|_2 = 14.9$, demonstrating an improvement of 7.5% in $\mathcal{H}_2$ performance compared to the G shaping controller Ψ. Selecting $b > 8.5$ in the G shaping design step, no feasible solution was obtained. Looking at the right part of Figure 4.3, the $\mathcal{H}_2$ performance improves at the expense of a higher $\mathcal{H}_\infty$ norm, approximating the $\mathcal{H}_\infty$ bound for lower values of $\|H_{\Psi_4,4}\|_2$.

Remark 6. *Although, theoretically speaking, the choice of the A_{22} matrix might influence the performance realized by the fixed-order controller, extensive numerical experiments have shown that selecting A_{22} different from the suggested values (i.e., $A_{22} = 0$ in discrete-time and $A_{22} = -I$ in continuous-time) has a negligible effect on the closed-loop performance.*
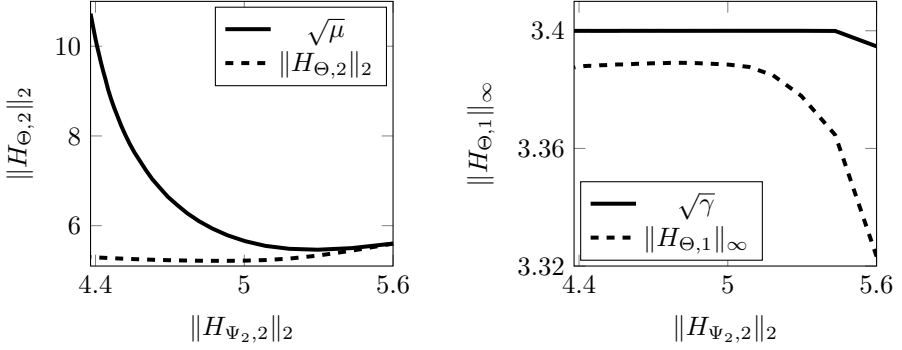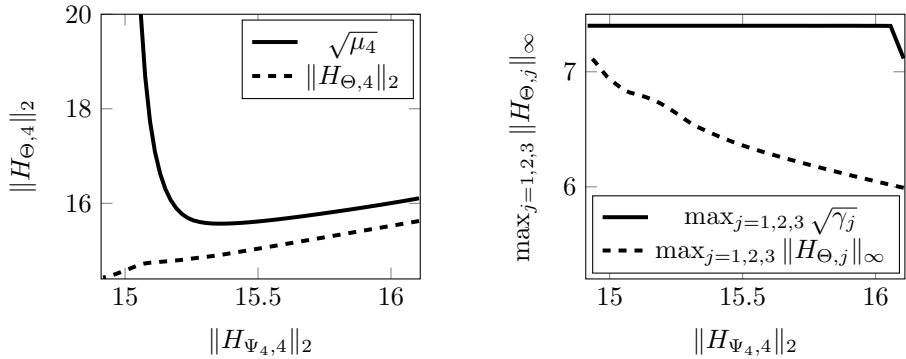
Figure 4.3: Using different G shaping controllers Ψ_j, $j \in \mathcal{S}$, allows the design of fixed-order controllers which are less conservative than a full-order G shaping design.

4.5 Fixed-order multi-$\mathcal{H}_\infty$ control of a lab-scale overhead crane

To demonstrate the practical viability of the fixed-order controller design approach (presented in Chapter 3) for LTI systems, this section provides experimental results of fixed-order multi-$\mathcal{H}_\infty$ controllers on a lab-scale overhead crane.

4.5.1 Model description

The system under consideration (shown in Figure 4.4) consists of a cart on a rail, to which a load is connected through a cable of fixed length. The horizontal cart and load position are denoted by x_{cart} [m] and x_{load} [m], respectively, while ϕ [rad] is the swing angle. The cable length is denoted by $\alpha = 0.45$ [m], implying a resonance frequency of 0.74Hz. A horizontal reference velocity of the cart defines the control input u [m/s], since an input voltage scales to horizontal cart velocity through a high bandwidth proportional feedback controller. The quantities x_{cart} and ϕ are measured in real time. Then, based on the assumption that the cable is stiff, x_{load} is expressed as

$$x_{\text{load}} = x_{\text{cart}} + \alpha \sin(\phi).$$

Consequently, assuming small swing angles (i.e., $\sin(\phi) \approx \phi$), perfect velocity tracking and no friction forces, the following continuous-time transfer function
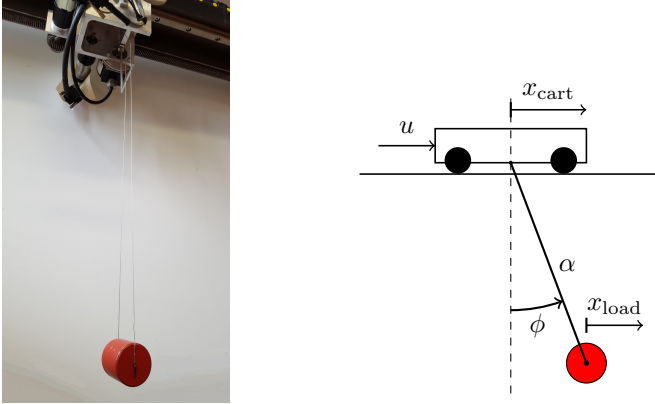
Figure 4.4: The overhead crane setup (left) and its schematic representation (right).

from u to x_{load} is derived:

$$\frac{g}{s(\alpha s^2 + g)}, \tag{4.5}$$

where g [m/s^2] denotes the gravitational acceleration. Converting (4.5) to state-space form allows direct application of our fixed-order controller synthesis approach.

However, since closed-loop performance is directly affected by the model accuracy, a more accurate system model than (4.5) is identified. Using multisine excitation, five frequency response functions (FRFs) are measured and averaged, and subsequently a 3rd order transfer function is fitted, see Figure 4.5. The corresponding discrete-time LTI model with a sampling period of 0.02s is given by

$$G : \begin{cases} x(t+1) = \begin{bmatrix} 2.9910 & -2.9905 & 0.9995 \\ 1 & 0 & 0 \\ 0 & 1 & 0 \end{bmatrix} x(t) + \begin{bmatrix} 1 \\ 0 \\ 0 \end{bmatrix} u(t), \\ 10^3 \cdot x_{\text{load}}(t) = \begin{bmatrix} 0.6571 & -1.272 & 0.7173 \end{bmatrix} x(t) + 3.408 \, u(t). \end{cases} \tag{4.6}$$

4.5.2 Controller design

The objective is to design fixed-order controllers (4.2) for the lab-scale overhead crane modeled by (4.6), achieving fast and accurate reference positioning of the load while avoiding excitation of the resonance frequency. At the same time, model uncertainty and measurement noise should be taken into account
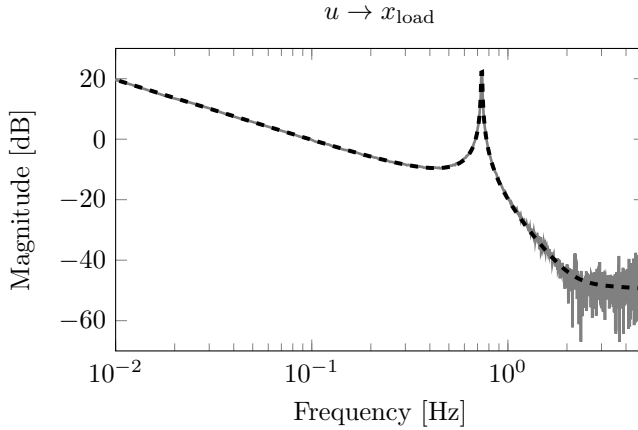
Figure 4.5: Averaged FRF (solid gray) and the fitted transfer function (dashed black).
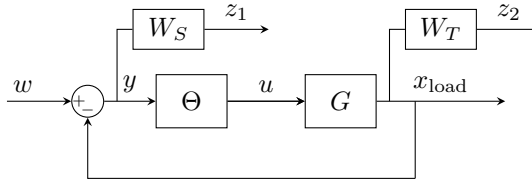
Figure 4.6: Block diagram of the lab-scale overhead crane model (4.6) interconnected with a fixed-order controller Θ. Two additional LTI systems W_S and W_T are incorporated to model the desired control objectives.

to guarantee the required level of robustness, and thus avoid stability and performance issues.

We define a reference signal w for the horizontal load position, and a corresponding error signal $y := w - x_{\text{load}}$. The controller input is selected as y, such that a nonzero input signal u is generated whenever the load is not on its desired position. The closed-loop interconnection of the LTI model (4.6) with a fixed-order controller (4.2) (denoted by Θ) is shown in Figure 4.6. Two additional discrete-time LTI systems (or, equivalently, transfer functions) W_S and W_T are incorporated to guarantee the aforementioned control objectives. Appropriate selection of W_S and W_T is briefly explained next.

The required level of robustness is characterized by the relative uncertainty of the measured FRFs with respect to the fitted FRF. Namely, assuming that the model (4.6) is subject to multiplicative uncertainty, and following the lines on
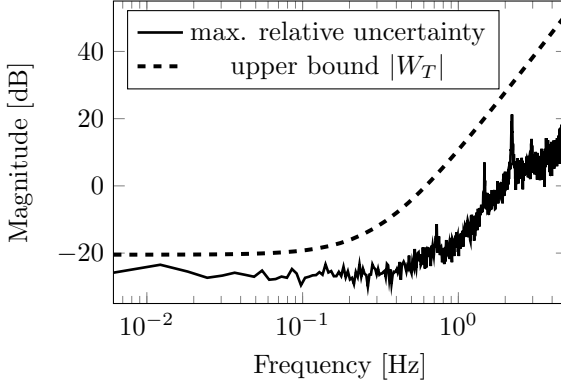
Figure 4.7: Maximum relative uncertainty and upper bound $|W_T|$.

pages 275-276 of [111], the closed-loop uncertain system is robustly stable if

$$\|W_T T\|_\infty < 1, \tag{4.7}$$

where T denotes the so-called complementary sensitivity (i.e., the transfer function from w to x_{load}), and W_T is a weighting function whose magnitude $|W_T|$ is an upper bound for the maximum relative model uncertainty. Figure 4.7 shows the maximum relative uncertainty and the bound $|W_T|$, corresponding to the selected third order transfer function W_T, as a function of frequency.

Closed-loop bandwidth, and thus reference tracking performance, is characterized by the so-called sensitivity function S (i.e., the transfer function from w to y). We consider the continuous-time transfer function

$$W(s) := \frac{s/A_\infty + \omega_{\text{c}}}{s + A_0 \omega_{\text{c}}}, \tag{4.8}$$

where ω_{c} is the crossover frequency [rad/s], while $\lim_{s \to 0} W(s) = 1/A_0$ and $\lim_{s \to \infty} W(s) = 1/A_\infty$. Selecting $\omega_{\text{c}} = 1$, $A_0 = -40$dB and $A_\infty = 20$dB, this transfer function is discretized using the Tustin approximation, resulting in the first order transfer function W_S. Then, optimizing bandwidth is equivalent to minimizing the positive scalar γ_1 subject to

$$\|W_S S\|_\infty < \gamma_1.$$

To achieve perfect reference positioning (i.e., no steady state error), $S(1) = 0$ is required. However, note that the latter is not enforced by the performance weight (4.8), since this transfer function has no pole in $s = 0$. Namely, stable

weighting functions are required to apply the full-order controller synthesis approach presented in, amongst others, [103]. Consequently, the low-frequency pole of W_S appears in the full-order controller, together with a zero at $z = 1$ due to integrating action in the model (4.6). An a posteriori manual pole-zero cancellation in the controller, corresponding to the low-frequency pole and the zero at $z = 1$, results in an open-loop transfer function with integrating action, and thus fulfills the requirement $S(1) = 0$. Since the uncontrolled system (i.e., the system of the form (4.1) with input $\begin{bmatrix} w & u \end{bmatrix}'$ and output $\begin{bmatrix} z & y \end{bmatrix}$) is of order 7, applying the approach [103] in combination with an a posteriori manual pole-zero cancellation results in a controller of order 6. It is worth to mention that, very recently, a more elegant approach that allows the incorporation of unstable weighting functions has been developed [63].

Adopting the notation of Section 3.4.3 (see page 42), we define the closed-loop transfer functions $H_{\Theta,1} : w \to z_1$ and $H_{\Theta,2} : w \to z_2$ (see Figure 4.6), and select the set of performance channels as $\mathcal{S} = \mathcal{S}_{\mathcal{H}_\infty} = \{1, 2\}$ and the corresponding set of selection matrices $R_1 = R_2 = 1$, $L_1 = \begin{bmatrix} 1 & 0 \end{bmatrix}$, and $L_2 = \begin{bmatrix} 0 & 1 \end{bmatrix}$. Then, the multi-$\mathcal{H}_\infty$ control problem translates to

$$
\begin{aligned}
&\underset{\Theta, \gamma_1, \gamma_2}{\text{minimize}} && \gamma_1 \\
&\text{subject to:} && \|H_{\Theta,1}\|_\infty < \gamma_1, \quad \|H_{\Theta,2}\|_\infty < \gamma_2, \\
& && \gamma_1 < b_1, \qquad\quad\; \gamma_2 < 1.
\end{aligned}
\tag{4.9}
$$

where an optional bound b_1 is incorporated to bound the feasible set associated with the optimization problem. It is worth to emphasize that this multi-objective formulation with constraints $\|H_{\Theta,1}\|_\infty < \gamma_1$ and $\|H_{\Theta,2}\|_\infty < \gamma_2$ is always less conservative than the mixed-sensitivity formulation (see [65])

$$
\left\| \begin{matrix} H_{\Theta,1}/\gamma_1 \\ H_{\Theta,2}/\gamma_2 \end{matrix} \right\|_\infty < 1.
$$

4.5.3 Numerical evaluation

In order to design fixed-order multi-$\mathcal{H}_\infty$ controllers for the lab-scale overhead crane, a full-order controller is computed with the approach [103], by solving the optimization problem (4.9) without imposing a bound b_1 and applying a manual pole-zero cancellation in the controller. This full-order controller is substituted for Ψ in the fixed-order $\mathcal{H}_\infty$ synthesis LMIs (3.14) (i.e.: $\Psi_1 = \Psi_2 = \Psi$), which are then sequentially applied to obtain solutions of (4.9) for all orders $0 \leq q \leq 5$ (see page 41 and Figure 3.2 on page 41).

The numerical results are summarized in Table 4.3, showing the selected bound b_1 and the obtained $\mathcal{H}_\infty$ bounds and $\mathcal{H}_\infty$ norms for each controller order

Table 4.3: Numerical results of multi-$\mathcal{H}_\infty$ controller synthesis for the lab-scale overhead crane model (4.6). For each controller order $0 \leq q \leq 6$, the selected bound b_1, bounds γ_i and a posteriori calculated norms $\|H_{\Theta,i}\|_\infty$, $i = 1, 2$ corresponding to the optimization problem (4.9) are shown.

q	b_1	γ_1	$\|H_{\Theta,1}\|_\infty$	γ_2	$\|H_{\Theta,2}\|_\infty$
6	–	0.57	0.57	1.00	0.92
5	0.65	0.60	0.57	0.97	0.94
4	3.1	3.02	0.58	1.00	0.96
3	54	52.5	23.3	0.96	0.91
2	66	64.7	56.7	0.94	0.77
1	53	52.4	49.9	0.91	0.79
0	57	55.9	51.8	0.88	0.86

$0 \leq q \leq 6$. Table 4.3 confirms that the fixed-order $\mathcal{H}_\infty$ synthesis LMIs yield stabilizing controllers satisfying the robustness bound $\|H_{\Theta,2}\|_\infty < 1$ for all orders $0 \leq q \leq 6$. Although more conservative $\mathcal{H}_\infty$ bounds result for lower controller orders, similar closed-loop performance is achieved for $4 \leq q \leq 6$, suggesting that a controller of order 4 is sufficient for this application. We observed that decreasing b_1 leads to lower closed-loop $\mathcal{H}_\infty$ norms. As can be inferred from the Bode magnitude plot of $H_{\Theta,2}$ and Θ, shown for all controller orders $0 \leq q \leq 6$ in Figure 4.8, the high-order controllers invert the resonance frequency of the system (4.6) (see [119] and references therein). While the latter may cause undesired closed-loop behavior, in this case it is perfectly legitimate since the resonance frequency has been reliably identified.

A desired bandwidth can no longer be achieved for the orders $q \leq 3$. To clarify this, note that the resonance frequency can no longer be sufficiently suppressed by the controller, see Figure 4.8. Therefore, this resonance will appear in the Bode magnitude plot corresponding to $H_{\Theta,2}$. Consequently, low controller gains are required to satisfy the robustness bound, implying a low bandwidth. To obtain feasible solutions of (4.9) for $0 \leq q \leq 3$, it was necessary to manually decrease the gain of the controller that was substituted in the fixed-order LMIs.

4.5.4 Experimental validation

To validate the designed fixed-order multi-$\mathcal{H}_\infty$ controllers, they are experimentally tested on the lab-scale overhead crane. For each controller order $0 \leq q \leq 6$, the experimental closed-loop response to a smoothed reference step is determined. Figure 4.9a shows the simulated and experimental closed-loop responses to a smoothed step of 0.5m for the controllers of order $4 \leq q \leq 6$. The
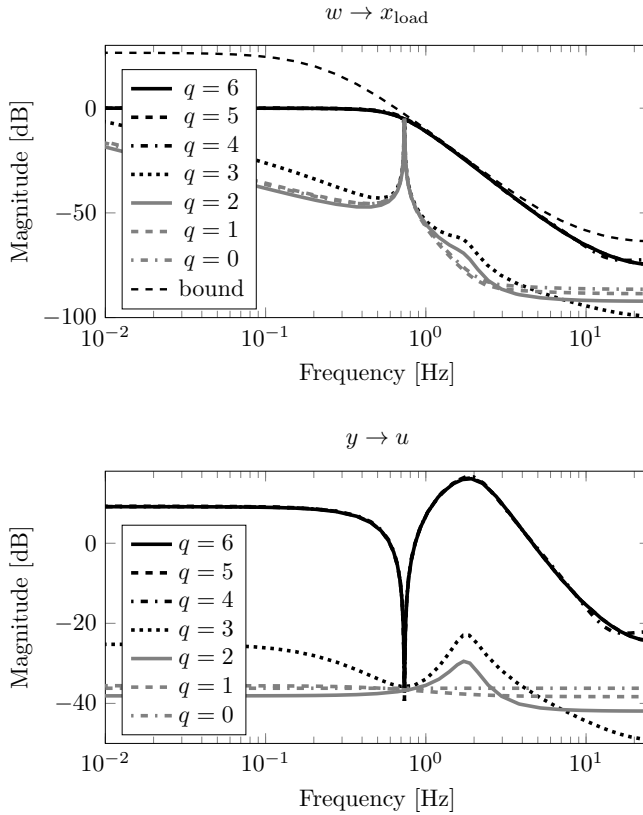
Figure 4.8: Bode magnitude plots of the complementary sensitivity $T : w \to x_{\mathsf{load}}$ (top) and the fixed-order controller $\Theta : y \to u$ (bottom), for all controller orders $0 \leq q \leq 6$.

experimental responses feature slightly more overshoot than the corresponding simulations, which we attribute to saturation of the control input u. However, it should be emphasized that the controllers of order $4 \leq q \leq 6$ feature similar performance, confirming that the controllers of order $q > 4$ are needlessly complex for this application. At the same time, Figure 4.9b shows that the closed-loop responses corresponding to the low-order controllers ($0 \leq q \leq 3$) are clearly below par. Consequently, a controller of order $q = 4$ is optimal in terms of simplicity and performance for this specific application. The fact that the computed fourth order controller achieves similar performance as a significantly more complicated full-order controller strongly sustains the value of our fixed-order controller design approach.
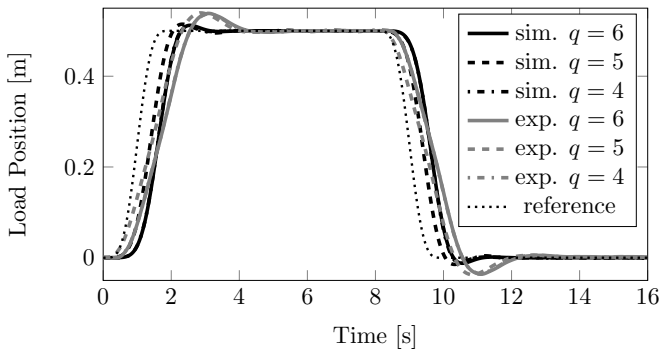
(a) Controller orders $4 \leq q \leq 6$.
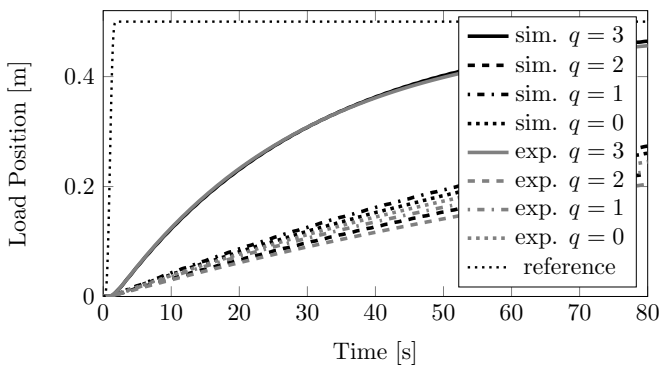
(b) Controller orders $0 \leq q \leq 3$.

Figure 4.9: Closed-loop simulated (black) and experimental (gray) responses to a smoothed reference step.

4.6   Summary

This chapter has presented numerical and experimental validations of the fixed-order controller design approach (presented in Chapter 3) applied to LTI systems. Despite its conservatism, numerous fixed-order controllers with similar closed-loop performance as an optimal full-order $\mathcal{H}_\infty$ or $\mathcal{H}_2$ controller were obtained, either by direct or iterative application of the fixed-order synthesis conditions. It was moreover shown how, by exploiting the freedom to select a different full-order controller for each performance specification, multi-objective fixed-order controllers were computed that outperform full-order controllers resulting from well-known (conservative) LMI approaches. The practical viability of our LMI framework for fixed-order controller synthesis was confirmed by experimental

validations of multi-$\mathcal{H}_\infty$ controllers on a lab-scale overhead crane.

RECAPITULATION

- The existence of a convex reformulation of the fixed-order $\mathcal{H}_\infty/\mathcal{H}_2$ synthesis problem for LTI systems is unknown, even when only one performance specification is imposed.

- Despite the potential conservatism of the LMI framework for fixed-order $\mathcal{H}_\infty/\mathcal{H}_2$ controller design (presented in Chapter 3), it often results in fixed-order $\mathcal{H}_\infty$ ($\mathcal{H}_2$) controllers with similar performance as (optimal) $\mathcal{H}_\infty$ ($\mathcal{H}_2$) full-order controllers.

- Our LMI framework (presented in Chapter 3) allows the computation of fixed-order multi-objective controllers that outperform full-order controllers resulting from the Lyapunov and G shaping paradigm, by exploiting the freedom to select a different full-order controller for each performance specification in the fixed-order synthesis LMIs.

- The practical viability of the fixed-order synthesis approach (presented in Chapter 3) for the class of LTI systems is confirmed by experimental validations of fixed-order multi-$\mathcal{H}_\infty$ controllers on a lab-scale overhead crane.

Chapter 5

Fixed-order controller design for LPV systems

In this chapter, the fixed-order LMI framework from Chapter 3 is applied to design fixed-order multi-objective $\mathcal{H}_\infty/\mathcal{H}_2$ controllers for LPV systems. Hence, it is assumed that the system is affected by parameters that are a priori unknown but measurable in real time. Both the number of states and the parameter dependency of the controller are a priori fixed. By applying a numerically attractive relaxation technique, tractable sufficient LMIs for fixed-order synthesis are derived, allowing the design of high performance fixed-order $\mathcal{H}_\infty/\mathcal{H}_2$ controllers. The practical viability of the approach is assessed by experimental validations on a lab-scale overhead crane with varying cable length.

5.1 Introduction

Bridging the gap between the restricted class of LTI systems and the general class of nonlinear systems, the modern framework of LPV systems has gained popularity since the nineties. It has been successful in many applications ranging from wafer stages [121] to racing motorcycles [22]. See the interesting recent survey [55] and book [82] for a complete overview.

Full-order dynamic output feedback control, amongst others, received substantial attention in the field of LPV control [7, 28, 99, 100, 127]. The design of *fixed-order* LPV controllers (i.e., with a prefixed order and parameter dependency), on the other hand, has not yet been extensively studied and applied. For instance, the approaches presented in [10, 67] solely provide conditions for controller

orders larger or equal to the plant order minus the number of (exact) state measurements, while the algorithms for fixed-order synthesis presented in [6, 47], which are very successful for LTI systems, cannot handle LPV dynamics. At the same time, sequential convex programming methods, e.g. [116], can cope with LPV dynamics, but are computationally very demanding. Additionally, the approach [37] relies on the design of numerous random initial controllers, which are subsequently used for the design of a single LPV controller. This results in a numerically costly procedure for the computation of a suitable LPV controller. Moreover, the latter approach does not allow all system matrices to be parameter-dependent. Although the 2-step approach presented in [3] (using a stabilizing state feedback for a specific augmented system as a starting point) is readily extendable to handle LPV dynamics, no guidelines are provided on how to select an initial state feedback to obtain a high performance fixed-order controller.

In this chapter, the novel fixed-order synthesis approach from Chapter 3 is applied to design fixed-order LPV controllers with a rational parameter dependency, where the polynomial degree of the numerator and denominator as well as the number of states are prefixed. The resulting approach allows polynomial parameter dependencies of all system matrices, handles multiple design objectives, and provides intuitive guidelines for the selection of an initial full-order controller. Moreover, known bounds on the rate of parameter variation are taken into account to obtain less conservative results compared to unbounded rates of variation. Namely, as motivated in [28, 88] and references therein, taking into account bounds on the rate of parameter variation is essential to reduce conservatism that is inherent in the LPV synthesis approaches based on quadratic stability [5]. Homogenization and polynomial approximations (see Section 2.4.2) are used to obtain tractable LMI formulations that guarantee feasibility of the parameter-dependent synthesis conditions. The combination of all properties above makes our method attractive, both computationally and practically, compared to existing approaches. The merits of the proposed methodology are illustrated by experimental validations on a lab-scale overhead crane with varying cable length, comparing the experimental performances of a full-order controller with a significantly simpler fixed-order LPV controller.

5.2   Problem formulation

Consider the finite-dimensional LPD state-space representation (3.1) (see page 30), and assume that the parameter α is a priori unknown, real-time measurable and time-varying. Then, the dynamics under consideration are LPV

(see Table 2.1 on page 9), and thus take the form

$$\begin{cases} \delta x &=& A(\alpha)x &+& B_w(\alpha)w &+& B_u(\alpha)u, \\ z &=& C_z(\alpha)x &+& D_{zw}(\alpha)w &+& D_{zu}(\alpha)u, \\ y &=& C_y(\alpha)x &+& D_{yw}(\alpha)w \end{cases} \tag{5.1}$$

with state $x : \mathbb{T} \to \mathbb{R}^{n_x}$, exogenous input $w : \mathbb{T} \to \mathbb{R}^{n_w}$, control input $u : \mathbb{T} \to \mathbb{R}^{n_u}$, regulated output $z : \mathbb{T} \to \mathbb{R}^{n_z}$ and measured output $y : \mathbb{T} \to \mathbb{R}^{n_y}$, where all system matrices are real continuous functions of $\alpha : \mathbb{T} \to \mathbb{R}^N$, bounded for all $t \in \mathbb{T}$, and have appropriate dimensions. By considering $\alpha \in \mathcal{T}$, see (2.4) on page 8, a priori known bounds on the rate of parameter variation are taken into account.

We are interested in the design of fixed-order dynamic output feedback LPV controllers

$$\begin{cases} \delta x_{\mathrm{c}} &=& A_{\mathrm{c}}(\alpha)x_{\mathrm{c}} &+& B_{\mathrm{c}}(\alpha)y, \\ u &=& C_{\mathrm{c}}(\alpha)x_{\mathrm{c}} &+& D_{\mathrm{c}}(\alpha)y, \end{cases} \tag{5.2}$$

with $x_{\mathrm{c}} \in \mathbb{R}^q$, $q < n_x$, and with an a priori fixed parameter dependency, that exponentially stabilize the LPV system (5.1) such that one ore more closed-loop $\mathcal{H}_\infty/\mathcal{H}_2$ performance specifications are guaranteed.

Due to the fact that the LPV system (5.1) and the fixed-order controller (5.2) depend on time-varying parameters, the corresponding $\mathcal{H}_\infty$ and $\mathcal{H}_2$ synthesis LMIs (3.14) and (3.17) feature infinite-dimensional optimization variables and infinitely many constraints, and are thus numerically intractable (see Section 2.4 on page 18). To resolve this issue, the next section discusses how the structure of the compact convex polytope $\Omega \subset \mathbb{R}^{2N}$ (defined as in (2.2) on page 8) is exploited to derive a finite set of sufficient LMIs for fixed-order $\mathcal{H}_\infty/\mathcal{H}_2$ synthesis.

5.3 Relaxations

It is clear that the parameter-dependent synthesis LMIs (3.17) and (3.14), which should hold for all $\alpha \in \mathcal{T}$, give rise to numerically intractable optimization problems. Therefore, this section presents an approach to derive a finite set of LMIs whose feasibility guarantees that the parameter-dependent LMIs (3.17) and (3.14) are feasible for all $(\alpha, \Delta\alpha) \in \Omega$, and hence for all $\alpha \in \mathcal{T}$. The chosen relaxation technique, which is closely related to the approach presented in [28, 88], exploits the convex polytopic structure of the parameter-domain Ω (see (2.4)), and relies on polynomial parameter dependencies and Pólya's theorem [30, 49, 101]. In contrast to the approach [28, 88], where each point $(\alpha, \Delta\alpha) \in \Omega$ is expressed as a convex combination of *all* the vertices of Ω,

we propose to apply a simplicial subdivision of the domain and subsequently apply homogenization (see Section 2.4.2) to derive a finite set of sufficient LMIs. Namely, for the application presented in Section 5.4, we noticed that such a subdivision results in a significant reduction of numerical complexity while the level of conservatism is maintained.

Considering the discrete-time case (the continuous-time case is analogous), the relaxation approach consists of the following steps:

1. First, each function value $(\alpha, \Delta\alpha) \in \Omega$ is expressed as a convex combination of (a subset of) the vertices of Ω. We propose to divide Ω into a finite set of convex polytopes with fewer vertices than Ω, which are denoted by $\Omega^{(i)}$, $i = 1, \ldots, D$, where $D \in \mathbb{N}_+$ is the number of polytopes. For $(\alpha, \Delta\alpha) \in \Omega^{(i)}$, the linear relation

$$\begin{bmatrix} \alpha \\ \Delta\alpha \end{bmatrix} = \begin{bmatrix} F_1^{(i)} \\ F_2^{(i)} \end{bmatrix} \beta^{(i)} = F^{(i)} \beta^{(i)}, \tag{5.3}$$

holds, where each column of $F^{(i)}$ corresponds to a vertex of $\Omega^{(i)}$, and $\beta^{(i)}$ assumes values in a unit simplex of dimension M_i, with M_i the number of vertices of $\Omega^{(i)}$. Relation (5.3) implies that

$$\alpha_+ := \alpha + \Delta\alpha = F_1^{(i)} \beta^{(i)} + F_2^{(i)} \beta^{(i)} = (F_1^{(i)} + F_2^{(i)}) \beta^{(i)},$$

for all $(\alpha, \Delta\alpha) \in \Omega^{(i)}$, $i = 1, \ldots, D$. Consequently, defining (amongst others)

$$\widehat{P}^{(i)}(\beta^{(i)}) := P(F_1^{(i)} \beta^{(i)}) = P(\alpha),$$

$$\widetilde{P}^{(i)}(\beta^{(i)}) := P((F_1^{(i)} + F_2^{(i)}) \beta^{(i)}) = P(\alpha_+),$$

$(\alpha, \Delta\alpha) \in \Omega^{(i)}$, $i = 1, \ldots, D$, the parameter-dependent LMIs (3.14) and (3.17) are readily expressed in terms of the parameters $\beta^{(i)} : \mathbb{N} \to \mathbb{R}^{M_i}$, $i = 1, \ldots, D$, resulting in the following equivalent parameter-dependent

LMIs for $\mathcal{H}_\infty$ synthesis

$$\widehat{R}_{\Psi,\infty}^{(i)}(\beta^{(i)})' \begin{bmatrix} -\widehat{P}^{(i)}(\beta^{(i)}) & 0 & 0 & 0 \\ 0 & \widetilde{P}^{(i)}(\beta^{(i)}) & 0 & 0 \\ 0 & 0 & -\gamma I & 0 \\ 0 & 0 & 0 & I \end{bmatrix} \widehat{R}_{\Psi,\infty}^{(i)}(\beta^{(i)})+$$

$$\mathrm{He}\left\{ \begin{bmatrix} 0 \\ 0 \\ I \end{bmatrix} \begin{bmatrix} \widehat{Z}^{(i)}(\beta^{(i)})\widehat{\widetilde{C}}_y^{(i)}(\beta^{(i)}) & \widehat{Z}^{(i)}(\beta^{(i)})\widehat{\widetilde{D}}_{yw}^{(i)}(\beta^{(i)}) & -\widehat{Y}^{(i)}(\beta^{(i)}) \end{bmatrix} \right\}$$

$$\prec 0, \quad (5.4)$$

for $i = 1, \ldots, D$. The parameter-dependent matrix $\widehat{Z}^{(i)}(\beta^{(i)})$ is explicitly given by

$$\widehat{Z}^{(i)}(\beta^{(i)}) = U'\widehat{\Theta}^{(i)}(\beta^{(i)})+$$

$$\widehat{Y}^{(i)}(\beta^{(i)})\left(\begin{bmatrix} 0_{q\times q} & 0 & 0 \\ 0 & \widehat{A}_{22}^{(i)}(\beta^{(i)}) & 0 \\ 0 & 0 & 0_{n_u \times n_y} \end{bmatrix} - \widehat{\Psi}^{(i)}(\beta^{(i)}) \right).$$

To guarantee feasibility of (3.14), the parameter-dependent LMIs (5.4) should hold for all trajectories $\beta^{(i)} : \mathbb{N} \to \mathbb{R}^{M_i}$, $i = 1, \ldots, D$ corresponding to $\alpha \in \mathcal{T}$. It is emphasized that, due to a coupling between α and $\Delta\alpha$, the trajectories $\beta^{(i)}$, $i = 1, \ldots, D$ are constrained. (The parameter-dependent $\mathcal{H}_2$ synthesis LMIs in terms of $\beta^{(i)}$, $i = 1, \ldots, D$ are derived in a similar fashion.)

2. The next step is to get rid of the time-dependency of the parameter-dependent LMIs (5.4), which is achieved by ignoring the implicit coupling between the trajectories of α and $\Delta\alpha$. Namely, then $\beta^{(i)}$ is allowed to be any function varying in the unit simplex of dimension M_i, $i = 1, \ldots, D$, such that the dependency of $\beta^{(i)}$ on time becomes irrelevant. Hence, imposing the parameter-dependent LMIs (5.4) for all points $\beta^{(i)}$ in the unit simplex of dimension M_i, $i = 1, \ldots, D$ yields sufficient conditions for the LMI (3.14) to hold for all $\alpha \in \mathcal{T}$.

3. Since the resulting set of LMI conditions, that should hold for all $\beta^{(i)}$ in the unit simplex of dimension M_i, $i = 1, \ldots, D$, are standard parameter-dependent LMIs, well-known techniques can be applied to derive a finite set of sufficient LMIs, see for instance [66, 87, 102, 104]. In this work, we apply

the approach of [87], relying on homogeneous polynomial dependencies of all LMI variables on parameters that lie in a unit simplex. Since all the LMI variables are assumed to have a polynomial parameter dependency on $\alpha \in \mathcal{T}$, the parameter-dependent LMIs (5.4) are rewritten as *homogeneous* polynomially parameter-dependent LMIs without loss of generality. To this end, we define the set of M-dimensional sequences whose elements sum to p as

$$\mathcal{K}_M(p) := \left\{ l = (l_1, \ldots, l_M) \,\middle|\, \sum_{j=1}^{M} l_j = p \right\},$$

with cardinality

$$\mathcal{J}_M(p) = \frac{(M + p - 1)!}{p!(M - 1)!}.$$

Consequently, assuming that the LMI variables $P(\alpha)$ and $P(\alpha_+)$ have a polynomial parameter dependency of degree p, they are expressed in terms of $\beta^{(i)}$, $i = 1, \ldots, D$ as follows

$$P(\alpha) = \widehat{P}^{(i)}(\beta^{(i)}) = \sum_{l \in \mathcal{K}_{M_i}(p)} (\beta^{(i)})^l \widehat{P}_l^{(i)},$$

$$P(\alpha_+) = \widetilde{P}^{(i)}(\beta^{(i)}) = \sum_{l \in \mathcal{K}_{M_i}(p)} (\beta^{(i)})^l \widetilde{P}_l^{(i)},$$

for $(\alpha, \Delta\alpha) \in \Omega^{(i)}$, $i = 1, \ldots, D$, where $(\beta^{(i)})^l = \prod_{j=1}^{M_i} (\beta_j^{(i)})^{l_j}$. The number of coefficients $\widehat{P}_l^{(i)}$ (and $\widetilde{P}_l^{(i)}$) equals $\mathcal{J}_{M_i}(p)$. Substituting all polynomially parameter-dependent variables in (5.4), homogenization of all terms results in parameter-dependent LMIs with a homogeneous polynomial dependency on $\beta^{(i)}$, $i = 1, \ldots, D$. Since $\beta^{(i)}$ takes values in a unit simplex, $i = 1, \ldots, D$, imposing negative definiteness on the matrix coefficients of the homogeneous polynomially parameter-dependent LMIs (5.4) results in a finite set of sufficient conditions.

The numerical complexity of the resulting LMI problem is affected by the polynomial degree of the homogeneous polynomially parameter-dependent LMIs (i.e. the polynomial degree of the LMI variables), the number D of subdomains and the number of vertices M_i of each subdomain $\Omega^{(i)}$, $i = 1, \ldots, D$. Specifically, to derive a finite set of sufficient LMIs for $P(\alpha) \succ 0$ to hold, where $P(\alpha)$ has a polynomial parameter dependency of degree p on α, results in the following
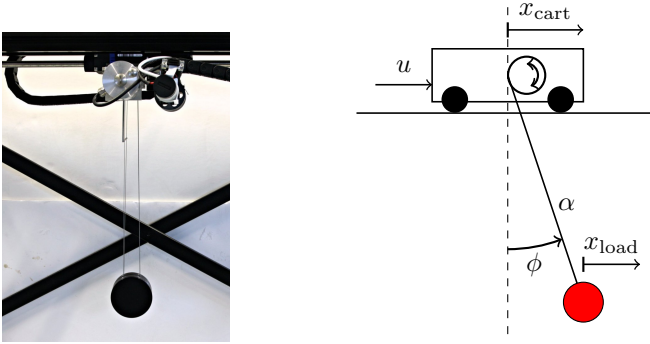
Figure 5.1: The overhead crane setup (left) and its schematic representation (right).

number of LMI blocks[1]

$$\sum_{i=1}^{D} \mathcal{J}_{M_i}(p) = \sum_{i=1}^{D} \frac{(M_i + p - 1)!}{p!(M_i - 1)!}.$$

The practical benefits of subdividing the parameter domain Ω for complicated control problems are illustrated below.

5.4 Fixed-order LPV control of an overhead crane

This section considers the design of fixed-order multi-objective $\mathcal{H}_2/\mathcal{H}_\infty$ LPV controllers for a lab-scale overhead crane with varying cable length. First, a description of the overhead crane LPV model and the control objective are provided. Then, exploiting subdivision of the parameter domain, the approach from Chapter 3 is applied to design fixed-order LPV controllers for the overhead crane model, followed by experimental validations. The LMIs are implemented and solved in MATLAB using the software packages Yalmip [72] and SeDuMi [113].

5.4.1 Model description

The system under consideration (shown in Figure 5.1) consists of a velocity controlled cart on a rail, to which a load is attached through a cable with

---

[1]Imposing positive/negative definiteness on a coefficient of a homogeneous polynomially parameter-dependent LMI results in a so-called LMI block.

varying length. The horizontal cart and load position are denoted by x_{cart} [m] and x_{load} [m], respectively, while $\alpha \in [0.35, 0.75]$ [m] defines the cable length and ϕ [rad] is the swing angle. The system input is a voltage $u \in [-10, 10]$ [V], which scales to cart velocity through a high bandwidth velocity controller. The quantities x_{cart} and ϕ, as well as the varying cable length α, are measured in real-time. To account for disturbance rejection in the control objective, an additional input d_ϕ is defined, modeling the effect of an initial swing angle disturbance. Specifically, selecting d_ϕ as the unit impulse function corresponds to an initial swing angle of 0.1rad and a horizontal load velocity of 0m/s. A multiple-input multiple-output 4$^{\text{th}}$ order LPV model with an affine dependency on α and a sampling period of 0.01s is identified using the SMILE technique [29, 127], and represented in state-space form as

$$
G : \left\{
\begin{array}{rcl}
x(t+1) & = & A(\alpha(t))x(t) \quad + \quad B(\alpha(t)) \begin{bmatrix} u(t) \\ d_\phi(t) \end{bmatrix}, \\[2ex]
\begin{bmatrix} x_{\text{cart}}(t) \\ \phi(t) \end{bmatrix} & = & C(\alpha(t))x(t) \quad + \quad D \begin{bmatrix} u(t) \\ d_\phi(t) \end{bmatrix}.
\end{array}
\right.
\tag{5.5}
$$

Figure 5.2 depicts Bode magnitude plots corresponding to each input-output channel of the LPV model (5.5), evaluated for 5 equidistant fixed cable lengths $\alpha \in [0.35, 0.75]$m. Note that, since u scales to cart velocity through a high bandwidth velocity controller, the transfer function $u \to x_{\text{cart}}$ corresponds to an integrator multiplied by a constant gain. Additionally, it is worth mentioning that a swing angle disturbance has no effect on the cart position, which is due to high friction between the cart and the rail.

Taking into account bounds on the rate of parameter variation, we select the set of admissible parameter trajectories as in (2.4) where Ω is the compact convex polytope with the following set of vertices:

$$
\left\{ \begin{bmatrix} \alpha_L \\ 0 \end{bmatrix}, \begin{bmatrix} \alpha_L \\ b \end{bmatrix}, \begin{bmatrix} \alpha_U - b \\ b \end{bmatrix}, \begin{bmatrix} \alpha_U \\ 0 \end{bmatrix}, \begin{bmatrix} \alpha_U \\ -b \end{bmatrix}, \begin{bmatrix} \alpha_L + b \\ -b \end{bmatrix} \right\}
\tag{5.6}
$$

where $\alpha_L = 0.35$, $\alpha_U = 0.75$, and $b = 0.004$, corresponding to a cable length varying between 0.35m and 0.75m, and a maximum cable hoisting velocity of 0.4m/s. The convex polytopic domain Ω, together with a possible simplicial subdivision, is depicted in Figure 5.3.

5.4.2   Control objective

The aim is to design fixed-order LPV controllers of the form (3.2) for the identified LPV model (5.5), achieving a good trade-off between reference tracking
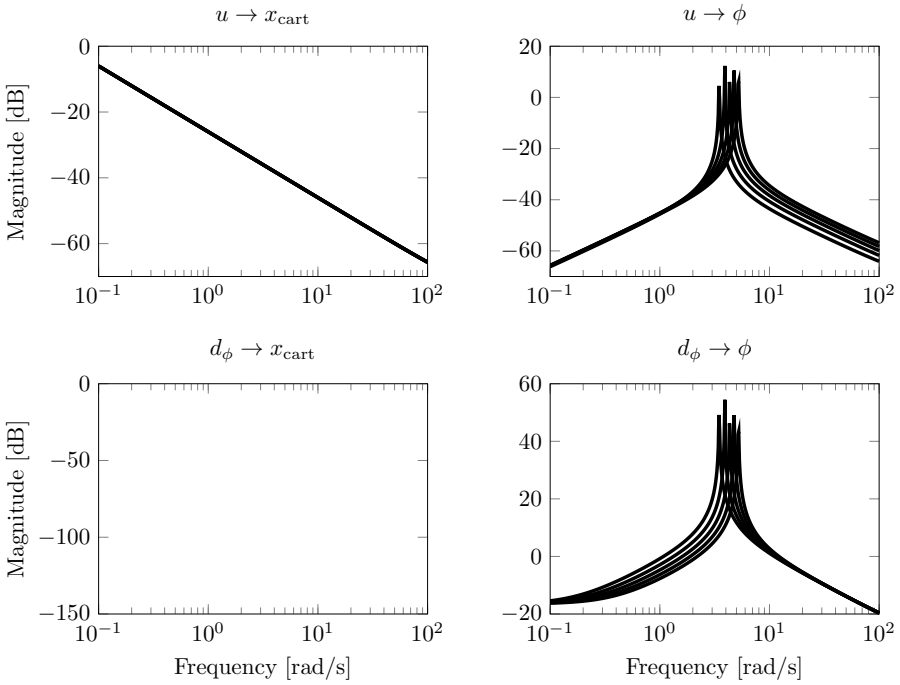
Figure 5.2: Bode magnitude plots for each input-output channel of the LPV system (5.5), evaluated for 5 equidistant cable lengths $\alpha \in [0.35, 0.75]$.
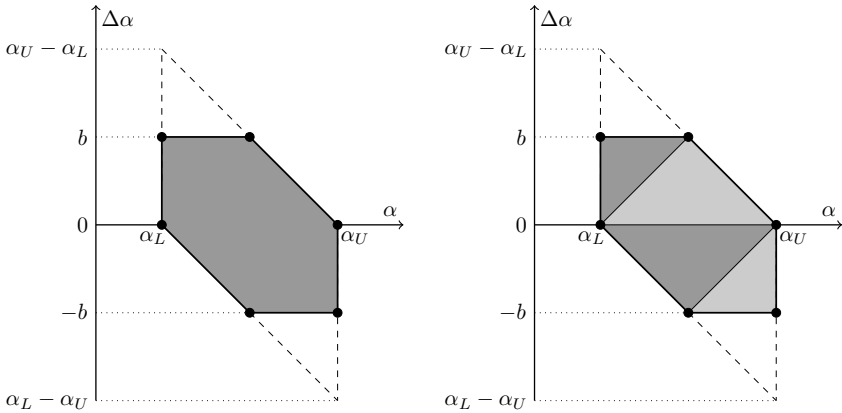
Figure 5.3: Left: visual representation of the set Ω, being the convex hull of (5.6). For a given bound b, $(\alpha, \Delta\alpha)$ assumes values in the gray region. Right: a possible subdivision of Ω in four triangular subdomains $\Omega^{(i)}$, $i = 1, \ldots, 4$, for the case $0 < b < \alpha_U - \alpha_L$.
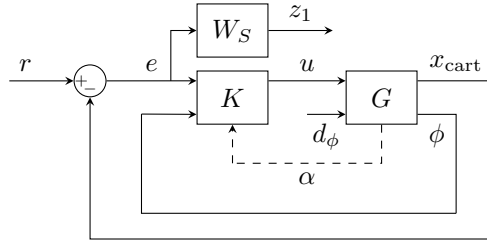
Figure 5.4: Block diagram of the overhead crane model (5.5) interconnected with a dynamic output feedback LPV controller (3.2). An LTI system W_S is incorporated to optimize bandwidth.

of the load position and rejection of swing angle disturbances under the influence of a varying cable length.

We define a reference signal r for the horizontal cart position, and a corresponding error signal $e := r - x_{\text{cart}}$. Note that $x_{\text{load}} \approx r$ whenever $x_{\text{cart}} \approx r$ and $\phi \approx 0$. The controller input is selected as $y := \begin{bmatrix} e & \phi \end{bmatrix}'$. To assure a high bandwidth and good reference tracking, we consider a weight function described by the continuous-time transfer function

$$W(s) := \frac{s/A_\infty + \omega_c}{s + A_0\omega_c}, \tag{5.7}$$

where ω_c is the crossover frequency [rad/s], while $\lim_{s\to 0} W(s) = 1/A_0$ and $\lim_{s\to\infty} W(s) = 1/A_\infty$. Selecting $\omega_c = 0.2$, $A_0 = -60$dB and $A_\infty = 100$dB in (5.7), this transfer function is discretized using zero-order hold, resulting in a discrete-time LTI model $W_S : e \to z_1$. Figure 5.4 provides a schematic overview of the interconnected system. An $\mathcal{H}_\infty$ performance specification is selected for the channel $r \to z_1$ to assure a high bandwidth, while an $\mathcal{H}_2$ performance specification is imposed on the channel $d_\phi \to \phi$ to account for the rejection of swing angle disturbances. Our choice for $\mathcal{H}_2$ performance stems from the fact that, in this case, minimization of the $\mathcal{H}_2$ norm relates to minimization of the energy in the autonomous response to an initial swing angle deviation.

5.4.3 Full-order $\mathcal{H}_\infty/\mathcal{H}_2$ controller design

The aim of this section is to design strictly proper full-order LPV controllers for the LPV model (5.5). Hence, controllers of the form

$$\begin{cases} x_c(k+1) & = & A_c(\alpha(k))x(k) + B_c(\alpha(k)) \begin{bmatrix} e(k) \\ \phi(k) \end{bmatrix}, \\ u(k) & = & C_c(\alpha(k))x(k), \end{cases} \tag{5.8}$$

Table 5.1: $\mathcal{H}_\infty$ performance bounds γ for full-order LPV control design and associated details on numerical complexity, for different values of μ and different degrees p of the Lyapunov matrix, using subdivision into four convex polytopes ($D = 4$) or no subdivision ($D = 1$) of the parameter domain Ω. The provided $\mathcal{H}_\infty$ bound, the number of LMI variables V and LMI blocks B (max. size = 22), and the computation times t_c (in seconds) illustrate the merits of simplicial subdivision as the polynomial degree p increases.

μ		0.25			0.6			1		
p		1	2	3	1	2	3	1	2	3
γ	$D = 4$	1.62	1.53	1.51	0.12	0.12	0.12	0.09	0.09	0.09
	$D = 1$	1.62	1.53	1.51	0.12	0.12	0.12	0.09	0.09	0.09
V		403	554	705	403	554	705	403	554	705
B	$D = 4$	72	120	180	72	120	180	72	120	180
	$D = 1$	63	168	378	63	168	378	63	168	378
t_c	$D = 4$	17.5	47.7	53.7	15.7	28.6	45.5	14.9	26.9	45.3
	$D = 1$	17.9	56.2	138	14.3	43.9	119	14.2	42.6	120

with $x_c \in \mathbb{R}^{n_x}$ ($n_x = 5$). Following the lines in [28] (see also [32]), parameter-dependent sufficient LMIs for the design of a controller (5.8) satisfying multiple $\mathcal{H}_\infty/\mathcal{H}_2$ performance objectives result, relying on a well-known nonlinear change of controller variables [103]. For these parameter-dependent LMIs, a finite set of sufficient LMIs is derived using the approach discussed in Section 5.3. The following two cases are distinguished:

- $D = 1$: No subdivision of the parameter domain Ω. In this case, the LMI relaxation approach is identical to the approach proposed in [28].

- $D = 4$: Subdivision of Ω into four convex polytopes. In the remainder of this chapter, we consider the specific subdivision shown in the right part of Figure 5.3 on page 71.

The $\mathcal{H}_\infty$ performance bound γ is minimized subject to a prefixed bound μ on the $\mathcal{H}_2$ performance. A lower value of μ guarantees better swing angle disturbance rejection at the expense of a lower bandwidth and a higher γ value, and vice-versa. Table 5.1 gives an overview of the obtained bounds γ for different prefixed bounds μ and different polynomial degrees p of the Lyapunov matrix, distinguishing between the cases $D = 1$ and $D = 4$. In addition, the provided number of scalar LMI variables, LMI blocks and computation times give insight into the numerical complexity.
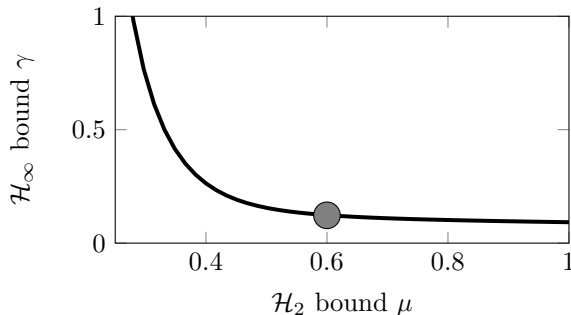
Figure 5.5: The trade-off between the prefixed $\mathcal{H}_2$ bound μ and the guaranteed $\mathcal{H}_\infty$ bound γ. The gray dot corresponds to the desired trade-off.

First of all, note that $D = 1$ and $D = 4$ yield the same bounds γ (up to two decimal digits) for each of the considered cases. In other words, subdivision of the parameter domain does not affect the closed-loop performance (for this specific example). However, the number of LMI blocks, and hence the computation times, are clearly influenced by subdivision. Table 5.1 indicates that the selected subdivision becomes more attractive as complexity of the associated LMI problem grows. On the other hand, no subdivision is preferable for simple LMI problems. Obviously, the number of LMI variables is independent of the selected subdivision.

Since increasing p does not result in significantly lower bounds γ, we select $p = 1$ (and $D = 4$) to compute a full-order controller as a starting point for the fixed-order LPV synthesis. An important consequence of selecting a low degree p is a full-order controller with *simple* polynomial parameter dependency (of degree 2 in this case), which is necessary to keep the fixed-order synthesis LMIs numerically attractive. For different prefixed values of μ, a bound γ is computed, resulting in the trade-off curve depicted in Figure 5.5. Controllers with different trade-offs have been implemented and tested experimentally. Based on the experimental responses on a reference step r and an impulse disturbance d_ϕ, we select the full-order controller corresponding to $\mu = 0.6$ with a $\mathcal{H}_\infty$ bound $\gamma = 0.123$, which is indicated by the gray dot in Figure 5.5. The state-space model (5.2) of this controller is characterized by 105 scalars.

5.4.4 Fixed-order $\mathcal{H}_\infty/\mathcal{H}_2$ controller design

Now we apply the approach proposed in Chapter 3 to design fixed-order LPV controllers for the practical LPV model (5.5), starting from the full-order

$\mathcal{H}_\infty/\mathcal{H}_2$ LPV controller with the optimal performance trade-off computed in Section 5.4.3. The closed-loop performances corresponding to different controller structures are compared.

In the parameter-dependent LMIs (3.14) and (3.17), we exploit the freedom to select different optimization variables for each performance specification, as explained in Section 3.4.3 on page 42. An affine Lyapunov matrix is selected for both the $\mathcal{H}_\infty$ and $\mathcal{H}_2$ performance, and the matrix $A_{22}(\alpha)$ is set to zero. Furthermore, the matrix $\Psi(\alpha) \in \mathbb{R}^{(n_x+n_u)\times(n_x+n_y)}$ is constructed from the computed full-order LPV controller with the desired performance trade-off (corresponding to the gray dot in Figure 5.5).

For the design of fixed-order LPV controllers, the state dimension $q = 2$ is selected and the following parameterizations are considered:

- **Affine (24 scalars):** We choose $Y_{11}(\alpha)$, $Y_{13}(\alpha)$, $Y_{31}(\alpha)$, $Y_{33}(\alpha)$ constant, and select $\bar{\Theta}(\alpha)$ to have an affine dependency on α.

- **Polynomial (degree 2, 36 scalars):** $Y_{11}(\alpha)$, $Y_{13}(\alpha)$, $Y_{31}(\alpha)$, $Y_{33}(\alpha)$ are set constant, while a polynomial dependency on α of degree 2 is selected for $\bar{\Theta}(\alpha)$.

- **Rational (affine/affine, 48 scalars):** $Y_{11}(\alpha)$, $Y_{13}(\alpha)$, $Y_{31}(\alpha)$, $Y_{33}(\alpha)$ and $\bar{\Theta}(\alpha)$ are all chosen affinely dependent on α.

For each controller parameterization, the bandwidth is optimized while the same $\mathcal{H}_2$ performance bound as for the full-order design ($\mu = 0.6$) is maintained. Numerical issues occur when solving the synthesis LMIs, resulting in unreliable closed-loop performance bounds. Therefore, guaranteed performance bounds γ are computed a posteriori by solving analysis LMIs.

Feasible solutions are obtained for all the considered cases. Table 5.2 provides an overview of the obtained $\mathcal{H}_\infty$ upper bounds γ, the computation times t_c (in seconds) and the number of scalar LMI variables associated with the computation of each fixed-order LPV controller. The number of full LMI blocks equals 180 for each case, with a maximum size of 28. As expected, an affine controller parameterization corresponds to a more conservative $\mathcal{H}_\infty$ bound than polynomial and rational parameterizations, while the numerical complexity of the associated synthesis problems is comparable.

The $\mathcal{H}_\infty$ upper bounds corresponding to the fixed-order LPV controller design are considerably higher compared to the full-order design. However, despite these conservative performance bounds, the polynomially and rationally parameter-dependent fixed-order LPV controllers have similar closed-loop performance (for

(a) Fixed-order LPV controller with affine parameter dependency.

(b) Fixed-order LPV controller with polynomial (degree 2) parameter dependency.

(c) Fixed-order LPV controller with rational (affine/affine) parameter dependency.
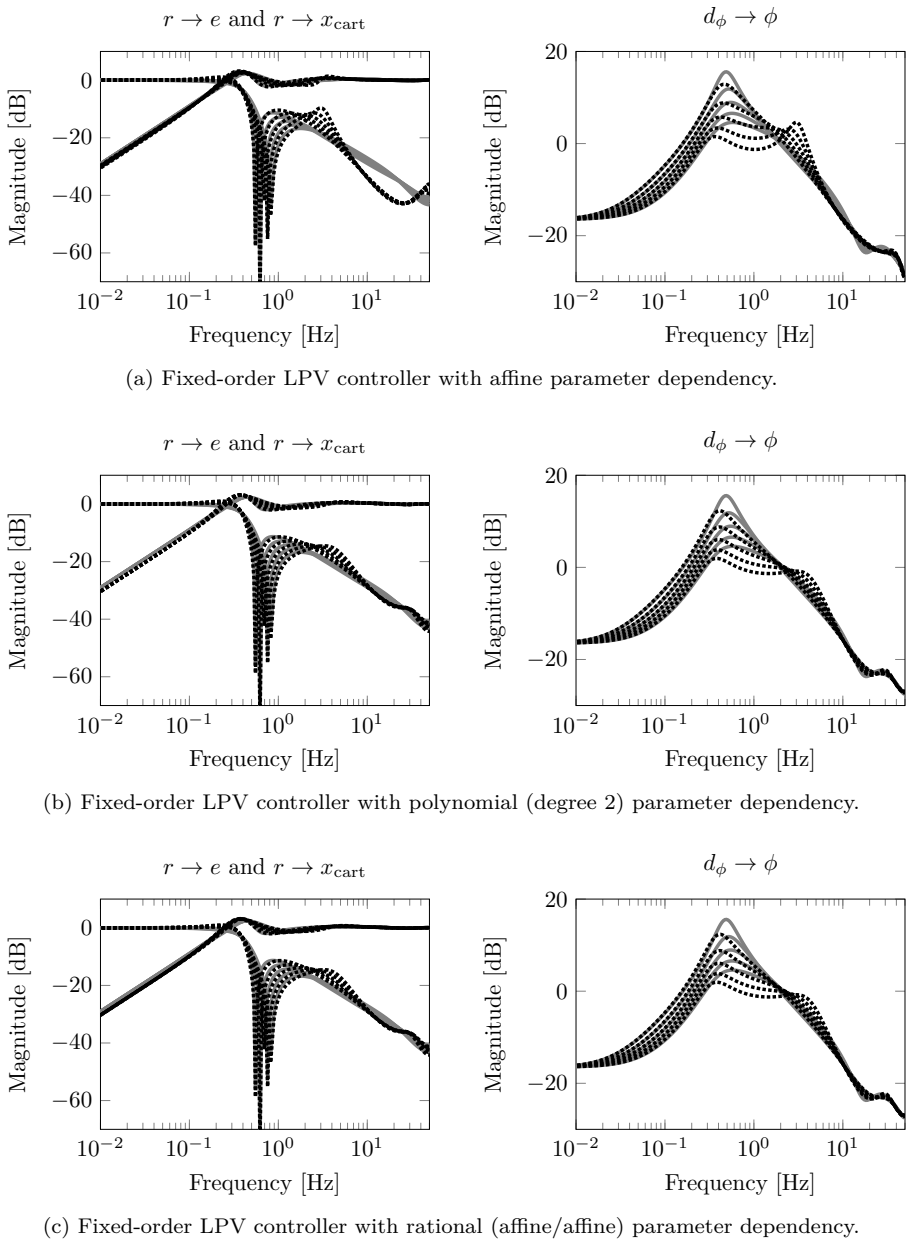
Figure 5.6: Bode magnitude plots of the closed-loop system corresponding to the fixed-order LPV controllers (dotted black) versus the full-order LPV controller (solid gray), evaluated for 5 equidistant cable lengths $\alpha \in [0.35, 0.75]$.

Table 5.2: The $\mathcal{H}_\infty$ bounds γ, computation times t_c (in seconds), and the number of scalar LMI variables corresponding to affine, polynomial, and rational controller parameterizations for $q = 2$. The number and maximum size of LMI blocks equals 180, respectively, 28 for each case.

	affine	polynomial	rational
γ	63.1	29.1	28.5
t_c	34.7	38.1	34.2
LMI variables	345	366	354

fixed cable lengths), and moreover clearly resemble the performance of the full-order controller. The latter is indicated in Figure 5.6 on page 76, showing Bode magnitude plots of the closed-loop system corresponding to the fixed-order LPV controllers versus the full-order LPV controller, evaluated for 5 equidistant fixed cable lengths α in the interval $[0.35, 0.75]$m. In the next section, we compare the experimental performances of the polynomially parameter-dependent fixed-order LPV controller and the full-order LPV controller for *varying* cable lengths.

5.4.5 Experimental results

Now we discuss the experimental validation of the fixed-order LPV controller design approach from Chapter 3 on the lab-scale overhead crane described in Section 5.4.1. The closed-loop performance of the full-order and the fixed-order LPV controllers, computed in Section 5.4.3 and Section 5.4.4, respectively, is investigated under the influence of a varying cable length. To this end, the following two experiments are performed:

- **Reference tracking:** A reference trajectory corresponding to a back and forth motion with a displacement of 0.4m is applied for the horizontal cart position in closed loop. This reference trajectory consists of piecewise 9th order polynomials (instead of discontinuous step functions) to avoid actuator saturation. Whenever a change in reference occurs, the cable is hoisted linearly at a rate of 0.4m/s as depicted in Figure 5.7, which is the maximum rate of parameter variation that the system can handle.

- **Disturbance rejection:** This experiment consists of three phases (see Figure 5.8):

  1. Starting from a system that is initially at rest, the horizontal cart position is changed rapidly without activating the controller, causing a freely swinging load.
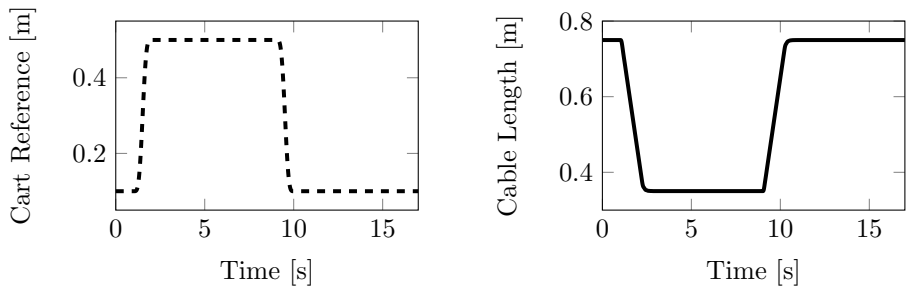
Figure 5.7: Reference for the cart position (left, dashed) and the cable length trajectory (right, solid) corresponding to the reference tracking experiment.
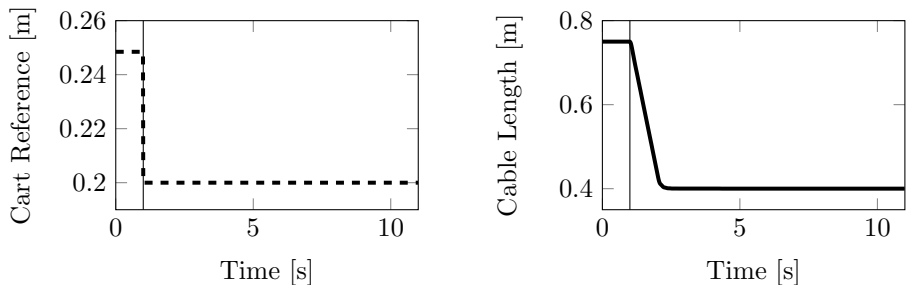
Figure 5.8: Reference for the cart position (left, dashed) and the cable length trajectory (right, solid) corresponding to the disturbance rejection experiment. The controller is activated at time $t = 1$ second, indicated by the thin vertical black line.

2. The load is freely swinging, while the horizontal cart position is constant.

3. When the deviation of the load reaches a maximum amplitude, and hence the load velocity is zero, the controller is activated. A fixed reference for the cart position is set, while the load is hoisted linearly.

We observed that the experimental performance of the full-order LPV controller is as desired. However, even for fixed cable lengths, undesired high-frequency chattering occurs when the affinely parameter-dependent fixed-order LPV controller is activated, implying that this controller is unsuitable for practical implementation. We attribute this undesired behavior to the high gain for the channels $r \rightarrow x_{\text{cart}}$ and $d_\phi \rightarrow \phi$ for frequencies around 3Hz, see Figure 5.6a. At the same time, the polynomially and rationally parameter-dependent fixed-order

LPV controllers have similar closed-loop performance as the full-order controller, as expected from Figure 5.6b and Figure 5.6c.

The results in Figure 5.9 (on page 80) and Figure 5.10 (on page 81) confirm that the polynomially parameter-dependent fixed-order LPV controller yields desired closed-loop behavior. Figure 5.9a and Figure 5.9b show the experimental (dotted black) and the simulated (solid gray) responses of the fixed-order, respectively, full-order LPV controller to a smooth reference trajectory (dashed gray) for the horizontal cart position and a cable length trajectory as in Figure 5.7. Similarly, the responses to an initial swing angle disturbance are shown in Figure 5.10a and Figure 5.10b. In the latter figures, the controller is activated at time $t = 1$ second, and the corresponding cable length trajectory is given in Figure 5.8. Note that, compared to the responses of the full-order LPV controller, the fixed-order LPV controller exhibits slightly more overshoot and a slightly slower response. However, realizing that the fixed-order LPV controller is described with only 36 scalars compared to 105 scalars for the full-order LPV controller, this modest difference in performance is impressive.

The fixed-order LPV controller with a rational parameter dependency features similar closed-loop behavior as the fixed-order LPV controller with a polynomial parameter dependency, both in simulations and experiments, as expected from Figure 5.6c.

5.5   Summary

This chapter has demonstrated the practical applicability of the fixed-order LMI framework (see Chapter 3) for LPV systems. For this class of systems, a numerically attractive relaxation technique was applied to derive tractable sufficient LMIs for fixed-order synthesis, resulting in an intuitive approach for fixed-order multi-objective $\mathcal{H}_\infty/\mathcal{H}_2$ LPV controller design. The viability of the proposed fixed-order LPV controller design approach for realistic engineering problems was confirmed by experimental validations of high performance fixed-order $\mathcal{H}_\infty/\mathcal{H}_2$ feedback controllers on a lab-scale overhead crane with varying cable length, which is accurately modeled as an LPV system. Namely, despite conservative performance bounds, fixed-order LPV controllers were designed that clearly resemble the performance of a high performance full-order controller.
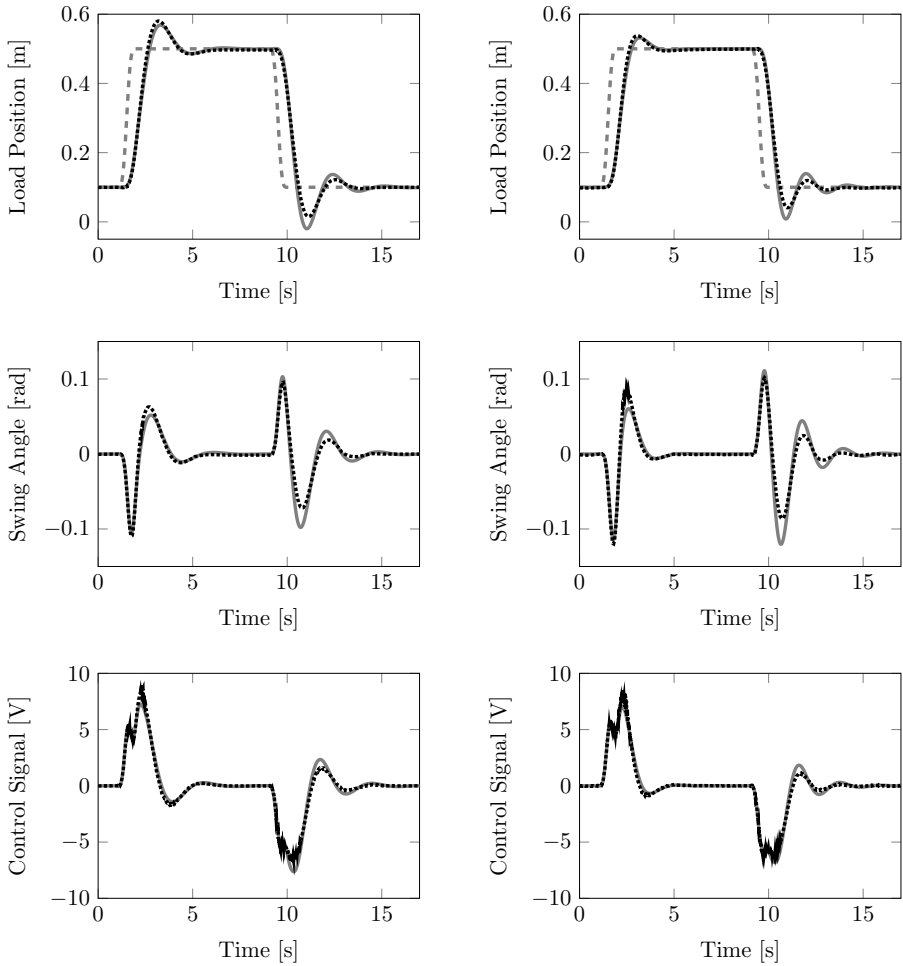
(a) Fixed-order LPV controller (2 states, polynomial degree 2).

(b) Full-order LPV controller (5 states, polynomial degree 2).

Figure 5.9: Reference tracking performance of the fixed-order (Figure 5.9a) and the full-order (Figure 5.9b) LPV controller. The experimental (dotted black) and simulated (solid gray) responses to a smooth reference trajectory (dashed gray) for the horizontal cart position are shown. Although the fixed-order LPV controller (36 scalars) yields slightly more overshoot and a slightly slower response compared to the full-order LPV controller (105 scalars), the overall performance is similar.
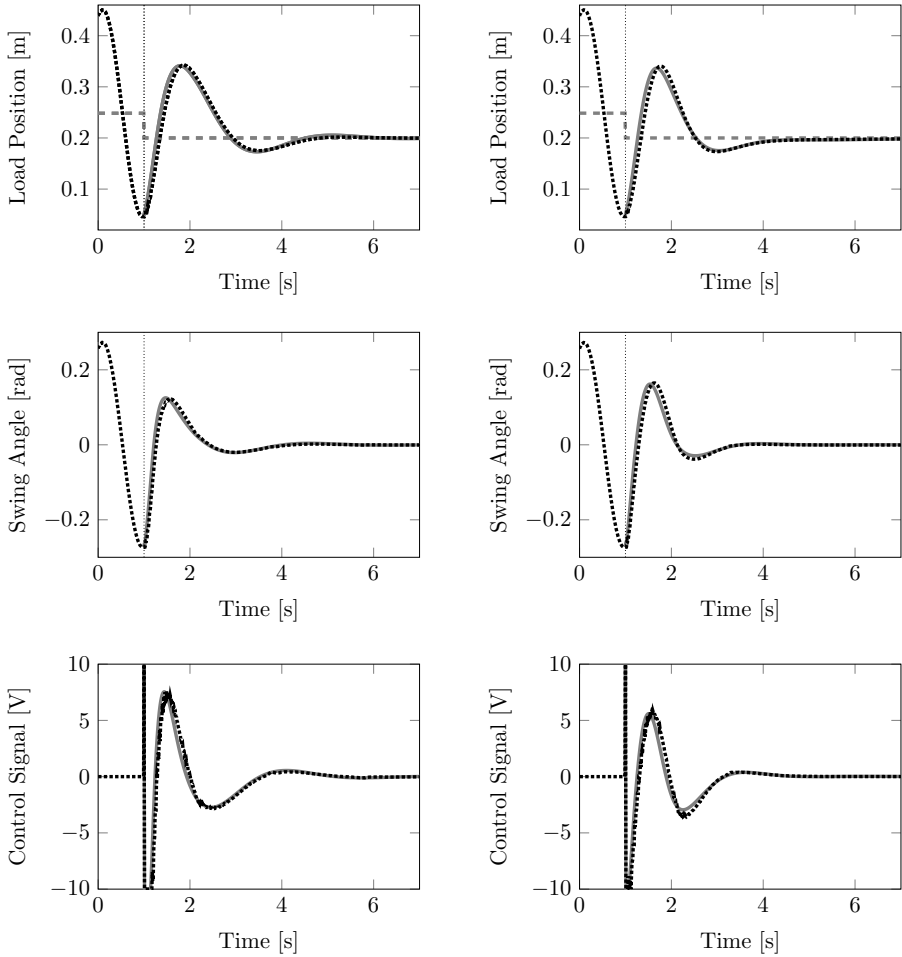
(a) Fixed-order LPV controller (2 states, polynomial degree 2).

(b) Full-order LPV controller (5 states, polynomial degree 2).

Figure 5.10: Disturbance rejection performance of the fixed-order (Figure 5.10a) and the full-order (Figure 5.10b) LPV controller. The experimental (dotted black) and simulated (solid gray) responses to an initial swing angle disturbance are shown. The controller is activated at time $t = 1$ second. Although the fixed-order LPV controller (36 scalars) yields slightly more overshoot and a slightly slower response compared to the full-order LPV controller (105 scalars), the overall performance is similar.

Recapitulation

- Applying the LMI framework to LPV systems results in an intuitive controller design approach, where the number of states and the parameter dependency of the controller are a priori fixed.

- To succesfully apply the fixed-order controller design approach from Chapter 3 to realistic LPV systems, a clever relaxation technique is necessary to obtain a numerically attractive optimization problem. Especially for complicated systems, subdivision of the polytopic domain into polytopes with fewer vertices seems promising, since this considerably reduces the number of sufficient LMIs.

- Taking into account bounded rates of parameter variation is essential to reduce conservatism that is inherent in the LPV synthesis approaches based on quadratic stability.

- Despite the conservatism of the fixed-order synthesis LMIs, high performance fixed-order multi-objective $\mathcal{H}_\infty/\mathcal{H}_2$ LPV controllers were obtained for a realistic engineering application.

Chapter 6

Fixed-order robust control of uncertain LTI systems

This chapter presents a convex approach to design fixed-order robust $\mathcal{H}_2/\mathcal{H}_\infty$ controllers for LTI systems affected by parametric uncertainty. Starting from an a priori computed stabilizing full-order parameter-dependent controller for the same system, which is designed under the assumption that the parameter is exactly known, the fixed-order LMI framework from Chapter 3 is exploited to compute fixed-order robust controllers with a guaranteed closed-loop $\mathcal{H}_\infty/\mathcal{H}_2$ performance for all parameter values. The result is a novel LMI procedure to iteratively compute less conservative robust controllers, utilizing a feasible solution of the fixed-order synthesis conditions as a starting point. Numerical comparisons with existing methods confirm the potential of the proposed robust controller design approach.

6.1 Introduction

The general fixed-order controller design problem for linear time-invariant (LTI) systems is challenging, even in the case of a single performance objective and without parametric uncertainty [50, 97, 103, 116]. This problem has already attracted many researchers since decades, and it still constitutes a field of active research to date due to its complexity.

As motivated in the introduction of Chapter 4 (see page 45), even for accurately known LTI systems the existence of a convex necessary and sufficient condition for fixed-order controller design is unknown. Although for the latter problem

several successful conservative convex approaches have been developed, the extension of these approaches to cope with parametric uncertainty is not evident [93].

Recently, an iterative LMI approach for robust static output feedback design is presented for continuous-time LTI systems subject to parametric uncertainty in [3], relying on an a priori computed parameter-dependent state feedback controller for a specific augmented system. This approach is readily extendable to design fixed-order robust controllers, and is based on the idea proposed in [92] for accurately known LTI systems. Additionally, sufficient LMIs for robust static output feedback design are proposed in [64, 107], incorporating scalar parameters in the LMIs to reduce conservatism at the expense of a higher numerical burden. In [96], an iterative LMI approach is presented to gradually compute fixed-order robust controllers with better performance for discrete-time polytopic systems.

In this chapter, the LMI framework presented in Chapter 3 is extended with an iterative LMI procedure to allow the design of high performance robust $\mathcal{H}_\infty/\mathcal{H}_2$ controllers for LTI systems with parametric uncertainty. In contrast to the aforementioned approaches, the resulting design approach handles any prefixed controller order, allows polynomial parameter dependencies of all system matrices, considers multiple performance objectives, and allows significant reductions of conservatism by iterative computation of robust controllers with better performance. The benefits of our approach are illustrated by numerical comparisons with existing methods.

6.2   Problem formulation

We consider the finite-dimensional LPD state-space representation (3.1) (see page 30), and assume that the parameter α is unknown but constant. The corresponding dynamics are uncertain LTI (see Table 2.1 on page 9), and hence take the form

$$\begin{cases} \delta x &= A(\alpha)x &+ B_w(\alpha)w &+ B_u(\alpha)u, \\ z &= C_z(\alpha)x &+ D_{zw}(\alpha)w &+ D_{zu}(\alpha)u, \\ y &= C_y(\alpha)x &+ D_{yw}(\alpha)w \end{cases} \qquad (6.1)$$

with state $x : \mathbb{T} \to \mathbb{R}^{n_x}$, exogenous input $w : \mathbb{T} \to \mathbb{R}^{n_w}$, control input $u : \mathbb{T} \to \mathbb{R}^{n_u}$, regulated output $z : \mathbb{T} \to \mathbb{R}^{n_z}$ and measured output $y : \mathbb{T} \to \mathbb{R}^{n_y}$. All system matrices are assumed to have a polynomial dependency on the time-invariant parameter $\alpha \in \Lambda$, where $\Lambda \in \mathbb{R}^N$ is a bounded convex polytope.

The aim is to design robust dynamic output feedback controllers

$$\begin{cases} \delta x_{\mathrm{c}} & = & A_{\mathrm{c}} x_{\mathrm{c}} & + & B_{\mathrm{c}} y, \\ u & = & C_{\mathrm{c}} x_{\mathrm{c}} & + & D_{\mathrm{c}} y, \end{cases} \tag{6.2}$$

with a preselected fixed order q ($0 \leq q \leq n_x$) that stabilize the uncertain system (6.1) and satisfy one or more closed-loop $\mathcal{H}_2$ and/or $\mathcal{H}_\infty$ performance specifications for all $\alpha \in \Lambda$. Hence, we consider optimization of the worst-case performance.

For any fixed value of $\alpha \in \Lambda$, let $H_\Theta(\alpha)$ denote the closed-loop system defined as in (3.4) on page 31. Then, for a fixed $\alpha \in \Lambda$, the $\mathcal{H}_\infty$ and $\mathcal{H}_2$ norm of $H_\Theta(\alpha)$ are indicated by $\|H_\Theta(\alpha)\|_\infty$, respectively, $\|H_\Theta(\alpha)\|_2$. The corresponding worst-case $\mathcal{H}_\infty$ and $\mathcal{H}_2$ performances of $H_\Theta(\alpha)$ are respectively given by $\max_{\alpha \in \Lambda} \|H_\Theta(\alpha)\|_\infty$ and $\max_{\alpha \in \Lambda} \|H_\Theta(\alpha)\|_2$.

6.3   Iterative LMI procedure

Relying on the LMI framework presented in Chapter 3, a convex procedure to iteratively reduce conservatism in a fixed-order robust $\mathcal{H}_2/\mathcal{H}_\infty$ control design is presented now. For the sake of clarity, we consider the single-objective fixed-order robust $\mathcal{H}_\infty$ control problem. The extension to handle $\mathcal{H}_2$ or multi-objective controller designs is straightforward.

A flowchart explaining the iterative LMI procedure for fixed-order robust $\mathcal{H}_\infty$ synthesis is shown in Figure 6.1. First a stabilizing parameter-dependent full-order controller is computed for the uncertain system (6.1) using, for instance, the convex approaches presented in [7, 28]. Subsequently, the LMI framework presented in Section 3.4 can be applied to design fixed-order robust controllers. It should be remarked that, compared to the LTI and LPV case, the selection of an initial full-order controller for fixed-order robust controller synthesis is complicated, since a high performance initial controller often leads to infeasibility of the fixed-order synthesis LMIs. To circumvent the latter issue, we propose the following approach: first, using a parameter-dependent full-order controller with good $\mathcal{H}_\infty$ performance, try to compute a fixed-order robust controller using (3.14) (see page 37). Whenever the latter LMI is infeasible, gradually relax the $\mathcal{H}_\infty$ bound that was used in the full-order controller design step by fixing it to a suboptimal value, solve the corresponding feasibility problem to obtain a suboptimal parameter-dependent full-order controller, and use this suboptimal full-order controller in the robust fixed-order synthesis step.

Suppose that the convex synthesis condition (3.14) provides a feasible solution. Then, as visualized in Figure 6.1, robust controllers with improved (not
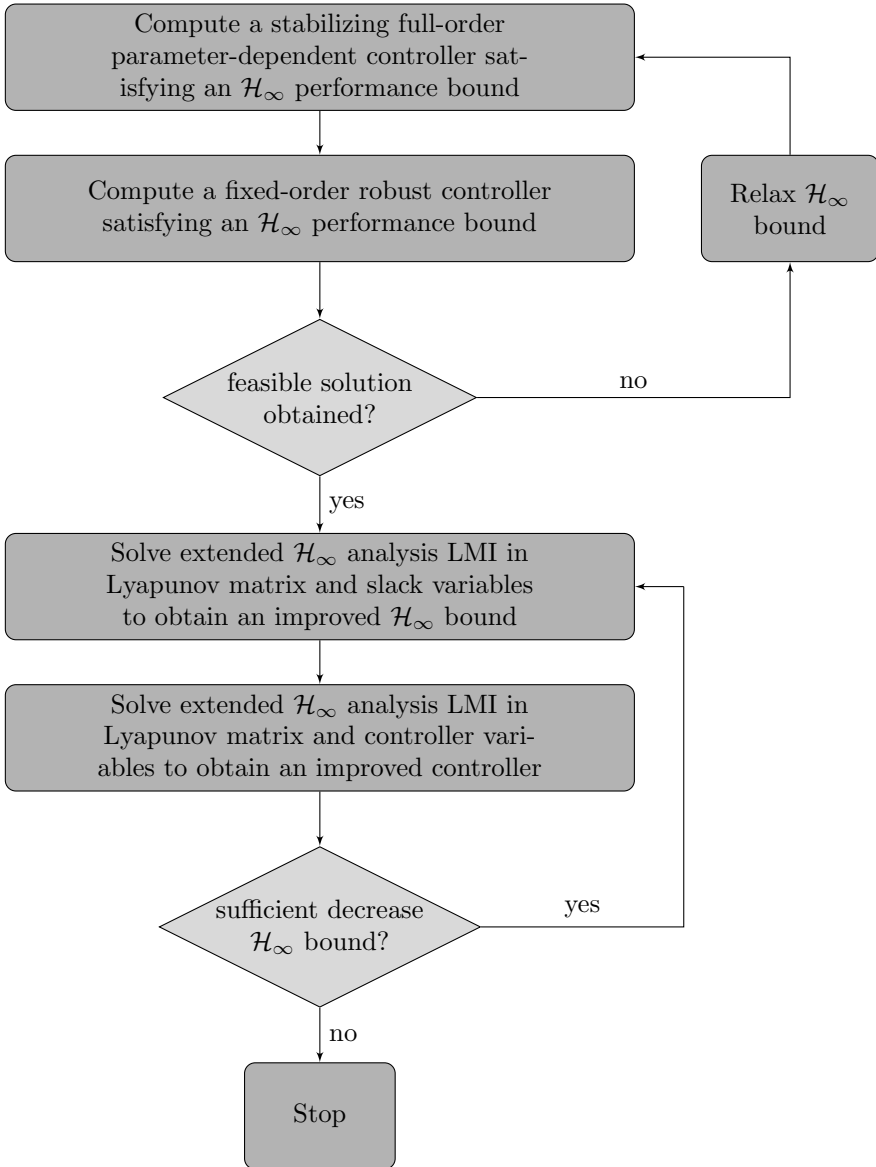
Figure 6.1: Flowchart of the iterative LMI procedure for fixed-order robust $\mathcal{H}_\infty$ control design.

necessarily strictly) worst-case $\mathcal{H}_\infty$ performance are obtained by alternately solving the analysis condition (3.9) (see page 33) in the optimization variables $P(\alpha)$, $X_1(\alpha)$, $X_2(\alpha)$, $X_3(\alpha)$, respectively, $P(\alpha)$, $\Theta_a(\alpha)$. The matrix $\Psi(\alpha)$ is fixed in the analysis LMI (3.14), since it does not influence the solution.

Specifically, the following LMI procedure is applied to iteratively compute robust controllers (of the same order) with improved worst-case $\mathcal{H}_\infty$ performance:

1. Using the convex synthesis condition (3.14), compute a robust controller $\Theta^{(0)}$ with a preselected fixed order q and a guaranteed worst-case $\mathcal{H}_\infty$ performance $\gamma^{(0)}$.

2. Set $k := 1$.

3. Substitute the solution variable $\Theta^{(k-1)}$ in the analysis condition (3.9), and optimize over the Lyapunov matrix $P(\alpha)$ and the slack variables $X_j(\alpha)$, $j = 1, 2, 3$, such that the performance bound $\gamma_a^{(k)}$ is minimized. Since substitution of the solution corresponding to the previous step implies that the constraint (3.9) is satisfied for $\gamma_a^{(k)} = \gamma^{(k-1)}$, we obtain $\gamma_a^{(k)} \leq \gamma^{(k-1)}$.

4. Substitute the solution variables $X_j(\alpha)$ (of the previous step) in the analysis condition (3.9), and optimize the performance bound $\gamma^{(k)}$ over the Lyapunov matrix $P(\alpha)$ and the controller variables $\Theta^{(k)}$, $A_{12}(\alpha)$, $A_{22}(\alpha)$ and $C_2(\alpha)$ (see (3.7) on page 32). Since $\Theta^{(k-1)}$ is a solution, we get that $\gamma^{(k)} \leq \gamma_a^{(k)}$.

5. If $|\gamma^{(k)} - \gamma^{(k-1)}|/\gamma^{(k-1)} < \epsilon$, with ϵ a predefined tolerance, stop. Else, set $k := k + 1$ and return to step 3.

It is remarked that, since the choice of $\Psi(\alpha)$ is irrelevant in the $\mathcal{H}_\infty$ analysis condition (3.9), theoretically speaking any value of $\Psi(\alpha)$ can be used in Step 3 and Step 4 without affecting the solution.

6.4   Numerical validation

This section considers two numerical examples to validate the iterative fixed-order robust $\mathcal{H}_2/\mathcal{H}_\infty$ controller design approach presented in Section 6.3, by means of comparisons with existing approaches. The LMIs are implemented and solved in MATLAB using the software packages Yalmip [72] and SeDuMi [113].

6.4.1   Robust $\mathcal{H}_\infty$ control

Consider the discretized mass-spring-damper system from Example II in [1], consisting of two masses $m_1 = 2$ [kg] and $m_2 = 1$ [kg], two springs with coefficients $k_1 \in [1, 4]$ [N/m] and $k_2 = 0.5$ [N/m], and a damper with uncertain damping constant $d \in [1, 4]$ [Ns/m]. The dynamics are expressed in the form (6.1) as follows

$$A(\alpha) = \begin{bmatrix} 1 & 0 & 0.1 & 0 \\ 0 & 1 & 0 & 0.1 \\ -\frac{0.1(k_1+k_2)}{m_1} & \frac{0.1k_2}{m_1} & 1 - \frac{0.1d}{m_1} & 0 \\ \frac{0.1k_2}{m_2} & -\frac{0.1k_2}{m_2} & 0 & 1 - \frac{0.1d}{m_2} \end{bmatrix},$$

$$B_w = \begin{bmatrix} 0 \\ 0.1 \\ 0.1 \\ 0 \end{bmatrix}, \quad B_u = \begin{bmatrix} 0 \\ 0 \\ \frac{0.1}{m_1} \\ 0 \end{bmatrix}, \quad C_z = \begin{bmatrix} 0 \\ 1 \\ 0 \\ 0 \end{bmatrix}', \quad C_y = \begin{bmatrix} 0 & 0 \\ 0 & 0 \\ 1 & 0 \\ 0 & 1 \end{bmatrix}',$$

$D_{zw} = 0$, $D_{zu} = 0$ and $D_{yw} = 0$, where only the A-matrix is uncertain and affinely dependends on the two-dimensional parameter

$$\alpha := \begin{bmatrix} k_1 & d \end{bmatrix}' \in [1, 4] \times [1, 4] = \Lambda.$$

The aim is to compute fixed-order robust controllers with optimal worst-case closed-loop $\mathcal{H}_\infty$ performance. As a starting point, a stabilizing full-order controller $\Psi(\alpha)$ with an affine dependency on α is computed with the approach [28]. Minimization of the $\mathcal{H}_\infty$ bound yields a parameter-dependent controller $\Psi(\alpha)$ for which the LMI (3.14) is infeasible. Therefore, we compute a suboptimal parameter-dependent $\mathcal{H}_\infty$ controller by fixing the $\mathcal{H}_\infty$ performance bound $\gamma = 12$ in the associated $\mathcal{H}_\infty$ synthesis LMIs and solving the corresponding feasibility problem, resulting in a suboptimal parameter-dependent controller with a guaranteed $\mathcal{H}_\infty$ performance of 7.66. Subsequently, fixed-order robust controllers of all orders $q = 0, \ldots, 4$ are computed by substituting $\Psi(\alpha)$ and $A_{22}(\alpha) = 0$ in the synthesis condition (3.14), and selecting an affine parameterization for the parameter-dependent LMI variables. The resulting worst-case $\mathcal{H}_\infty$ bounds are shown in the second row of Table 6.1, and are subject to conservatism (especially for $q = 0$). Therefore, the corresponding fixed-order robust controllers are used as a starting point in the iterative procedure proposed in Section 6.3 to compute less conservative robust controllers, taking all pameter-dependent LMI variables affine in α, and defining a tolerance $\epsilon = 10^{-3}$. For all controller orders, Figure 6.2 shows the worst-case $\mathcal{H}_\infty$ bound as a function of iterations, where the results of Step 3 and Step 4 corresponding to an iteration are indicated in black, respectively, gray. The third row of Table 6.1 shows the $\mathcal{H}_\infty$ bound $\gamma^{(k)}$ that is

Table 6.1: Worst-case $\mathcal{H}_\infty$ performance bounds for each order $q = 0, \ldots, 4$, resulting from Theorem 8 ($\gamma^{(0)}$) and subsequent application of the iterative procedure ($\gamma^{(k)}$, with k the number of iterations).

q	4	3	2	1	0
$\gamma^{(0)}$	9.39	15.5	10.3	14.0	4.39×10^4
$\gamma^{(k)}$ (k)	6.60 (15)	6.60 (40)	6.85 (34)	7.55 (8)	7.55 (20)

obtained after k iterations (when the LMI procedure terminated), and reveals a significant reduction of conservatism for all orders. Compared to the robust static output feedback design approach [1], which provided an $\mathcal{H}_\infty$ performance bound of 8.54 (i.e., for the case $q = 0$), we achieved a relative improvement of 12%. Moreover, no feasible solution was obtained with the robust static output feedback design approaches [32, 35, 36].

6.4.2 Robust multi-objective $\mathcal{H}_\infty/\mathcal{H}_2$ control

We consider a slightly modified version of the 3$^{\text{rd}}$ order discrete-time LTI model used in Example 4 of [32]:

$$\delta x = \begin{bmatrix} 2 & 0 & 1 \\ 1 & 0.5 & 0 \\ 0 & 1 & -\alpha_1 \end{bmatrix} x + \begin{bmatrix} 0 & 0 \\ 1 & 0 \\ 0 & 0 \end{bmatrix} w_2 + \begin{bmatrix} 1 \\ 0 \\ 0 \end{bmatrix} w_\infty + \begin{bmatrix} 1 \\ 0 \\ 0 \end{bmatrix} u,$$

with exogenous outputs

$$z_2 = \begin{bmatrix} x \\ u \end{bmatrix}, \quad z_\infty = \begin{bmatrix} 1 & 0 & 0 \end{bmatrix} x,$$

and measurement equation

$$y = \begin{bmatrix} 0 & 1 & 0 \end{bmatrix} x + \begin{bmatrix} 0 & \alpha_2 \end{bmatrix} w_2,$$

where $\alpha = \begin{bmatrix} \alpha_1 & \alpha_2 \end{bmatrix}' \in [0.45, 0.55] \times [0.9, 1.1] = \Lambda$.

The goal is to compute a robust full-order controller minimizing a bound μ on the worst-case $\mathcal{H}_2$ performance from w_2 to z_2, while an a priori imposed bound $\gamma = 3.5$ on the worst-case $\mathcal{H}_\infty$ performance from w_∞ to z_∞ is satisfied. Note that, due to an uncertain matrix relating w_2 to y, the approach [96] cannot be applied. First, a multi-objective parameter-dependent controller with an affine dependency on α is computed with the approach [28], resulting in the $\mathcal{H}_2$ bound $\mu = 19.04$, as shown in Table 6.2. A tighter bound $\mu_{\text{ana}} = 16.35$ is
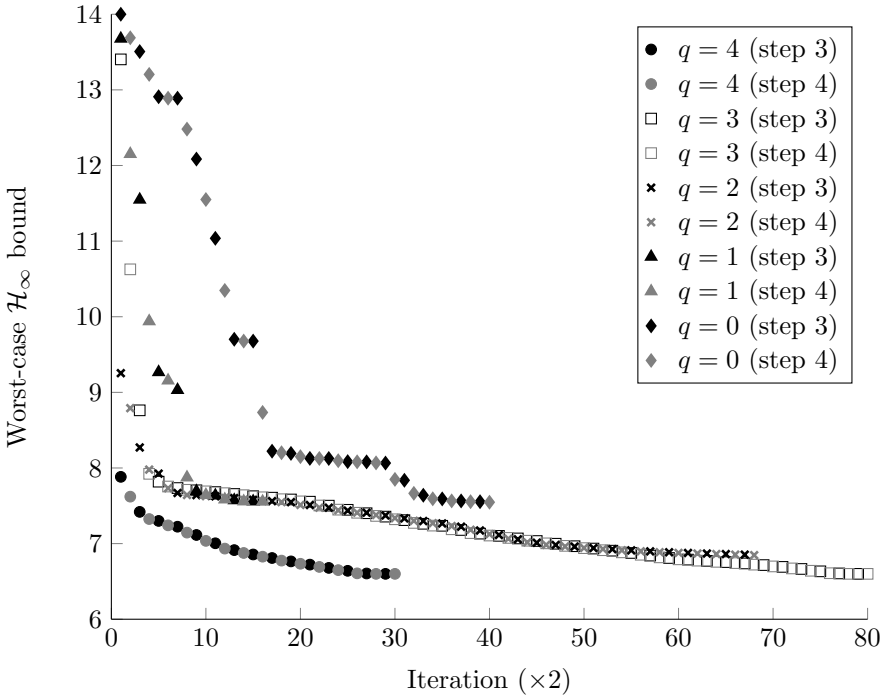
Figure 6.2: The iterative LMI procedure from Section 6.3 outperforms the approaches [1, 32, 35, 36], by computing high performance fixed-order robust $\mathcal{H}_\infty$ controllers. For each controller order, step 3 and step 4 of the iterative LMI procedure (see page 87) are indicated in gray, respectively, black.

computed by a posteriori solving an analysis LMI. Substituting the parameter-dependent controller for $\Psi(\alpha)$ (and $A_{22}(\alpha) = 0$) in the synthesis conditions of Theorem 8 and Theorem 9, a full-order robust controller guaranteeing a closed-loop $\mathcal{H}_\infty$ performance of 17.90 is computed, and a corresponding tighter bound $\mu_{\mathrm{ana}} = 16.38$. Applying the iterative procedure with $\epsilon = 10^{-4}$, a robust controller with a $\mathcal{H}_\infty$ bound $\mu = 16.33$ and $\mu_{\mathrm{ana}} = 16.31$ is computed in 10 iterations, outperforming the parameter-dependent controller.

6.5 Summary

This chapter has presented an iterative LMI procedure to design fixed-order robust $\mathcal{H}_2/\mathcal{H}_\infty$ controllers for LTI systems with parametric uncertainty,

Table 6.2: Comparison of the worst-case $\mathcal{H}_2$ performance bounds resulting from synthesis (μ) and a posteriori analysis (μ_{ana}), and the prefixed (a posteriori computed) $\mathcal{H}_\infty$ bounds γ (γ_{ana}), corresponding to the parameter-dependent, robust, and improved robust controller.

	μ	μ_{ana}	γ	γ_{ana}
Parameter dependent [28]	19.04	16.35	3.5	3.08
Robust (Theorems 8 and 9)	17.90	16.38	3.5	3.37
Improved robust (10 iterations)	16.33	16.31	3.5	3.35

extending the LMI framework for fixed-order controller design of Chapter 3. Starting from an a priori computed parameter-dependent full-order controller stabilizing the uncertain system for all parameter values, the sufficient LMIs from Chapter 3 were exploited to compute an initial fixed-order robust controller satisfying a closed-loop $\mathcal{H}_\infty$ and/or $\mathcal{H}_2$ performance specification. By iteratively applying the extended analysis LMIs presented in Section 3.3, alternating between optimization of different LMI variables, conservatism in this initial robust controller design was significantly reduced. The numerical example in Section 6.4.1 confirmed that, despite the potential conservatism of an initial robust $\mathcal{H}_\infty$ controller, application of the iterative LMI procedure resulted in high performance controllers, outperforming modern approaches available in the literature. In addition, the design of a robust controller with similar performance as a parameter-dependent controller (see Section 6.4.2) showed the potential of our approach for multi-objective robust control problems.

RECAPITULATION

- To obtain high performance fixed-order robust controllers, the fixed-order LMI framework is applied in conjunction with an iterative LMI procedure.

- The proposed iterative LMI procedure is an essential extension for robust control design. Namely, compared to the LTI and LPV case, the selection of an initial full-order controller (in the fixed-order synthesis LMIs) to obtain high performance fixed-order robust controllers is complicated, often implying conservative results.

- Conservatism in a fixed-order robust $\mathcal{H}_\infty/\mathcal{H}_2$ control design is significantly reduced by iteratively solving the extended analysis LMIs (3.9) and (3.11) (see page 33, respectively, page 34) in different optimization variables.

- The effectiveness of our approach is demonstrated by numerical comparisons with existing robust controller design approaches.

Chapter 7

Fixed-order controller design for LTD systems

This chapter presents a combined approach to design fixed-order multi-objective $\mathcal{H}_\infty/\mathcal{H}_2$ controllers for continuous-time linear time-delay (LTD) systems with delays in the state, input and/or output. This combined approach relies on the following steps. First, a novel Krylov based model order reduction technique is applied to obtain an accurate low-order LTI approximation of the original LTD system. Subsequently, exploiting the LMI framework for fixed-order controller design presented in Chapter 3, a fixed-order controller is designed for the delay-free approximation. Finally, the controller is validated on the original LTD system. The successful design of a fixed-order multi-$\mathcal{H}_2$ controller for a realistic LTD model of an experimental heat transfer setup confirms the potential of our approach for realistic industrial applications.

7.1 Introduction

The design of fixed-order (i.e., practical) controllers for LTD systems is challenging. Namely, this problem is equivalent to the design of a fixed-order controller for an infinite-dimensional LTI system [24], which is known to be nonconvex (see Section 4.1). To alleviate this issue, we propose a novel approach to reduce the infinite-dimensional system to a finite-dimensional LTI system, subsequently apply the approach of Chapter 3 to design a fixed-order controller for this reduced system, and validate the fixed-order controller in closed-loop with the original LTD system.

While results related to the reduction of LTD systems to finite-dimensional LTI systems are rare, and many problems related to the latter are generally considered to be unsolved [91], the availability of accurate delay-free models is favorable for many purposes. Namely, amongst others, such models make numerical simulation of large-scale systems computationally feasible and provide tractable models for control design.

In the proposed model order reduction approach (see Section 7.3), the presence of state delays is addressed by rewriting the original LTD system as an equivalent infinite-dimensional LTI system, as in [24]. Discretization of this system leads to a standard finite-dimensional LTI model, which is suitable for model reduction purposes. The followed discretization approach is based on a spectral approximation, inspired by [20]. Since the accuracy of the discretization depends on the choice of the interpolation points, we select the points such that the accuracy of the eigenvalues is optimized and, at the same time, structure and sparsity is introduced in the system matrices. Furthermore, we prove that the transfer function of the discretized system matches several moments with the transfer function of the original LTD system. Since the discretized LTI system usually features a large state dimension, we project it on a subspace using a Padé via Krylov like model reduction method, such that preservation of the moment matching properties is guaranteed. In addition, by exploiting the structure of the problem during the construction of the Krylov space, as in [59], the process is made dynamic in the sense that the number of discretization points in the spectral approximation does not need to be chosen beforehand, hence the model reduction process can always be resumed if the accuracy of the reduced model is insufficient. Finally, delays in input and output are replaced by Padé approximations, which also satisfy the property of matching multiple moments at zero.

For model reduction of linear systems based on moment matching, the Padé-via-Lanczos method and its variations are probably best known [11, 38, 42, 46]. These methods build a two-sided Krylov subspace with the system matrix and the input and output vectors as starting vectors. The advantage of two-sided methods is that both the input and the output are taken into account in the reduced models, which leads to matching twice as many moments for a given dimension of the reduced model compared to the case where only the input is taken into account. Despite this advantage, the proposed model order reduction approach relies on a one-sided Krylov-Padé method, since this allows us to fully exploit problem structure. Moreover, the proposed approach leads to an accurate approximation of the smallest characteristic roots of the time-delay system. Since the rightmost characteristic roots are typically among the smallest ones [80], this makes the reduced model suitable for control design purposes.

Section 7.4 discusses how the above model reduction technique is combined with

the controller design approach of Chapter 3 to successfully design fixed-order controllers for a realistic LTD model of an experimental heat transfer setup.

7.2 Problem formulation

We consider a continuous-time LTD system of the form

$$
\begin{cases}
\dot{x}(t) &= A_0 x(t) + \sum_{i=1}^{m_x} A_i x(t - \tau_i) + \sum_{i=1}^{m_u} B_i u_i(t - \mu_i), \\
y_i(t) &= C_i x(t - \nu_i) + \sum_{j=1}^{m_u} D_{ij}\, u_j(t - \nu_i - \mu_j), \quad i = 1, \ldots, m_y,
\end{cases}
\tag{7.1}
$$

where $x(t) \in \mathbb{R}^{n_x}$ is the state, $u_i(t)$, $i = 1, \ldots, m_u$ are the (multidimensional) inputs, and $y_i(t)$, $i = 1, \ldots, m_y$ correspond to the (multidimensional) outputs at time t. The quantities τ_i, $i = 1, \ldots, m_x$, μ_i, $i = 1, \ldots, m_u$ and ν_i, $i = 1, \ldots, m_y$ represent time-delays in the system states, inputs and outputs, respectively, where the largest state delay is denoted by $\tau_{\max} = \max_{i \in \{1, \ldots, m_x\}} \tau_i$.

The inputs u_i and outputs y_i are grouped in vectors as follows:

$$
\mathbf{u} = \begin{bmatrix} u'_1 & \cdots & u'_{m_u} \end{bmatrix}' : \mathbb{T} \to \mathbb{R}^{n_u}, \quad \mathbf{y} = \begin{bmatrix} y'_1 & \cdots & y'_{m_y} \end{bmatrix}' : \mathbb{T} \to \mathbb{R}^{n_y},
$$

where we assume that the number of scalar inputs does not exceed the dimension of the system state, i.e., $n_u \leq n_x$. Without loss of generality, the input $\mathbf{u}$ and output $\mathbf{y}$ are subdivided as

$$
\mathbf{u} = \begin{bmatrix} \mathbf{u}_1 \\ \mathbf{u}_2 \end{bmatrix}, \quad \mathbf{y} = \begin{bmatrix} \mathbf{y}_1 \\ \mathbf{y}_2 \end{bmatrix},
$$

to distinguish between exogenous inputs $\mathbf{u}_1$ and control inputs $\mathbf{u}_2$ on the one hand, and regulated outputs $\mathbf{y}_1$ and measured outputs $\mathbf{y}_2$ on the other hand. Then, the main objective is to design a fixed-order dynamic output feedback LTI controller

$$
K : \begin{cases}
\delta x_{\mathrm{c}} &= A_{\mathrm{c}} x_{\mathrm{c}} & + & B_{\mathrm{c}} \mathbf{y}_2, \\
\mathbf{u}_2 &= C_{\mathrm{c}} x_{\mathrm{c}} & + & D_{\mathrm{c}} \mathbf{y}_2,
\end{cases}
\tag{7.2}
$$

with $x_{\mathrm{c}} \in \mathbb{R}^q$, $q \in \mathbb{N}$, exponentially stabilizing the LTD system (7.1) and guaranteeing one or more closed-loop $\mathcal{H}_\infty / \mathcal{H}_2$ performance specifications from (parts of) $\mathbf{u}_1$ to (parts of) $\mathbf{y}_1$.

Defining the block matrices

$$
\mathbf{B} = \begin{bmatrix} B_1 & \cdots & B_{m_u} \end{bmatrix}, \quad \mathbf{C} = \begin{bmatrix} C_1 \\ \vdots \\ C_{m_y} \end{bmatrix}, \quad \mathbf{D} = \begin{bmatrix} D_{11} & \cdots & D_{1m_u} \\ \vdots & & \vdots \\ D_{m_y 1} & \cdots & D_{m_y m_u} \end{bmatrix}.
$$
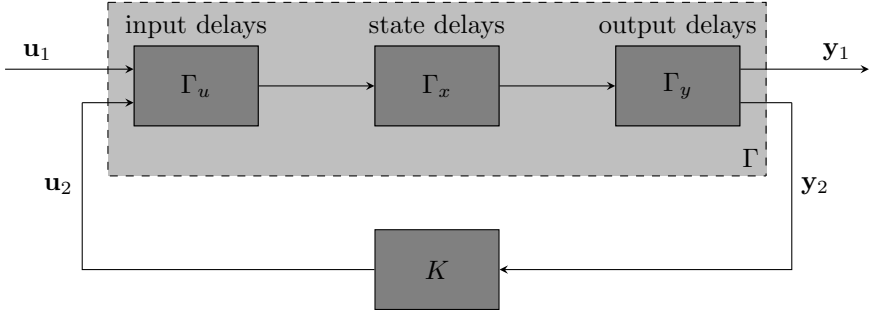
Figure 7.1: The objective is to design a fixed-order LTI controller (7.2) for the LTD system (7.1), such that the closed-loop system is exponentially stable and satisfies one or more $\mathcal{H}_\infty/\mathcal{H}_2$ performance specifications from (parts of) $\mathbf{u}_1$ to (parts of) $\mathbf{y}_1$.

and the transfer functions

$$\Gamma_x(s) = \mathbf{C}\left(sI - A_0 - \sum_{i=1}^{m_x} A_i e^{-s\tau_i}\right)^{-1}\mathbf{B} + \mathbf{D}, \qquad (7.3)$$

$$\Gamma_y(s) = \mathrm{diag}\left(e^{-s\nu_1}I, \ldots, e^{-s\nu_{m_y}}I\right),$$

$$\Gamma_u(s) = \mathrm{diag}\left(e^{-s\mu_1}I, \ldots, e^{-s\mu_{m_u}}I\right),$$

the transfer function of (7.1) is expressed as

$$\Gamma(s) := \Gamma_y(s)\Gamma_x(s)\Gamma_u(s). \qquad (7.4)$$

It should be emphasized that the transfer function Γ_x corresponds to an LTD system with only state delays, while Γ_y and Γ_u characterize the output, respectively, input delays of the LTD system (7.1). Namely, the decomposition (7.4) is exploited to efficiently compute an LTI approximation of the LTD system (7.1), which is the context of the following section. Subsequently, the approach of Chapter 3 can be applied to design fixed-order $\mathcal{H}_\infty/\mathcal{H}_2$ controllers for the approximating LTI system, and hence for the original LTD system when this approximation is sufficiently accurate. Figure 7.1 schematically visualizes the main control objective.

7.3   Krylov based model order reduction

This section presents a Krylov based model order reduction approach for LTD systems of the form (7.1). In fact, relying on the decomposition

(7.4), this approach consists of two steps. First, Section 7.3.1 presents a numerically attractive Krylov based technique to obtain a finite-dimensional LTI approximation of the transfer function Γ_x, corresponding to an LTD system with only state delays. Then, Section 7.3.2 discusses how Padé approximations are used to obtain approximating LTI models of the transfer functions Γ_u and Γ_y, characterizing input and output delays, respectively.

7.3.1 Approximation of LTD systems with only state delays

To obtain a finite-dimensional LTI approximation of an LPD system with only state delays, the approach of [79] is adopted and extended to the MIMO case. Specifically, we consider the transfer function Γ_x, corresponding to the time-domain representation

$$\begin{cases} \dot{x}(t) &= A_0 x(t) + \sum_{i=1}^{m_x} A_i x(t - \tau_i) + \mathbf{B}\mathbf{u}(t), \\ \mathbf{y}(t) &= \mathbf{C}x(t) + \mathbf{D}\mathbf{u}(t). \end{cases} \tag{7.5}$$

Finite-dimensional approximation

An approach to analyze the time-delay system (7.5) is to rewrite it as an ordinary differential equation on a function space. Discretizing the corresponding operators yields an approximation of (7.5) in the form of a finite-dimensional LTI system, involving large matrices and no delays. The latter is briefly summarized next, followed by a discussion on several useful properties of the discretized system. As a main result, we show that the specific discretization fulfills a moment matching property, playing an important role in the derivation of the reduced model.

A spectral discretization To obtain an infinite-dimensional LTI representation of (7.5), we define a new state variable z_1 which, at time t, equals the trajectory of the state x on the interval $[t - \tau_{\max}, t]$, see Figure 7.2, and consider the space $X := \mathbb{R}^{n_x} \times \mathcal{L}_2([t - \tau_{\max}, t], \mathbb{R}^{n_x})$. Then, defining the derivative operator $\mathcal{A}: X \to X$ as

$$\mathcal{D}(\mathcal{A}) = \left\{ z = (z_0, z_1) \in X : z_1(t) \in \mathcal{C}^1([t - \tau_{\max}, t], \mathbb{R}^{n_x}), \ z_0(t) = x(t) \right\},$$

$$\mathcal{A}z(t) = \left(A_0 z_0(t) + \sum_{i=1}^{m_x} A_i z_1(t - \tau_i), \dot{z}_1(t) \right), \quad z \in \mathcal{D}(\mathcal{A}),$$
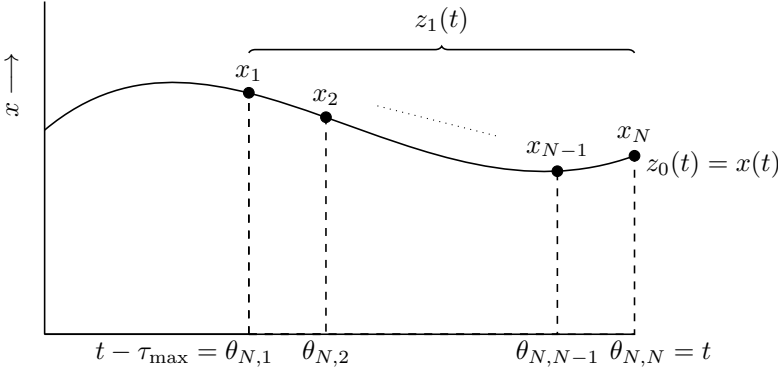
Figure 7.2: An infinite-dimensional LTI representation of the LTD system (7.5) is derived by defining a state $z_1(t)$ as the evolution of the trajectory of state x on the interval $[t - \tau_{\max}, t]$. Subsequently, discretizing $z(t)$ into a finite set of states $x_1, \ldots, x_N$ yields a finite-dimensional LTI approximation.

and the operators $\mathcal{B} : \mathbb{R}^{n_u} \to X$ and $\mathcal{C} : X \to \mathbb{R}^{n_y}$ as

$$
\begin{aligned}
\mathcal{B}\mathbf{u} &= (\mathbf{B}\mathbf{u}, 0), \quad \mathbf{u} \in \mathbb{R}^{n_u}, \\
\mathcal{C}z &= \mathbf{C}z_0, \qquad z = (z_0, z_1) \in X.
\end{aligned}
$$

the LTD system (7.5) can be rewritten as the infinite-dimensional LTI system

$$
\begin{cases}
\dot{z} &= \mathcal{A}z &+ \mathcal{B}\mathbf{u}, \\
\mathbf{y} &= \mathcal{C}z &+ \mathbf{D}\mathbf{u},
\end{cases}
\tag{7.6}
$$

where $z(t) \in \mathcal{D}(\mathcal{A}) \subset X$. Note that, in the definition of $\mathcal{A}$, the system dynamics of (7.5) are used to determine the derivative at the boundary (i.e., at time t).

System (7.6) can be discretized using a *spectral method* (see, e.g. [20, 117]). Given a positive integer N and $t \in \mathbb{R}_+$, we consider a mesh Ω_N of N distinct points in the interval $[t - \tau_{\max}, t]$:

$$
\Omega_N = \{\theta_{N,i}, \ i = 1, \ldots, N\},
\tag{7.7}
$$

where

$$
t - \tau_{\max} \leq \theta_{N,1} < \ldots < \theta_{N,N-1} < \theta_{N,N} = t.
$$

This allows us to replace the continuous space X with the space X_N of discrete functions defined over the mesh Ω_N. That is, any state trajectory $z \in X$ is discretized into a block vector $x = \begin{bmatrix} x_1' & \cdots & x_N' \end{bmatrix}' \in X_N$ with components

$$
x_i = z(\theta_{N,i}) \in \mathbb{R}^{n_x}, \quad i = 1, \ldots, N,
$$

which is also indicated in Figure 7.2. We let $\mathcal{P}_N x$, $x \in X_N$, be the unique $\mathbb{R}^{n_x}$ valued interpolating polynomial of degree smaller than or equal to $N - 1$, satisfying

$$\mathcal{P}_N x(\theta_{N,i}) = x_i, \quad i = 1, \ldots, N.$$

In this way we can approximate the operator $\mathcal{A}$ over X with the matrix $A_N : X_N \to X_N$, defined as

$$\begin{cases} (A_N x)_i & = & \frac{d\mathcal{P}_N x}{dt}(\theta_{N,i}), \quad i = 1, \ldots, N - 1, \\ (A_N x)_N & = & A_0 \mathcal{P}_N x(t) + \sum_{i=1}^{m_x} A_i \mathcal{P}_N x(t - \tau_i). \end{cases} \tag{7.8}$$

Using the Lagrange representation of $\mathcal{P}_N x$,

$$\mathcal{P}_N x = \sum_{k=1}^{N} l_{N-1,k} x_k,$$

where the Lagrange polynomials $l_{N-1,k}$ are real valued polynomials of degree $N - 1$ satisfying

$$l_{N-1,k}(\theta_{N,i}) = \begin{cases} 1 & \text{if } i = k, \\ 0 & \text{if } i \neq k, \end{cases}$$

we get an explicit form for the matrix A_N,

$$A_N = \begin{bmatrix} d_{1,1} & \cdots & d_{1,N} \\ \vdots & & \vdots \\ d_{N-1,1} & \cdots & d_{N-1,N} \\ a_1 & \cdots & a_N \end{bmatrix} \in \mathbb{R}^{N n_x \times N n_x}, \tag{7.9}$$

where

$$\begin{cases} d_{i,k} & = & \dot{l}_{N-1,k}(\theta_{N,i}) I_{n_x}, \\ a_k & = & A_0 l_{N-1,k}(t) + \sum_{i=1}^{m_x} A_i l_{N-1,k}(t - \tau_i). \end{cases}$$

In a similar fashion, $\mathcal{B}$ and $\mathcal{C}$ are approximated by

$$B_N = \begin{bmatrix} 0 & \cdots & 0 & 1 \end{bmatrix}' \otimes \mathbf{B}, \quad C_N = \begin{bmatrix} 0 & \cdots & 0 & 1 \end{bmatrix} \otimes \mathbf{C},$$

respectively, resulting in the following finite-dimensional approximation of the LTD system (7.5):

$$\begin{cases} \dot{z} & = & A_N z & + & B_N \mathbf{u}, \\ \mathbf{y} & = & C_N z & + & \mathbf{D} \mathbf{u}, \end{cases} \tag{7.10}$$

with $z : \mathbb{T} \to \mathbb{R}^{N n_x}$. In the frequency domain this approximation is described by the transfer function

$$\Gamma_x^N(s) := C_N \left(sI - A_N\right)^{-1} B_N + \mathbf{D}. \tag{7.11}$$

Properties The discretized system (7.10) has the favorable property that several moments (i.e., the function and its derivatives) of the original transfer function (7.3) and its approximation (7.11) coincide at zero and infinity. Specifically, at the origin the first N moments coincide, while at infinity the function value and the first derivative coincide. This is formalized in the following theorem (see [79], Theorem 2.1).

Theorem 10 (Matching moments)**.** *The transfer functions* (7.3) *and* (7.11) *satisfy*

$$\left.\frac{d^i \Gamma_x^N(s)}{ds^i}\right|_{s=0} = \left.\frac{d^i \Gamma_x(s)}{ds^i}\right|_{s=0}, \quad i = 0, \ldots, N-1, \tag{7.12}$$

and

$$\left.\frac{d^i \Gamma_x^N(s^{-1})}{ds^i}\right|_{s=0} = \lim_{\substack{s \to 0 \\ \Re(s)=0}} \frac{d^i \Gamma_x(s^{-1})}{ds^i}, \quad i = 0, 1. \tag{7.13}$$

That is, the moments of $\Gamma_x^N(s)$ *and* $\Gamma_x^N(s)$ *at zero match up to the* $(N-1)$*th moment, and the moments at infinity match up to the first moment*[1].

The properties described by Theorem 10 are *independent* of the choice of the grid points. Hence, other desired properties can be imposed by an optimal choice of the distribution of the grid points. Therefore, the grid points are specified as

$$\theta_{N,i} = \frac{\tau_{\max}}{2}(\alpha_{N,i} - 1), \quad \alpha_{N,i} = -\cos\left(\frac{\pi i}{N}\right), \quad i = 1, \ldots, N, \tag{7.14}$$

corresponding to scaled and shifted zeros of the so-called Chebyshev polynomial of the second kind and order $N-1$. With the choice of the Chebyshev grid (7.14), the convergence of the individual eigenvalues of A_N to corresponding characteristic roots is fast. More specifically, in [20] it is proven that spectral accuracy (approximation error $O(N^{-N})$) is obtained. An additional property of using a Chebyshev grid, observed in extensive numerical simulations, is that the eigenvalues of A_N which have not yet converged to corresponding characteristic roots, are located to the left of the eigenvalues that have already converged (see, for instance, the plots in [20]). Additionally, this choice of grid points allows a sparse system representation characterized by the transfer function

$$\Gamma_x^N(s) = F_N \left(sG_N - I\right)^{-1} H_N + \mathbf{D}. \tag{7.15}$$

Appendix C.1 provides the explicit derivation of the sparse system matrices F_N, G_N and H_N from the approximation (7.10) (see [79], Lemma 3.1).

---

[1]In the right hand side of (7.13) we consider the limit along the imaginary axis. When dropping this restriction, the limit does not exist since $s = \infty$ is an essential singularity of both Γ_x and Γ.

As a matter of fact, an *adaptive* construction of the sparse approximation (7.15) is possible, in the sense that an increase of the number of grid points N can be dealt with by extending the corresponding matrices. This is formalized in Appendix C.2.

Constructing a reduced-order model

As discussed in the previous section, the discretized system (7.10) features attractive approximation properties. However, a major drawback is that the order (Nn_x) of (7.10) is considerably larger than the order (n_x) of the original time-delay system (7.5). On the other hand, (7.10) attains a standard LTI form, thus conceptually allowing an order reduction by applying a standard Krylov based technique. While the latter usually involves an explicit construction of the large matrices in (7.10), we will show that this can be avoided by exploiting the sparse structure of (7.15), hence allowing an efficient implementation. Moreover, the construction is dynamic in the sense that the value of N in (7.11) does not need to be fixed a priori.

Dynamic construction of a Krylov space   The model reduction is achieved by projecting the large and sparse matrices F_N, G_N and H_N from (7.15) on an appropriately defined subspace. Instrumental to this we use the dynamic construction of a Krylov space of G_N, presented in [59]. This construction is in turn inspired by methods for polynomial eigenvalue problems that exploit structure to reduce the storage cost of the Krylov vectors [12, 39, 78]. Appendix C.3 summarizes the construction of a Krylov space (in a slightly adapted form), allowing the derivation of reduced models based on a projection.

Reduced model by projection, moment matching properties   We now arrive at the derivation of an approximation of Γ_x^N, defined by (7.11) or, equivalently, (7.15), having a prescribed order k. A possible approach is to construct the Krylov space $\mathcal{K}_k(G_N, x_0)$ with Algorithm 1 (see Appendix C.3) and project the matrices F_N, G_N and H_N, corresponding to the sparse system representation (7.15), on this Krylov space. Assuming $N \geq k$, an orthogonal projection on the Krylov space yields a kth order approximation of $\Gamma_x^N(s)$:

$$\Gamma_x^{(k)}(s) = F^{(k)}(sG^{(k)} - I)^{-1}H^{(k)} + \mathbf{D}, \tag{7.16}$$

where

$$F^{(k)} = F_k V_k, \quad G^{(k)} = \mathcal{H}_k, \quad H^{(k)} = V_k' H_k, \tag{7.17}$$

and the matrices

$$V_k \in \mathbb{R}^{kn_x \times kn_u}, \quad \mathcal{H}_k \in \mathbb{R}^{kn_u \times kn_u}$$

refer to the output of Algorithm 1 presented in Appendix C.3. It is important to note that the matrices $F^{(k-1)}$ and $H^{(k-1)}$ are *submatrices* of $F^{(k)}$ and $H^{(k)}$. Therefore, they can be constructed in a dynamic way during the iterations of Algorithm 1, as is the case with the so-called Hessenberg matrix $\mathcal{H}_k$.

With a particular choice of block vector x_0, transfer function (7.16) satisfies the following moment matching property with the (original) transfer function Γ_x of LTD system (7.5).

Theorem 11 (Matching moments reduced model)**.** *Let $k \in \mathbb{N}$ sastisfy $k \geq 2$ and let $V_k \in \mathbb{R}^{kn_x \times kn_u}$. Assume that the columns of V_k form an orthogonal basis of $\mathcal{K}_k(G_k, R_0^{-1}\mathbf{B})$. Then the transfer function (7.16) satisfies*

$$\left. \frac{d^i \Gamma_x^{(k)}(s)}{ds^i} \right|_{s=0} = \left. \frac{d^i \Gamma_x(s)}{ds^i} \right|_{s=0}, \quad i = 0, \ldots, k-2, \tag{7.18}$$

and

$$\left. \frac{d^i \Gamma_x^{(k)}(s^{-1})}{ds^i} \right|_{s=0} = \lim_{\substack{s \to 0 \\ \Re(s)=0}} \frac{d^i \Gamma_x(s^{-1})}{ds^i}, \quad i = 0, 1. \tag{7.19}$$

Proof. See Appendix C.4. $\square$

Figure 7.3 provides a complete schematic overview of the Krylov based model order reduction approach applied to the LTD system (7.5). The overall approximation of Γ_x by the rational transfer function $\Gamma_x^{(k)}$ is described in Appendix C.5.

7.3.2 Taking into account input-output delays

The approximation of Γ_x by $\Gamma_x^{(k)}$ exhibits a good spectral approximation, in the sense that the smallest characteristic roots are accurately approximated and moments at zero and at infinity are preserved. In addition, the application of the Krylov method to $G_N \sim A_N^{-1}$ leads to non-converged eigenvalues of the reduced model having a favorable location, see [79].

Based on the decomposition (7.4), the overall transfer function Γ can be approximated by

$$\Gamma^{(k)} = \Gamma_y^{(k)} \Gamma_x^{(k)} \Gamma_u^{(k)}, \tag{7.20}$$

TDS with only state delays:
$A_0, \ldots, A_{m_x}$, **B**, **C**, **D**

Infinite-dimensional LTI system:
$\mathcal{A}, \mathcal{B}, \mathcal{C}$, **D**

finite-dimensional
approximation

N moments at 0
2 moments at ∞

LTI system of dimension Nn_x:
A_N, B_N, C_N, **D**

$k - 1$ moments at 0
2 moments at ∞

Sparse representation:
F_N, G_N, H_N, **D**

Krylov based
projection

$k - 1$ moments at 0
2 moments at ∞

Reduced LTI model of order k:
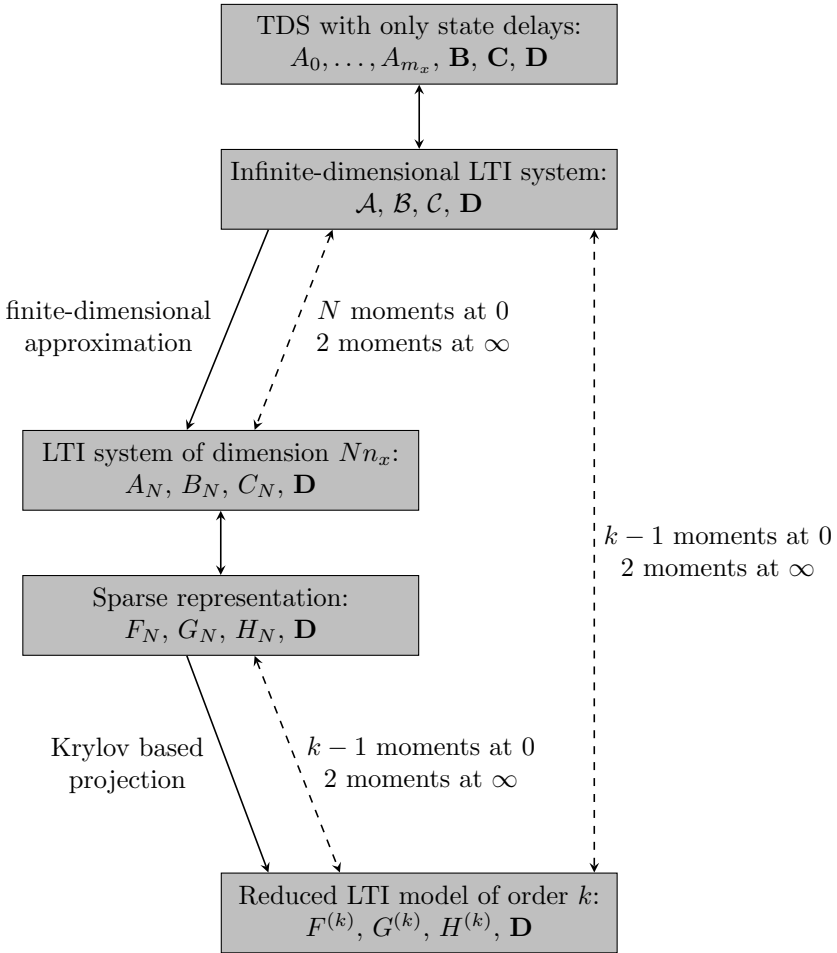$F^{(k)}$, $G^{(k)}$, $H^{(k)}$, **D**

Figure 7.3: Schematic overview of the numerically efficient Krylov based model order reduction approach.

where $\Gamma_y^{(k)}$ and $\Gamma_u^{(k)}$ are obtained from Γ_y and Γ_u using a (ℓ, ℓ)-Padé approximation of $e^{-s\mu_i}$, $i = 1, \ldots, m_u$, and $e^{-s\nu_i}$, $i = 1, \ldots, m_y$, with

$$\ell = \left\lceil \frac{k}{2} \right\rceil - 1. \tag{7.21}$$

Inherent to a Padé approximation, the introduced characteristic roots are in the open left half plane.

Due to the choice of order of Padé approximant (7.21) and the chain rule, moments of Γ are preserved at zero, in the sense that

$$\left. \frac{d^i \Gamma^{(k)}(s)}{ds^i} \right|_{s=0} = \left. \frac{d^i \Gamma(s)}{ds^i} \right|_{s=0}, \quad i = 0, \ldots, k-2.$$

In the presence of input and output delays, moments at infinity of Γ are in general not well defined since

$$\lim_{\substack{s \to 0 \\ \Re(s) = 0}} \frac{d^i \Gamma(s^{-1})}{ds^i}, \quad i \in \{0, 1\},$$

does not exists, except for $i = 0$ and Γ strictly proper. However, since the moment matching property holds between Γ_x and $\Gamma_x^{(k)}$ and a Padé approximation is characterized by a feedtrough at infinity equal to ± 1, the modulus of the feedthrough term of Γ as well as the asymptotic decay rate of the amplitude of the transfer function (up to -40dB/decade) carry over.

Finally, transfer function (7.20) can be realized by a LTI system of the form

$$\begin{cases} \dot{\xi}(t) &= A^{(k)}\xi(t) + B^{(k)}\mathbf{u}(t), \\ \mathbf{y}(t) &= C^{(k)}\xi(t) + \mathbf{D}\mathbf{u}(t). \end{cases} \tag{7.22}$$

The order of (7.22) is equal to $kn_u + \ell(m_y + m_u)$ in case all input and output channels are subject to delays. Note that, as a property inherited from a spectral discretization, the dimension of the LTI approximation does not depend on the number of state delays m_x.

Remark 7. *In case Γ has less outputs than inputs, it is favorable to approximate Γ_x', corresponding to*

$$\begin{cases} \dot{x}(t) &= A_0' x(t) + \sum_{i=1}^{m_x} A_i' x(t - \tau_i) + \mathbf{C}' \mathbf{y}(t), \\ \mathbf{u}(t) &= \mathbf{B}' x(t) + \mathbf{D}' \mathbf{y}(t), \end{cases}$$

in the first place, and use the transposed system of the resulting LTI approximation subsequently, without losing the properties mentioned above. This switch, which has been implemented in the software, leads to a dimension of the reduced model equal to $k \min(n_u, n_y) + \ell(m_y + m_u)$.

7.4 Fixed-order control of an experimental heat transfer setup

This section considers the design of fixed-order multi-objective controllers (7.2) for a realistic LTD model (7.1) of an experimental heat transfer setup. To compute a fixed-order controller for the LTD system, we apply the model order reduction technique from Section 7.3 to obtain a sufficiently accurate LTI approximation of the LTD model, and subsequently use the approach from Chapter 3 to design a fixed-order controller for this approximation. The effectiveness of this combined approach is assessed by a numerical validation of the performance of the closed-loop time-delay model. The LMIs are implemented and solved in MATLAB using the software packages Yalmip [72] and MOSEK [84].

7.4.1 Model description

The experimental setup, shown in Figure 7.4, consists of two closed and independent heating circuits with water as heat transfer medium. The main components of the system are a heater and a cooler for each circuit, which are connected with pipelines of extendable length, and a heat exchanger. The delays in the system, characterized by the ratios between the lengths of pipelines and the flow velocities, play a crucial role in the system dynamics.

We consider the realistic model from [81] (see also [120]). This LTD model of the form (7.1) has a state vector of dimension $n_x = 10$, corresponding to temperatures [°C] at different places of the setup. The measured output, denoted by $\mathbf{y}_2$, as in Figure 7.1, is equal to the state vector (i.e., all temperatures are measured). The control input $\mathbf{u}_2$ (see Figure 7.1) is the set-point value of the slave PI control loop (included in the model) that controls the performance of the left heater. An exogenous input d adjusts the performance of the left cooler and is considered here as a disturbance, while the controlled variable T_c (the last element of the state vector) is the temperature measured at the output of the left cooler. Furthermore, the system has 5 state delays ($\tau_1 = 3$s, $\tau_2 = 5$s, $\tau_3 = 15$s, $\tau_4 = 23$s, $\tau_5 = 29$s), 2 input delays ($\mu_1 = 6$s, $\mu_2 = 7$s) and no output delays.

7.4.2 Derivation of a reduced delay-free model

In this section, an LTI approximation of the realistic LTD model (see Section 7.4.1) is determined by applying the Krylov based model order reduction
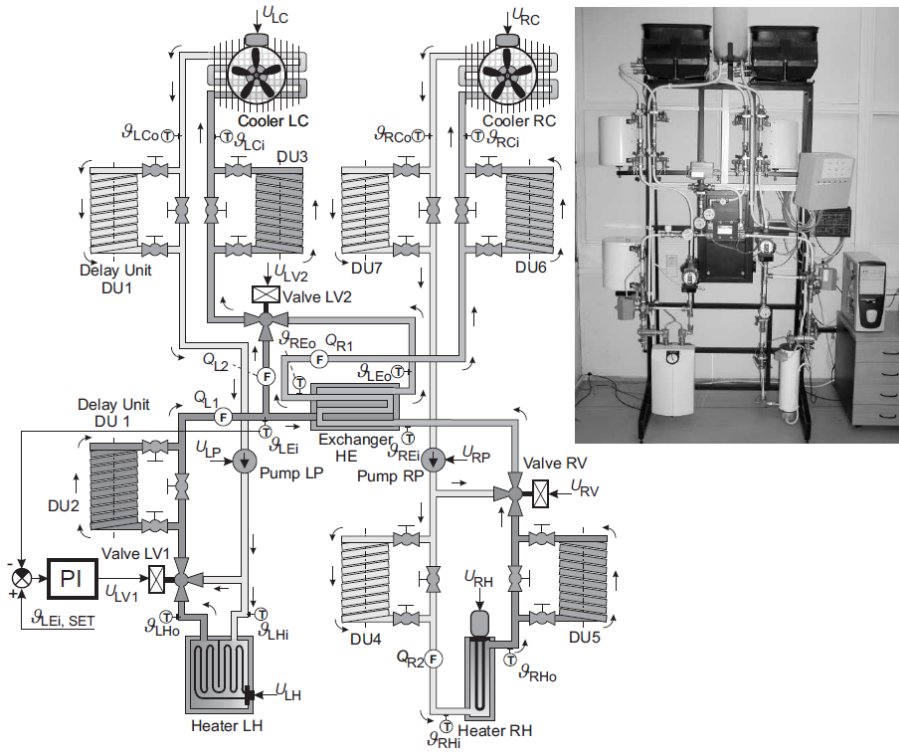
Figure 7.4: The experimental heat transfer setup and its schematic representation.

technique presented in Section 7.3.

It is important to realize that, while an accurate LTI approximation is desired, a low order approximation is attractive for control design. To satisfy these conflicting specifications, we select $k = 10$, corresponding to $k - 1$ matching momtents at zero and 2 at infinity (see Theorem 11). Since the input delay corresponding to the disturbance input d ($\mu_1 = 6$s) does not influence performance, it is set to zero without loss of generality. This results in an LTI system (7.22) of order 25. To assess the accuracy of this delay-free approximation, the relevant (single-input single-output) transfer functions of the original LTD system (7.1) and its LTI approximation (7.22) are compared. The corresponding Bode magnitude plots are shown in Figure 7.5, revealing a maximum error of approximately -40dB, which is satisfactory for this application. Note that, since 2 moments are matched at infinity, the asymptotic decay rates of the original time-delay system and its delay-free approximation correspond up to a
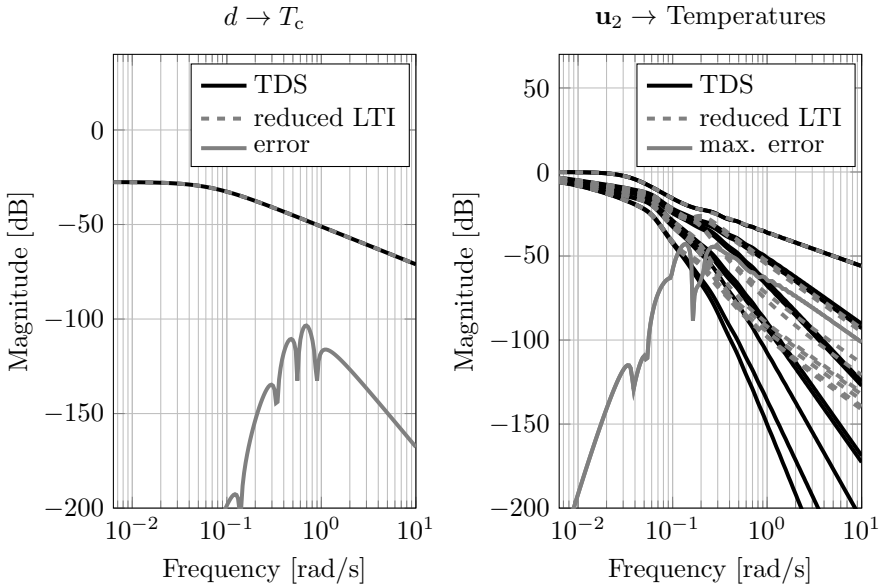
Figure 7.5: Bode magnitude plots corresponding to relevant input-output channels of the LTD model (solid black), its delay-free approximation (dashed gray), and the (maximum) error (solid gray). Left: $d \rightarrow T_c$, where T_c is the temperature at the output of the left cooler. Right: $\mathbf{u}_2$ to each measured temperature (i.e., each element of output vector $\mathbf{y_2}$).

decay rate of -40dB/decade.

7.4.3 Controller design

This section considers the design of a high performance fixed-order controller for the delay-free approximation (7.22) of the realistic heat transfer model (7.1), using the approach of Chapter 3. The aim is to achieve a fast response to a constant reference for the temperature T_c at the output of the left cooler, while limiting the energy consumed by the system.

To this end, a reference signal r is defined such that, in accordance with Figure 7.1, the exogenous input is composed as $\mathbf{u}_1 = \begin{bmatrix} d & r \end{bmatrix}'$. To counteract the effect of a disturbance d on the temperature T_c, an integrator is added to the LTI approximation by defining the error $e := r - T_c$ and introducing an additional state variable

$$z(t) := \int_0^t e(v)dv, \tag{7.23}$$

corresponding to an extra state equation $\dot{z} = r - T_c$. Subsequently, the regulated output $\mathbf{y}_1$ is constructed as $\mathbf{y}_1 = \begin{bmatrix} z & \mathbf{y}_2' \end{bmatrix}'$. The resulting LTI system, with input $\mathbf{u} = \begin{bmatrix} \mathbf{u}_1' & \mathbf{u}_2' \end{bmatrix}'$ and output $\mathbf{y} = \begin{bmatrix} \mathbf{y}_1' & \mathbf{y}_2' \end{bmatrix}'$, has a state, input and output dimension of, respectively, 26, 3 and 21.

Considering the closed-loop interconnection of this LTI system with a controller (7.2) (and grouping the controller variables as in (3.3) on page 31), a bound γ_1 on the $\mathcal{H}_2$ norm is minimized for the closed-loop channel $H_{\Theta,1} : r \to z$ to optimize performance, subject to a bound γ_2 on the $\mathcal{H}_2$ norm for the channel $H_{\Theta,2} : d \to \mathbf{y}_2$ to limit energy consumption. Specifically, the optimization problem for the design of a fixed-order controller (7.2) attains the following form:

$$\begin{aligned} \underset{\Theta, \gamma_1, \gamma_2}{\text{minimize}} \quad & \gamma_1 \\ \text{subject to:} \quad & \|H_{\Theta,1}\|_2 < \gamma_1, \quad \|H_{\Theta,2}\|_2 < \gamma_2, \\ & \gamma_1 < b_1, \qquad\qquad \gamma_2 < b_2, \end{aligned} \tag{7.24}$$

where the (optional) prefixed bounds $b_1 \in \mathbb{R}_+$ and $b_2 \in \mathbb{R}_+$ are incorporated to bound the feasible set associated with the optimization, and thus avoid numerical issues. We select the bounds $b_1 = 8$ and $b_2 = 2.5 \times 10^{-2}$.

First, a (conservative) full-order multi-$\mathcal{H}_2$ controller, denoted by Ψ, is computed with the Lyapunov shaping paradigm [103], with closed-loop $\mathcal{H}_2$ performances $\|H_{\Psi,1}\|_2 = 7.73$ and $\|H_{\Psi,2}\|_2 = 1.61 \times 10^{-2}$. This controller is obtained by solving the LMI feasibility problem corresponding to (7.24) (i.e., instead of optimizing γ_1). Namely, while minimization of γ_1 results in slightly better $\mathcal{H}_2$ performance of the closed-loop LTI system, the associated closed-loop LTD system is unstable. We attribute this to the fact that, in the latter case, the delay-free approximation of the closed-loop LTD system is not sufficiently accurate.

Substituting the obtained full-order controller Ψ in the fixed-order $\mathcal{H}_2$ synthesis LMIs (3.17), and selecting $A_{22} = -I_{26-q}$, controllers with a state dimension of $15 \leq q \leq 25$ are computed. (No feasible solutions were obtained for $q \leq 14$ with the selected bounds b_1 and b_2.) Initially γ_1 is optimized, and a feasibility problem is solved instead whenever numerical issues occur. The results are summarized in Table 7.1, showing the obtained $\mathcal{H}_2$ bounds γ_i, $\mathcal{H}_2$ norms $\|H_{\Theta,i}\|_2$, $i = 1, 2$, number of scalar LMI variables and computation times associated with the LMI optimization problem for each state dimension q. It is clear that, for $18 \leq q \leq 25$, the same closed-loop performance as the initial full-order controller is achieved, while for the cases $q = 17$ and $q = 16$ the performance is only slightly affected. At the same time, it should be emphasized that for $q = 15$ a significant improvement of performance is achieved compared to the full-order controller, see the discussion below Remark 5 on page 39.

Table 7.1: For each controller order $15 \leq q \leq 25$, the $\mathcal{H}_2$ bounds μ_i, a posteriori calculated $\mathcal{H}_2$ norms $\|H_{\Theta,i}\|_2$, $i = 1, 2$, number of scalar LMI variables and computation times t_c (in seconds) corresponding to the optimization problem (7.24) are shown. The controller of order $q = 15$ outperforms the initial full-order controller, confirming the merits of the fixed-order LMI framework presented in Chapter 3 for multi-objective control design.

q	μ_1	$\|H_{\Theta,1}\|_2$	μ_2	$\|H_{\Theta,2}\|_2 \times 10^2$	LMI variables	t_c
25	7.73	7.73	2.45	1.61	4506	76.8
24	7.73	7.73	2.45	1.61	4472	83.2
23	7.73	7.73	2.45	1.61	4440	77.8
22	7.73	7.73	2.45	1.61	4410	85.0
21	7.95	7.73	2.44	1.61	4382	44.1
20	7.95	7.73	2.44	1.61	4356	49.0
19	7.95	7.72	2.44	1.61	4332	42.7
18	7.95	7.74	2.44	1.61	4310	34.9
17	7.88	7.81	2.46	1.58	4290	31.6
16	7.95	7.83	2.44	1.57	4272	27.3
15	7.96	7.13	2.45	1.92	4256	51.1

Remark 8 (Exact state measurements). *In the LTD model (7.1) of the heat transfer setup, 10 exact state measurements are considered (i.e., it is assumed that no noise affects the measurements). Therefore, in the delay-free approximation (7.22) of (7.1), these same 10 states are, at least approximately, measured (as a linear combination of 26 states). As discussed in [9], this implies that a controller (7.2) with $q = 26 - 10 = 16$ states exists that achieves the same performance as an (optimal) full-order controller for the LTI system (7.22).*

Remark 8 clarifies that, for $16 \leq q \leq 25$, controllers with *similar* performance as the initial full-order controller Ψ are obtained, see Table 7.1. It is important to stress that, despite the potential conservatism of the approach of Chapter 3, the amount of introduced conservatism is negligible. As a matter of fact, a *reduction* of conservatism is achieved for $q = 15$, confirming the merits of our fixed-order LMI framework for multi-objective control design.

7.4.4 Validation

This section validates the performance of the controllers (7.2) with $q = 26$ and $q = 15$ states, designed in the previous section, in closed-loop with the original LTD model (7.1) of the experimental heat transfer setup and its delay-free

approximation (7.22). Comparisons are provided between the closed-loop LTD system and its delay-free approximation on the one hand, and between the performance of the full-order ($q = 26$) and fixed-order ($q = 15$) controller on the other hand.

Figure 7.6 shows several important transfer functions corresponding to the LTD system and its delay-free approximation, interconnected with the full-order ($q = 26$), respectively, fixed-order ($q = 15$) controller. These transfer functions show that, for both controllers, the delay-free model accurately approximates the closed-loop LTD system. Furthermore, it is clear that the performance of both controllers is similar. The controller with $q = 15$ states has a slightly higher bandwidth, suggesting a faster response as indicated by the left part of Figure 7.7. The added integrator (7.23) enforces the transfer functions $r \to e$ to be zero at zero frequency, implying that constant disturbances d are completely attenuated, see the right part of Figure 7.7. Note that the fixed-order controller yields a more agressive input response, see also Figure 7.8 on page 113, clarifying more overshoot in the responses shown in Figure 7.7b compared to Figure 7.7a.

7.5 Summary

This chapter has presented a combined approach to design fixed-order multi-objective $\mathcal{H}_\infty/\mathcal{H}_2$ controllers for LTD systems featuring delays in the state, input and/or output. In this combined approach, first a novel Krylov based model order reduction technique was applied in conjunction with standard Padé approximations to obtain an accurate low-order LTI approximation of the original LTD system. Subsequently, a fixed-order controller was designed for this approximating LTI model with the approach presented in Chapter 3. In a final step, the controller was validated on the original LTD system. This approach was applied to design fixed-order multi-$\mathcal{H}_2$ controllers for a realistic LTD model of an experimental heat transfer setup. For this LTD model with 10 states, 2 inputs, 10 outputs, and 7 delays, a delay-free approximation with 25 states was obtained. Both full-order ($q = 26$) and fixed-order ($q = 15$) controllers were designed for the approximation, and successfully validated on the original LTD model, confirming the potential of our combined approach for industrial engineering applications.
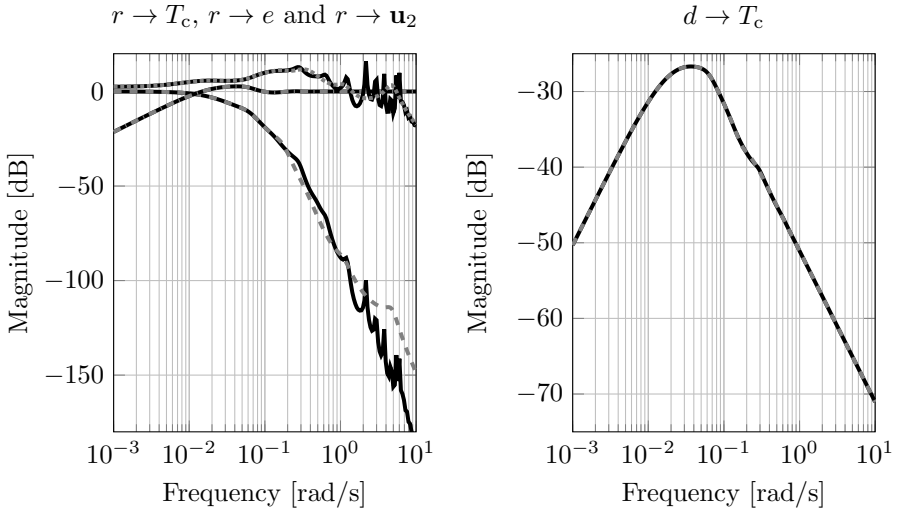
(a) Controller with $q = 26$ states
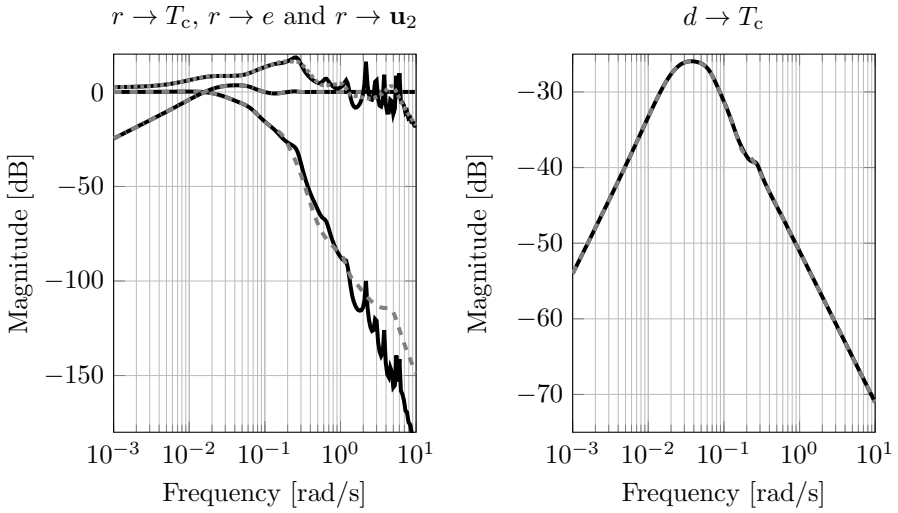
(b) Controller with $q = 15$ states

Figure 7.6: Bode magnitude plots corresponding to the LTD system (solid black) and its delay-free approximation (gray) in closed-loop with a controller of order $q = 26$ (top) and $q = 15$ (bottom). Left: the transfer functions $r \to T_{\mathrm{c}}$ (dashed), $r \to e$ (dashdotted) and $r \to \mathbf{u}_2$ (dotted). Right: the transfer function $d \to T_{\mathrm{c}}$.
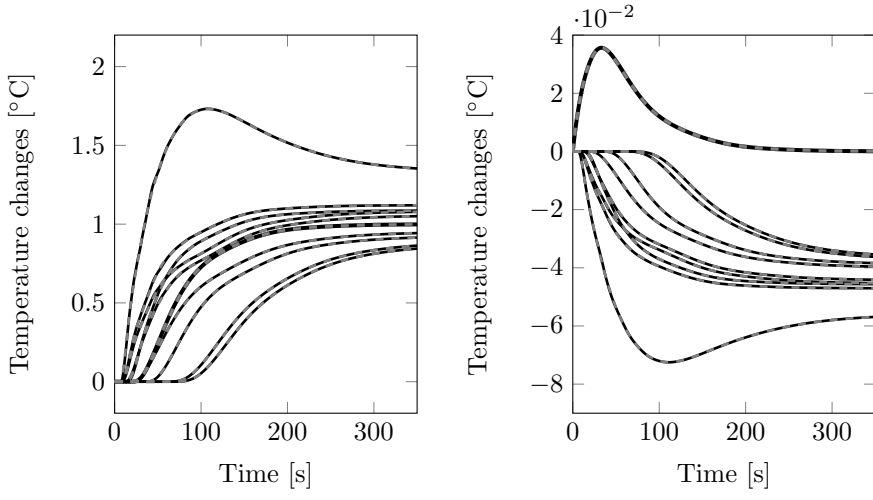
(a) Controller with $q = 26$ states
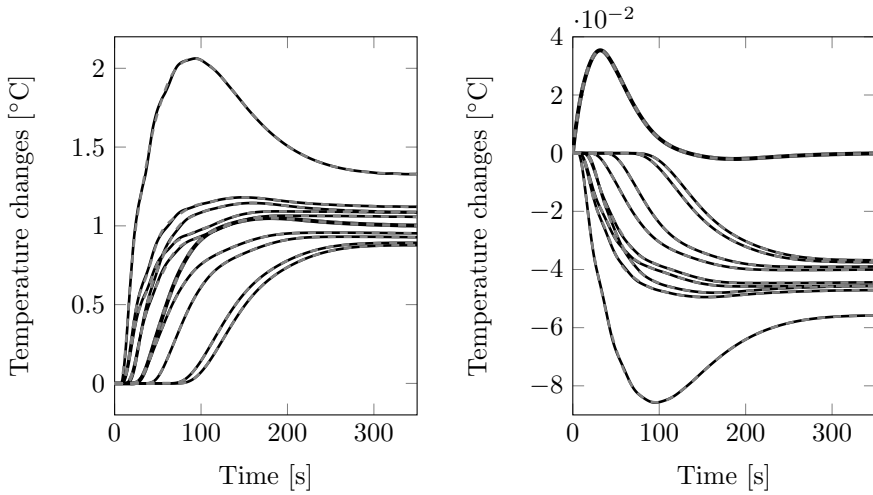
(b) Controller with $q = 15$ states

Figure 7.7: Reference tracking and disturbance rejection performance of the controllers with $q = 26$ states (top) and $q = 15$ states (bottom). The response of the regulated temperature T_c (thick) and the other measured temperatures (thin) to a reference step (left) and disturbance step (right) is shown for the closed-loop LTD system (black) and its delay-free approximation (dashed gray).
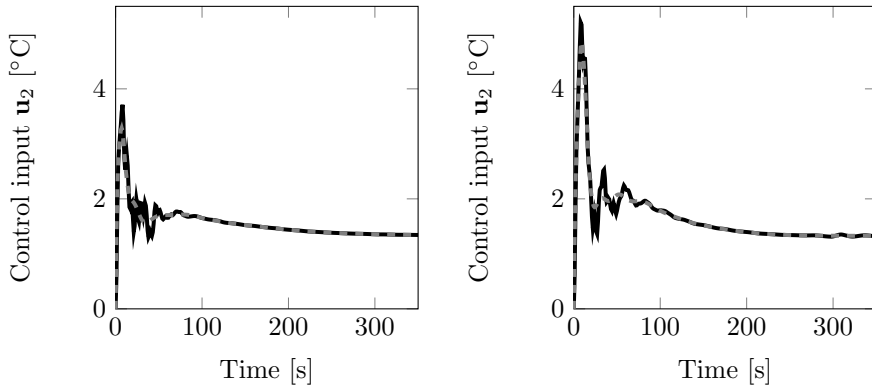
Figure 7.8: Response of the control input $\mathbf{u}_2$ to a reference step of the LTD system (solid black) and its delay-free approximation (dashed gray) in closed-loop with the full-order controller ($q = 26$, left) and the fixed-order controller ($q = 15$, right).

Recapitulation

- By combining a novel Krylov based model order reduction technique with the LMI framework for fixed-order controller design of Chapter 3, fixed-order $\mathcal{H}_\infty/\mathcal{H}_2$ controllers are designed for LTD systems.

- To obtain a delay-free approximation of an LTD system, the system is rewritten as an equivalent infinite-dimensional LTI system. Subsequently, a specific spectral discretization is applied, having the favorable property that several moments of the transfer function are preserved at zero and infinity. Additionally, proper selection of the set of grid points allows a sparse system representation.

- A Krylov based model order reduction approach is applied to systematically reduce the number of states of the delay-free approximation, exploiting sparsity and moreover satisfying attractive moment matching properties with the original LTD system.

- The practical viability of the combined fixed-order controller design approach for LTD systems is assessed by designing a high performance fixed-order multi-$\mathcal{H}_2$ controller for a realistic LTD model of an experimental heat transfer setup.

Chapter 8

Combined structure and control design

This chapter presents a parametric programming approach to design $\mathcal{H}_\infty/\mathcal{H}_2$ feedback controllers for LTI systems, while simultaneously optimizing structural parameters affecting the system dynamics. In this approach, closed-loop performance is optimized in function of these parameters by relying on well-known convex LPV synthesis approaches. By solving the corresponding primal and dual optimization problems, performance upper and lower bounds in function of the structural parameters are obtained, providing insight in the conservatism of the solution. Exploiting polynomial spline parameterizations, conservatism is reduced in a systematic and numerically efficient way. The effectiveness of the approach is validated by simultaneously designing a state feedback controller and optimizing structural parameters for earthquake isolation of a civil engineering structure.

8.1 Introduction

Generally speaking, combined structure and control design considers the simultaneous optimization of structural parameters and an active controller for a given system, with respect to predefined performance specifications. Since the design of structural parameters and a controller are not independent, simultaneous optimization allows superior performance and/or reduced actuator effort compared to controller design for a model with a priori fixed structural parameters [57, 109, 110]. However, it is well known that such a simultaneous design gives rise to intractable nonconvex optimization problems.

Several algorithms for combined structure and control design have been proposed (see [60, 125], amongst others), but are computationally demanding and do not guarantee convergence to a local optimum. Improved approaches using iterative LMI procedures have been presented in [45, 73], and more recently in [21].

This chapter presents an elegant and numerically attractive approach to simultaneously design structural parameters and an $\mathcal{H}_\infty/\mathcal{H}_2$ feedback controller for a given LTI system, relying on well-known convex LPV controller design approaches. By optimizing performance in function of the structural parameters and exploiting polynomial spline parameterizations, approximate performance bounds in function of the structural parameters are obtained. In contrast to the aforementioned approaches, this requires solving only one convex optimization problem. Moreover, while the approach presented [21] is restricted to affine parameterizations, our approach allows polynomial spline dependencies for all system matrices. The use of such general parameterizations is motivated by the following fact: when increasing the degree and the number of knots of the B-spline parameterizations, the solution converges to the optimal (i.e., gridded) solution. The effectiveness of our approach is validated by simultaneous optimization of structural parameters and a state feedback controller for earthquake isolation of a civil engineering structure.

8.2   Problem formulation

Consider the finite-dimensional LPD state-space model

$$
\begin{cases}
\delta x &=& A(\alpha)x &+& B_w(\alpha)w &+& B_u(\alpha)u, \\
z &=& C_z(\alpha)x &+& D_{zw}(\alpha)w &+& D_{zu}(\alpha)u, \\
y &=& C_y(\alpha)x &+& D_{yw}(\alpha)w
\end{cases}
\tag{8.1}
$$

with state $x : \mathbb{T} \to \mathbb{R}^{n_x}$, exogenous input $w : \mathbb{T} \to \mathbb{R}^{n_w}$, control input $u : \mathbb{T} \to \mathbb{R}^{n_u}$, regulated output $z : \mathbb{T} \to \mathbb{R}^{n_z}$ and measured output $y : \mathbb{T} \to \mathbb{R}^{n_y}$. It is assumed that all system matrices have a polynomial spline dependency on the time-invariant parameter $\alpha \in \Lambda$, where $\Lambda \subset \mathbb{R}^N$ is the Cartesian product of N bounded intervals:

$$
\Lambda = [\underline{\alpha}_1, \overline{\alpha}_1] \times [\underline{\alpha}_2, \overline{\alpha}_2] \times \cdots \times [\underline{\alpha}_N, \overline{\alpha}_N].
$$

The aim is to design a feedback controller

$$
K : \begin{cases}
\delta x_{\text{c}} &=& A_{\text{c}}x_{\text{c}} &+& B_{\text{c}}y, \\
u &=& C_{\text{c}}x_{\text{c}} &+& D_{\text{c}}y,
\end{cases}
\tag{8.2}
$$

with $x_c \in \mathbb{R}^q$ ($0 \leq q \leq n_x$) for the system (8.1), such that one or more closed-loop $\mathcal{H}_\infty/\mathcal{H}_2$ performance specifications and the structural parameter $\alpha \in \Lambda$ are simultaneously optimized.

8.3 Approach

This section briefly discusses a parametric programming approach for simultaneous optimization of a $\mathcal{H}_\infty/\mathcal{H}_2$ feedback controller and structural model parameters. The proposed approach relies on parameter-dependent LMIs for LPV synthesis, see Chapter 5 and references therein, considering the specific case of a time-invariant parameter. It is emphasized that, independent of the considered synthesis LMIs (i.e., ranging from state feedback to fixed-order dynamic output feedback), the approach can be straightforwardly applied.

The approach consists of the following two steps:

1. Using an available LPV controller synthesis approach, we design a parameter-dependent controller $K(\alpha)$ achieving a high closed-loop performance for *each* parameter value $\alpha \in \Lambda$ by solving only one convex optimization problem. This is achieved by optimizing a desired closed-loop performance bound $p(\alpha) > 0$ *as a function* of the time-invariant parameter $\alpha \in \Lambda$ as follows:

$$\underset{K(\cdot),p(\cdot)}{\text{minimize}} \quad \int_\Lambda p(\alpha)d\alpha$$

$$\text{subject to:} \quad \text{LPV synthesis LMIs depending on } K(\alpha),\, p(\alpha) \tag{8.3}$$

2. Minimize the obtained performance bound $p(\alpha)$ over $\alpha \in \Lambda$, and select the controller corresponding to the optimal value of α. Specifically, compute

$$\alpha_{\text{opt}} := \underset{\alpha \in \Lambda}{\arg\min}\, p(\alpha)$$

and select $K := K(\alpha_{\text{opt}})$.

Note that, in Step 1, performance is optimized *as a function* of the structural parameter α, in contrast to typical LPV synthesis approaches in which worst-case performance is usually optimized. Subsequently, in Step 2, the performance bound $p(\alpha)$ is minimized over $\alpha \in \Lambda$. It is emphasized that optimization of the performance bound for each parameter value in conjunction with a sufficiently accurate parameterization of optimization variables is indispensable for optimal selection of the structural parameter.

Remark 9 ($\mathcal{L}_1$ norm optimization)**.** *Mathematically speaking, the $\mathcal{L}_1$ norm of the strictly positive function $p(\alpha)$, defined as*

$$\|p\|_1 := \int_\Lambda p(\alpha)d\alpha,$$

is optimized in the optimization problem (8.3), as opposed to the $\mathcal{L}_\infty$ norm

$$\|p\|_\infty := \max_{\alpha \in \Lambda} p(\alpha)$$

in typical LPV controller design problems. The optimization of different norms (i.e., convex functions), such as the $\mathcal{L}_p$ norms with $1 < p < \infty$, might be considered. However, the latter is beyond the scope of this thesis.

In the ideal case of a perfect parameterization of the optimization variables, the optimal solution of (8.3) is attained, and thus the lowest achievable performance bound $p(\alpha)$ is achieved for each $\alpha \in \Lambda$. This implies that, whenever (8.3) is a necessary and sufficient synthesis condition (e.g., $\mathcal{H}_\infty$ state feedback design), the above approach yields the optimal structural parameter and corresponding optimal controller if the parameterization is sufficiently accurate.

Due to the generality of polynomial spline parameterizations (see Section 2.4.1 on page 19), they allow accurate approximations of the optimal solution of (8.3). Compared to polynomial parameterizations, considerably less conservative approximations might be obtained, which is due to the extra degree of freedom to select internal break points to locally influence LMI variables. Although the optimal placement of internal break points is a difficult problem, it is shown in the next section that systematic selection of break points might already be more attractive than selecting a higher polynomial degree, both in terms of conservatism and numerical complexity.

As a possible extension of the above approach, the so-called dual problem (see, for instance, [19]) associated with (8.3) can be derived, providing a lower bound $d(\alpha)$ on the solution of (8.3). A measure of conservatism is obtained by studying the so-called duality gap, which is quantified by the difference $p(\alpha) - d(\alpha)$, $\alpha \in \Lambda$. Obviously, a smaller duality gap corresponds to a more accurate approximation of the optimal solution. The next section demonstrates how B-spline parameterizations are exploited to systematically reduce the duality gap.

8.4 Earthquake isolation of a 3-store building

This section validates the proposed combined structure and control design approach, by simultaneously designing a state feedback controller and optimizing
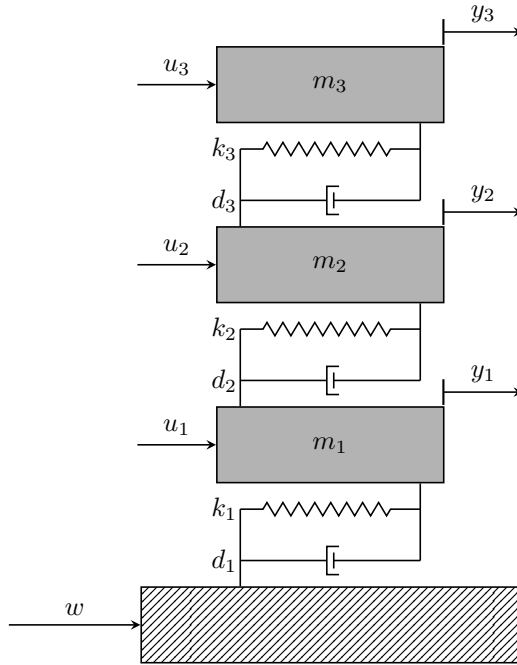
Figure 8.1: Schematic representation of the 3-store building model.

structural parameters for earthquake isolation of a 3-store building. A description of the considered model and the control objectives is provided in Section 8.4.1, respectively, Section 8.4.2. Subsequently, the numerical results discussed in Section 8.4.3 demonstrate the generality, flexibility and practical viability of our approach.

8.4.1 Model description

A schematic representation of the considered model of a 3-store building, which is borrowed from [21], is shown in Figure 8.1. The corresponding nominal structural parameters are given in Table 8.1. Each floor is modeled as a mass, while the building dynamics are captured by interconnecting two consecutive floors by a spring and a damper. The control inputs u_i, $i = 1, 2, 3$, are forces applied independently to each floor. An earthquake is modeled by a disturbance input w, representing ground acceleration.

Table 8.1: Nominal structural parameters of the 3-store model.

Floor masses [kg]	Stiffness coefficients [kN/m]	Damping coefficients [kN s/m]
$m_1 = 5897$	$k_1 = 33,732$	$d_1 = 67$
$m_2 = 5897$	$k_2 = 29,093$	$d_2 = 116$
$m_3 = 5897$	$k_3 = 28,621$	$d_3 = 57$

Defining the structural parameter

$$\alpha = \begin{bmatrix} m_1 & m_2 & m_3 & k_1 & k_2 & k_3 & d_1 & d_2 & d_3 \end{bmatrix}',$$

and mass, stiffness and damping matrices $M(\alpha) = \mathrm{diag}\{m_1, m_2, m_3\}$,

$$S(\alpha) = \begin{bmatrix} k_1 + k_2 & -k_2 & 0 \\ -k_2 & k_2 + k_3 & -k_3 \\ 0 & -k_3 & k_3 \end{bmatrix}, \quad D(\alpha) = \begin{bmatrix} d_1 + d_2 & -d_2 & 0 \\ -d_2 & d_2 + d_3 & -d_3 \\ 0 & -d_3 & d_3 \end{bmatrix},$$

respectively, the model dynamics are conveniently expressed in the state-space form (8.1) with

$$A(\alpha) = \begin{bmatrix} 0 & I_3 \\ -M(\alpha)^{-1}K(\alpha) & -M(\alpha)^{-1}D(\alpha) \end{bmatrix},$$

$$B_w(\alpha) = \begin{bmatrix} 0_{3\times 1} \\ 1 \\ 1 \\ 1 \end{bmatrix}, \quad B_u(\alpha) = \begin{bmatrix} 0 \\ M(\alpha)^{-1} \end{bmatrix}.$$

The associated system state is composed of the horizontal floor positions y_i, $i = 1, 2, 3$ with respect to the ground, and their velocities. To limit the interstory displacements $y_i - y_{i-1}$, $i = 1, 2, 3$ (with $y_0 := 0$), the regulated output is defined by

$$C_z(\alpha) = \left[\begin{array}{ccc|c} 1 & 0 & 0 & \\ -1 & 1 & 0 & 0_{3\times 3} \\ 0 & -1 & 1 & \end{array} \right], \quad D_{zw}(\alpha) = 0, \quad D_{zu}(\alpha) = 0.$$

Furthermore, assuming that all states are available for feedback, $C_y(\alpha) = I_6$ and $D_{yw}(\alpha) = 0$.

8.4.2 Control objective

We consider the simultaneous design of a state feedback control law $u = Fx$ (i.e., $q = 0$ in (8.2)) and optimization of one or more structural parameters for the 3-store model from Section 8.4.1. The control objective of [21] is adopted.

Suppose that w is a stochastic white Gaussian noise process with identity covariance matrix. Then, for a given prefixed bound on the energy (variance) of the regulated output z, we are interested in minimizing the control effort u (quantified by its standard deviation). It is clear from Definition 3 (on page 13) that the imposed objectives correspond to a multi-$\mathcal{H}_2$ state feedback control problem.

As discussed in [21], the corresponding optimization problem (8.3) is explicitly given by

$$\underset{Q(\cdot),L(\cdot),Z(\cdot)}{\text{minimize}} \quad \int_\Lambda \text{Tr}\{Z(\alpha)\}d\alpha \tag{8.4}$$

subject to:

$$\begin{bmatrix} Q(\alpha)A(\alpha)' + A(\alpha)Q(\alpha) + B_u(\alpha)L(\alpha) + L(\alpha)'B_u(\alpha)' & B_w(\alpha) \\ B_w(\alpha)' & -I \end{bmatrix} \prec 0,$$

$$C_z(\alpha)Q(\alpha)C_z(\alpha)' \prec \mu I,$$

$$\begin{bmatrix} Q(\alpha) & L(\alpha)' \\ L(\alpha) & Z(\alpha) \end{bmatrix} \succ 0, \quad \forall \alpha \in \Lambda,$$

with $Q(\alpha) \in \mathbb{S}_+^6$, $L(\alpha) \in \mathbb{R}^{3\times6}$ and $Z(\alpha) \in \mathbb{S}_+^3$, $\alpha \in \Lambda$, and where $\mu = 15$ is selected to bound the variance of the regulated output z. Λ is constructed from known lower and upper bounds on each structural parameter. The parameter-dependent state feedback controller is reconstructed as $F(\alpha) = L(\alpha)Q(\alpha)^{-1}$.

The associated dual problem (see, e.g., [19]) is given by

$$\underset{U(\cdot),V(\cdot)}{\text{maximize}} \quad \int_\Lambda \text{Tr}\{U_{12}(\alpha)B_w(\alpha)'\} + \text{Tr}\{U_{12}(\alpha)'B_w(\alpha)\} -$$
$$\text{Tr}\{U_{22}(\alpha)\} - \mu\text{Tr}\{V(\alpha)\}d\alpha \tag{8.5}$$

subject to:

$$U(\alpha) := \begin{bmatrix} U_{11}(\alpha) & U_{12}(\alpha) \\ U_{12}(\alpha)' & U_{22}(\alpha) \end{bmatrix} \succ 0,$$

$$V(\alpha) \succ 0,$$

$$\begin{bmatrix} A(\alpha)'U_{11}(\alpha) + U_{11}(\alpha)A(\alpha) + C_z(\alpha)'V(\alpha)C_z(\alpha) & U_{11}(\alpha)B_u(\alpha) \\ B_u(\alpha)'U_{11}(\alpha) & I \end{bmatrix} \succ 0,$$

where the constraints should hold for all $\alpha \in \Lambda$. The function

$$d(\alpha) = \text{Tr}\{U_{12}(\alpha)B_w(\alpha)'\} + \text{Tr}\{U_{12}(\alpha)'B_w(\alpha)\} - \text{Tr}\{U_{22}(\alpha)\} - \mu\text{Tr}\{V(\alpha)\}$$

is a lower bound on the optimal value function $p(\alpha) = \text{Tr}\{Z(\alpha)\}$ of the primal problem (8.4).

As explained in Section 2.4 on page 18, tractable LMI formulations are obtained by imposing a parameterization on the LMI variables and applying a relaxation. When a solution of (8.4) is obtained, the corresponding optimal structural parameter and state feedback controller are determined as

$$\alpha_{\mathrm{opt}} = \arg\min_{\alpha \in \Lambda} \mathrm{Tr}\{Z(\alpha)\},$$

respectively, $F := F(\alpha_{\mathrm{opt}})$.

8.4.3 Numerical results

Starting from the primal and dual optimization problems (8.4) and (8.5), respectively, B-spline parameterizations are exploited to derive tractable LMI conditions for simultaneous optimization of a multi-$\mathcal{H}_2$ state feedback controller and structural parameters for the 3-store model. First, only the stiffness coefficient k_2 is optimized, while the nominal values of the remaining structural parameters (see Table 8.1 on page 120) are selected. In a second case, the damping coefficient d_3 is optimized in addition to k_2. The LMIs are implemented and solved in MATLAB using the software packages Yalmip [72] and SDPT3 [115].

Case 1: optimization of k_2

We are interested in simultaneous optimization of the state feedback control gain F and the structural parameter k_2 over the interval $[\underline{k}_2, \overline{k}_2]$, where $\underline{k}_2$ and $\overline{k}_2$ represent half, respectively, double the nominal value of k_2. Note that, in this case, the system matrices of (8.1) affinely depend on k_2, such that selecting all LMI variables as polynomial splines results in parameter-dependent LMIs with a polynomial spline dependency.

Using 100 equidistant grid points on the interval $[\underline{k}_2, \overline{k}_2]$, multi-$\mathcal{H}_2$ state feedback controllers are computed by solving the parameter-independent version of optimization problem (8.4) for each grid point. The resulting tradeoff curve is shown in Figure 8.2, revealing an optimal value $k_2 \approx 4.9 \cdot 10^7$. It should be emphasized that, since the parameterization of LMI variables is a source of conservatism, only an approximation of the gridded solution can be obtained with parametric programming. On the other hand, parametric programming is more elegant in the sense that it only requires solving one convex optimization problem, while gridding procedures are numerically very demanding. For instance, in this case, gridding already requires solving 100 convex optimization
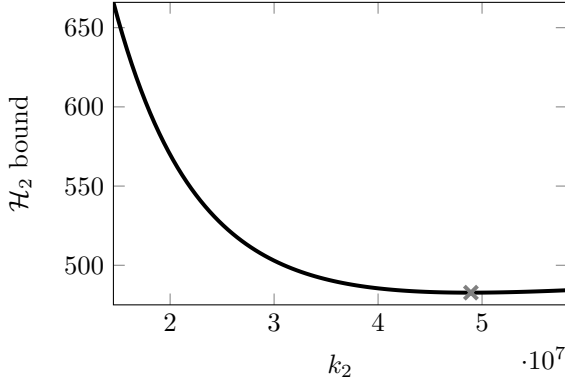
Figure 8.2: $\mathcal{H}_2$ performance as a function of the structural parameter k_2, obtained using 100 equidistant grid points on the interval $[\underline{k}_2, \overline{k}_2]$. The gray cross indicates the optimal value of k_2.

Table 8.2: Selected polynomial degrees of the LMI variables.

LMI variable	degree
$Q(\alpha), U(\alpha), V(\alpha)$	g
$F(\alpha), L(\alpha)$	$g+1$

problems. When N structural parameters are simultaneously optimized, this generalizes to 100^N convex problems.

To assess the benefits of our parametric programming approach, various possibilities to obtain approximate solutions of the $\mathcal{H}_2$ bound from Figure 8.2 are compared.

First, using polynomial parameterizations for all LMI variables, a degree elevation (of degree d) is compared with knot insertion (using m midpoint refinements, such that the number of inserted knots equals $2^m - 1$). According to the polynomial degrees in Table 8.2, a polynomial parameter dependency is selected for all LMI variables. Setting $g = 2$, the results in Table 8.3 are obtained, revealing that applying knot insertion instead of degree elevation yields better approximations of the gridded solution with a comparable numerical burden. The latter is further illustrated in Figure 8.3, comparing the primal and dual solutions corresponding to the cases $(d, m) = (4, 0)$ and $(d, m) = (0, 3)$.

Now we consider more general polynomial spline parameterizations for the LMI variables, allowing a comparison between increased polynomial degree g and more internal knots k. Table 8.4 shows the results for different values of (g, k),

Table 8.3: Degree elevation (of degree d) versus knot insertion (using m midpoint refinements) for polynomial LMI variables ($g = 2$).

degree d ($m = 0$)	0	1	2	4	8
primal objective	560.8	554.2	549.6	541.7	536.6
computation time [sec]	1.09	1.18	1.21	1.41	1.68
dual objective	445.9	451.4	460.0	464.7	469.4
computation time [sec]	1.62	1.16	1.02	1.10	1.24
midpoint refinements m ($d = 0$)	0	1	2	3	4
primal objective	560.8	550.3	532.2	529.2	528.0
computation time [sec]	1.04	1.21	1.24	1.50	1.93
dual objective	445.9	467.8	472.0	474.8	475.8
computation time [sec]	1.54	1.00	1.16	1.14	1.41
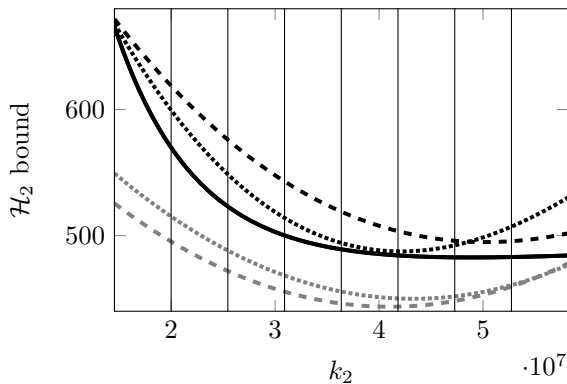
Figure 8.3: A comparison between the primal (black) and dual (gray) solutions corresponding to the cases $(d, m) = (4, 0)$ (dashed) and $(d, m) = (0, 3)$ (dotted) shows that a better approximation of the gridded solution is obtained using knot insertion. The thick solid black line and the thin vertical black lines correspond to the gridded solution, respectively, the positions of inserted knots for the case $(d, m) = (0, 3)$.

Table 8.4: Higher polynomial degree vs. more knots of LMI variables. (Without degree elevation or knot insertion.)

| degree g $(k = 0)$	2	3	4	5
primal objective	560.8	536.2	530.2	526.5
computation time [sec]	2.24	0.95	0.94	1.00
dual objective	445.9	481.1	495.4	501.0
computation time [sec]	1.31	0.78	0.84	1.02
number of knots k $(g = 2)$	0	1	2	3
primal objective	560.8	532.0	522.6	518.4
computation time [sec]	2.13	0.88	0.96	1.13
dual objective	445.9	487.2	497.7	503.5
computation time [sec]	1.34	0.83	0.93	1.06
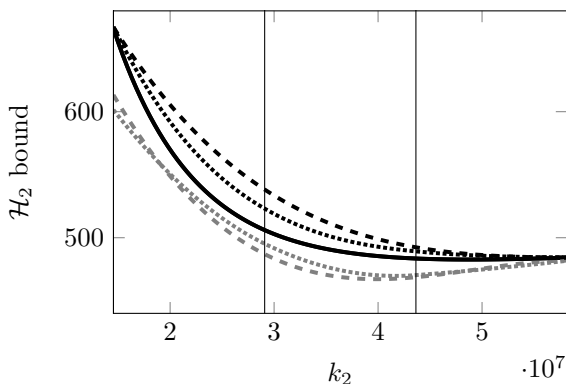
Figure 8.4: A comparison between the primal (black) and dual (gray) solutions corresponding to the cases $(g, k) = (4, 0)$ (dashed) and $(g, k) = (2, 2)$ (dotted) illustrates the benefit of B-spline LMI variables with internal knots. The thick solid black line and thin vertical black lines correspond to the gridded solution, respectively, the internal knot positions for the case $(g, k) = (2, 2)$.

without degree elevation and knot insertion (i.e., $(d, m) = (0, 0)$). It is clear that internal knots are more attractive than higher degrees of LMI variables, since this leads to better approximations of the gridded solution with a comparable numerical burden. Figure 8.4 confirms this by comparing the case $(g, k) = (4, 0)$ and $(g, k) = (2, 2)$.

Table 8.5: A comparison of the primal and dual solution with the gridded solution reveals a very accurate approximation and a drastic decrease of numerical complexity.

	30x30 grid	primal	dual
objective function (times 10^{-14})	6.46	6.49	6.37
computation time [sec]	≈ 1100	15.3	11.1

Case 2: optimization of (k_2, d_3)

The simultaneous design of a state feedback control gain F and the multi-dimensional structural parameter $(k_2, d_3) \in [\underline{k}_2, \overline{k}_2] \times [\underline{d}_3, \overline{d}_3] = \Lambda$ is considered now. The interval boundaries $\underline{k}_2$ and $\overline{k}_2$ are half, respectively, double the nominal value of k_2, while $\underline{d}_3$ and $\overline{d}_3$ are selected as half, respectively, exactly the nominal value of d_3. Using a 30×30 equidistant grid of Λ, a state feedback controller and a corresponding closed-loop $\mathcal{H}_2$ bound as a function of (k_2, d_3) are computed by solving 900 convex optimization problems (i.e., the parameter-independent version of (8.4)), where it takes approximately 1.25s to solve each convex optimization problem, implying a total time of almost 20 minutes to obtain an accurate gridded solution.

Subsequently, all LMI variables are chosen to have a polynomial spline dependency on (k_2, d_3) (see Section 2.4.1 on page 19). With $g = 2$, the degrees of Table (8.2) and $k = 4$ knots are selected in both k_2 and d_3, and the associated optimization problems (8.4) and (8.5) are solved. The corresponding objective functions and computation times are compared with the gridded solution in Table 8.5, resembling a very accurate approximation of the objective function for each parameter value and a drastic decrease of the computation time. Figure 8.5 illustrates how well the primal solution (transparent) approximates the gridded solution (opaque) of (8.4). The fact that the minimum of the primal solution (indicated by the black circle) is very close to the optimal value of the structural parameter (k_2, d_3) (indicated by the black square) clearly confirms the merits of our approach for combined structure and control design.

Remark 10 (Rational dependency on mass). *In the used state-space form, the dependency on mass is rational, such that polynomial spline parameterizations would fail when considering the masses as structural parameters. However, using the so-called descriptor form, the dependency of the system on all parameters is rendered polynomial. As discussed in [21], the LMIs are straightforwardly adapted to handle parameter-dependent descriptor systems, see also Section 2.4.2.*
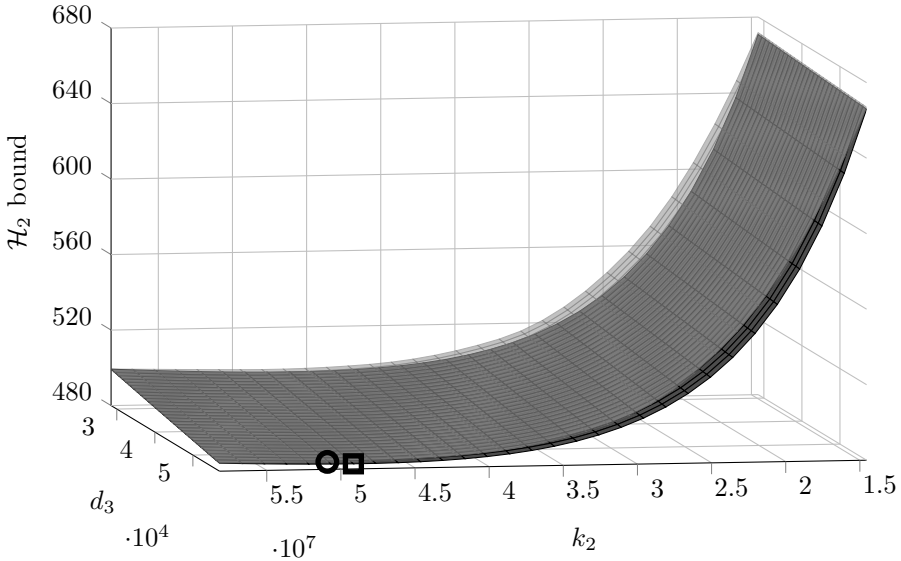
Figure 8.5: The gridded (opaque) and primal (transparent) solution. The fact that the minimum of the primal solution (indicated by the black circle) is very close to the optimal value of the structural parameter (indicated by the black square) clearly confirms the merits of B-spline parameterizations for structure and control design.

8.5   Summary

This chapter has presented a parametric programming approach for combined structure and control design, simultaneously optimizing an $\mathcal{H}_\infty/\mathcal{H}_2$ feedback controller and structural parameters affecting the system dynamics. The latter was achieved by rewriting the problem as a specific LPV synthesis problem (i.e., with time-invariant parameters), and optimizing a parameterized performance bound in function of the structural parameter. The approach was validated on a 3-store building model, by designing an active feedback controller while optimizing structural parameters for earthquake isolation. It was shown that polynomial spline parameterizations are very effective to obtain approximate solutions of combined structure and control design problems, especially compared to exhaustive gridding procedures. Namely, internal knots locally affect the solution, and thus might lead to considerable reductions of conservatism compared to polynomial parameterizations featuring similar numerical complexity. A lower bound on the closed-loop performance in function of the parameter was obtained by solving the dual of the considered (primal) optimization problem, providing insight in the conservatism of the solution.

Recapitulation

- Polynomial spline parameterizations are very effective to obtain approximate solutions of combined structure and control design problems.

- Convex LPV synthesis approaches allow simultaneous optimization of a controller and structural parameters, by optimizing closed-loop performance in function of the parameter (instead of worst-case performance).

- By solving the dual of the considered (primal) optimization problem, a lower bound on the closed-loop performance in function of the parameter is obtained, providing insight in the conservatism of the solution.

- Considering polynomial spline variables with internal knots, locally affecting the solution, might lead to considerable reductions of conservatism compared to polynomial parameterizations featuring similar numerical complexity. In addition, knot insertion is an attractive alternative to degree elevation.

- The merits of our approach are demonstrated by simultaneously designing a state feedback controller and optimizing structural parameters for earthquake isolation of a civil engineering structure.

Chapter 9

Concluding remarks

This thesis has presented a unifying convex framework to design fixed-order controllers for the broad class of LPD systems, including extensive numerical and experimental validations. This last chapter provides concluding remarks and suggestions for future research.

9.1 Conclusions

Since both accuracy and simplicity of a dynamical model are of utmost importance for a successful control design, the general class of LPD systems has been considered in this thesis. LPD systems exhibit a linear input-output relation, while the system dynamics are affected by parameters which are potentially time-varying and uncertain, thus bridging the gap between the restrictive class of LTI systems and general nonlinear systems. For some dynamical systems, LPD models provide the desired accuracy to guarantee stability and performance, while standard LTI techniques fail. On the other hand, stability and performance is incredibly hard to prove for the general class nonlinear systems. The constantly increasing demands from the manufacturing industry are the main incentive for the research and development communities to push the limits of accuracy and performance. In light of this, the following contributions to the design of practical and intuitive controllers for LPD systems have been presented.

9.1.1   Fixed-order controller design for LPD systems

The need for more accurate dynamical models complicates the design of practical and intuitive controllers. In this context, this thesis has presented an advanced methodology to design feedback controllers for LPD systems with guaranteed closed-loop stability and performance. The practicality of these controllers is due to their structural simplicity, which is enforced by a priori fixing the number of states and the parameter dependency. At the same time, the resulting controller designs are intuitive, since the imposed performance measures directly relate to bandwidth, actuator effort, robustness, overshoot, disturbance rejection, etc. Since the design of fixed-order controllers is intrinsically a very hard (i.e., nonconvex) problem, a novel framework of sufficient LMIs is presented in Chapter 3 to alleviate this issue. This framework relies on a set of a priori computed full-order LPD controllers that stabilize the LPD system for all possible parameter trajectories, which are used as parameters in sufficient LMIs for the fixed-order controller design. In these LMIs, continuous-time and discrete-time controller designs are unified, and multiple performance specifications can be taken into account.

For different subclasses of LPD systems, the main benefits of the fixed-order controller design approach are highlighted below.

LTI systems   In Chapter 4, the fixed-order controller design approach is applied to LTI systems. For single-objective $\mathcal{H}_\infty$ or $\mathcal{H}_2$ synthesis, intuitive guidelines are provided for the selection of an initial full-order controller, often resulting in optimal fixed-order controllers despite the conservatism inherent in the approach. Additionally, for multi-objective control the selection of a different initial full-order controller for each performance specification is motivated, since this potentially yields fixed-order controllers that outperform full-order controllers resulting from well-known (conservative) LMI approaches. Numerical comparisons with existing approaches, and experimental validations on a lab-scale overhead crane with fixed cable length, clearly illustrate the potential of the LMI framework for fixed-order LTI controller synthesis.

LPV systems   Exploiting a numerically efficient relaxation approach, the LMI framework for fixed-order controller design is applied to design practical controllers for LPV systems in Chapter 5. Taking into account bounds on the rate of parameter variation, high performance fixed-order multi-objective $\mathcal{H}_\infty/\mathcal{H}_2$ LPV controllers are designed for a lab-scale overhead crane with varying cable length, which is accurately modeled as an LPV system. The practical viability of the approach is assessed through successful experimental validations.

Uncertain LTI systems By imposing structural constraints on certain optimization variables, the LMI framework is applied to design robust fixed-order controllers for uncertain LTI systems in Chapter 6. To obtain high performance robust controllers, the extension of the fixed-order LMI framework with an iterative LMI procedure is essential. In this procedure, which requires an initial stabilizing robust controller, novel extended analysis LMIs are alternately solved in different optimization variables to gradually obtain less conservative fixed-order robust controllers.

9.1.2 Fixed-order controller design for LTD systems

Chapter 7 presents a combined approach to design fixed-order LTI controllers for LTD systems with delays in the state, input and output. In this approach, first a novel efficient Krylov based model order reduction technique is applied in conjunction with standard Padé approximations to obtain an accurate low-order LTI approximation of the original LTD system. Subsequently, a fixed-order controller is designed for this approximating model, using the approach presented in Chapter 3. Finally, the closed-loop performance of the resulting fixed-order controller is validated on the original LTD system. The successful design of fixed-order multi-$\mathcal{H}_2$ controllers for a realistic LTD model of an experimental heat transfer setup confirm the potential of the combined approach for industrial engineering applications.

9.1.3 Combined structure and control design

A parametric programming approach for combined structure and control design is presented in Chapter 8. In this approach, a feedback controller and structural parameters affecting the system dynamics are simultaneously optimized. This is achieved by rewriting the problem as a convex LPV synthesis problem with time-invariant parameters, and optimizing a parameterized performance bound in function of the structural parameter. Exploiting polynomial spline parameterizations, an accurate approximation of the optimal performance bound in function of the structural parameter is obtained. The effectiveness of the approach is validated by simultaneously designing a state feedback controller and optimizing structural parameters for earthquake isolation of a civil engineering structure.

9.2 Recommendations for future research

This section briefly discusses potential directions for future research.

Robust multi-objective control In the iterative LMI procedure, proposed in Chapter 6, extended analysis LMIs are alternately solved in different optimization variables to gradually obtain less conservative fixed-order controllers. Since, in the case of multiple performance objectives, the use of a different full-order controller for each performance specification might be favorable, it is worthwhile to extend the iterative LMI procedure by updating these controller variables in an additional step.

Efficiency iterative LMI procedure The main benefit of the iterative LMI procedure (see Chapter 6) is featured by significant reductions of conservatism compared to an initial fixed-order robust controller. However, convergence might be slow, and convergence to a local optimum of the underlying nonconvex problem is not guaranteed. Convex-concave decompositions (see [116]) provide an elegant alternative, since they yield an iterative LMI procedure with guaranteed convergence to a local optimum. It is remarked that the iterative LMI procedure can be straightforwardly applied to the LTI and LPV case.

Combined structure and control design The combined structure and control design approach (see Chapter 8) provides a performance upper/lower bound by solving only one convex (primal/dual) optimization problem. However, obtaining a good solution requires sufficiently accurate parameterizations of the optimization variables, usually involving several manual steps. By combining information from the primal and the dual solution, automated procedures could be derived to gradually obtain more accurate solutions.

More general parameterizations For, amongst others, LPV and robust control design, it would be beneficial to consider polynomial spline parameterizations instead of more restrictive polynomial parameterizations.

LMIs with scalar parameters For analysis and control of LPD systems, less conservative parameter-dependent LMI conditions can be derived by incorporating scalar parameters. However, this comes at the expense of an increased numerical burden, since such scalar parameters appear in products

with LMI variables. Gridding or a smart search procedure is required, and deserves further investigation.

Parameter domain modeling   In addition to bounds on the rate of parameter variation, known bounds on the rate of parameter acceleration (and, more general, higher order derivatives/differences) could be taken into account to further reduce conservatism in LPD analysis and synthesis approaches.

Experimental validations   The fixed-order controller design approach is successfully validated experimentally for LTI and LPV systems. However, experimental validations of fixed-order controllers for LTD systems (i.e., the experimental heat exhanger setup) and uncertain LTI systems would completely show its versatility and practical viability.

Gap between industry and academia   There is a strong industrial demand for software to design high performance controllers for complex dynamical systems. Namely, the current industrial decoupled PID-controller design standards are inadequate to cope with the complex, often uncertain and/or time-varying dynamics of these systems, leading to suboptimal performance, unreliable behavior and even instability. In addition, the tuning of PID-controllers is often very cumbersome and time consuming. The development of reliable, efficient and user-friendly software to support non-experts in the design of optimal controllers, yielding the best performance and robustness for a given implementation cost, constitutes an important direction for future research. Validations on experimental development cases and models of industrial cases would demonstrate the potential of this software for company applications.

Appendix A

Proofs

This appendix presents theoretical proofs of the theorems presented in Chapter 2 and Chapter 3.

A.1 Proof of Theorem 1

Suppose that there exist scalars $a, b, c > 0$ and $d \geq 1$ such that the conditions (2.6) hold for all $\alpha \in \mathcal{T}$ and all trajectories $x : \mathbb{T} \to \mathbb{R}^{n_x}$ of (2.5). Combining (2.6a) and (2.6b), we get

$$\Delta V(\alpha, x) \leq -c\|x\|^d \leq -\frac{c}{b} V(\alpha, x),$$

for all $\alpha \in \mathcal{T}$ and all trajectories $x : \mathbb{T} \to \mathbb{R}^{n_x}$. Using the definition of ΔV leads to

$$V(\alpha(t), x(t)) \leq V(\alpha(0), x(0)) f(t),$$

where $f(t) = e^{-ct/b}$ in continuous time, and $f(t) = (1 - \frac{c}{b})^t$ in discrete time. Now it follows from (2.6a) that

$$a\|x(t)\|^d \leq V(\alpha(t), x(t)) \leq V(\alpha(0), x(0)) f(t) \leq b\|x(0)\|^d f(t),$$

for all $\alpha \in \mathcal{T}$, all trajectories $x : \mathbb{T} \to \mathbb{R}^{n_x}$ and all $t \in \mathbb{T}$, and thus

$$\|x(t)\|^d \leq \frac{b}{a}\|x(0)\|^d f(t), \quad \forall \alpha \in \mathcal{T}, \ t \in \mathbb{T}.$$

Exponential stability follows by taking $c < b$ without loss of generality. $\qquad \square$

A.2   Proof of Theorem 2

Assume that there exists a bounded matrix $P(\alpha(t)) \in \mathbb{S}_+^{n_x}$, for $\alpha \in \mathcal{T}$, $t \in \mathbb{T}$, such that (2.8) holds for all $\alpha \in \mathcal{T}$, $t \in \mathbb{T}$. Since $P(\alpha(t))$ is positive definite and bounded, there exist constants $a, b > 0$ such that

$$aI_{n_x} \prec P(\alpha(t)) \prec bI_{n_x}, \quad \forall \alpha \in \mathcal{T},\ t \in \mathbb{T},$$

or, similarly,

$$a\|x\|_2^2 < x'P(\alpha)x = V(\alpha, x) < b\|x\|_2^2, \quad \forall \alpha \in \mathcal{T},\ x \in \mathbb{R}^{n_x} \backslash \{0\}.$$

Furthermore, (2.8) implies that there exists a scalar $c > 0$ and a bounded matrix $Q(\alpha(t)) \in \mathbb{S}_+^{n_x}$, for $\alpha \in \mathcal{T}$, $t \in \mathbb{T}$, such that

$$\begin{bmatrix} I \\ A(\alpha(t)) \end{bmatrix}' \Phi(\alpha(t)) \begin{bmatrix} I \\ A(\alpha(t)) \end{bmatrix} = -Q(\alpha(t)) \preceq -cI_{n_x}, \quad \forall \alpha \in \mathcal{T},\ t \in \mathbb{T}.$$

Noting that $\Delta V(\alpha, x)$ along trajectories of the LPD system (2.5) is given by

$$\Delta V(\alpha, x) = x' \begin{bmatrix} I \\ A(\alpha) \end{bmatrix}' \Phi(\alpha) \begin{bmatrix} I \\ A(\alpha) \end{bmatrix} x,$$

we obtain $\Delta V(\alpha, x) \leq -c\|x\|_2^2$, for all $\alpha \in \mathcal{T}$ and all trajectories $x : \mathbb{T} \to \mathbb{R}^{n_x}$ of (2.5), hence the conditions of Theorem 1 (see page 11) are satisfied. $\square$

A.3   Proof of Theorem 3

Suppose that, for some bounded scalar $\gamma > 0$, there exists a matrix $P(\alpha(t)) \in \mathbb{S}^{n_x}$, $\alpha \in \mathcal{T}$, $t \in \mathbb{T}$, such that the LMI (2.9) is feasible for all $\alpha \in \mathcal{T}$, $t \in \mathbb{T}$. Then, since (2.9) implies that

$$\begin{bmatrix} I \\ A(\alpha(t)) \end{bmatrix}' \Phi(\alpha(t)) \begin{bmatrix} I \\ A(\alpha(t)) \end{bmatrix} + C(\alpha(t))'C(\alpha(t)) \prec 0,$$

for all $\alpha \in \mathcal{T}$, $t \in \mathbb{T}$, exponential stability follows from $C(\alpha)'C(\alpha) \succeq 0$ and Theorem 2. Moreover, using the storage function $V(\alpha, x) = x'P(\alpha)x$, we obtain

$$\Delta V(\alpha, x) = \begin{bmatrix} x \\ w \end{bmatrix}' \begin{bmatrix} I & 0 \\ A(\alpha) & B(\alpha) \end{bmatrix}' \Phi(\alpha) \begin{bmatrix} I & 0 \\ A(\alpha) & B(\alpha) \end{bmatrix} \begin{bmatrix} x \\ w \end{bmatrix},$$

such that (2.9) can be rewritten as

$$\Delta V(\alpha, x) \quad < \quad -\begin{bmatrix} x \\ w \end{bmatrix}' \begin{bmatrix} 0 & I \\ C(\alpha) & D(\alpha) \end{bmatrix}' \begin{bmatrix} -\gamma I & 0 \\ 0 & I \end{bmatrix} \begin{bmatrix} 0 & I \\ C(\alpha) & D(\alpha) \end{bmatrix} \begin{bmatrix} x \\ w \end{bmatrix}$$

$$= \quad \gamma w'w - z'z,$$

which should hold for all $\alpha \in \mathcal{T}$. Integration/summation (continuous time/discrete time) yields the inequality

$$V(\alpha(T), x(T)) - V(\alpha(0), x(0)) < \gamma \|w(t)\|_{2,[0,T]}^2 - \|z(t)\|_{2,[0,T]}^2 \qquad (A.1)$$

for all $\alpha \in \mathcal{T}$, $T \in \mathbb{T}$. Consequently, using $x(0) = 0$ and positive definiteness of V, (A.1) implies that

$$0 < \gamma \|w(t)\|_2^2 - \|z(t)\|_2^2$$

for all $\alpha \in \mathcal{T}$, which is equivalent to

$$\sup_{\alpha \in \mathcal{T}} \sup_{w(t) \neq 0} \frac{\|z(t)\|_2}{\|w(t)\|_2} < \sqrt{\gamma},$$

proving that $\|H\|_\infty < \sqrt{\gamma}$. $\qquad\qquad\qquad \square$

A.4   Proof of Theorem 4

The proof for the discrete-time case, which is a straightforward extension of the proof presented in [27] to the case of LPD systems, is presented. For the continuous-time case, we refer to [112].

Let the LPD system (2.1) be exponentially stable, and assume that $D(\alpha) = 0$ for all $\alpha \in \mathcal{T}$. Then, according to Lemma 1, there exists a bounded matrix $\bar{Q}(\alpha(t))$, for $\alpha \in \mathcal{T}$, $t \in \mathbb{T}$, such that, for any $\alpha \in \mathcal{T}$,

$$\bar{Q}(\delta\alpha) = A(\alpha)\bar{Q}(\alpha)A(\alpha)' + B(\alpha)B(\alpha)', \quad \bar{Q}(\alpha(0)) = 0. \qquad (A.2)$$

Suppose that there exists a bounded parameter-dependent matrix $Q(\alpha(t)) \in \mathbb{S}_+^{n_x}$ for $\alpha \in \mathcal{T}$, $t \in \mathbb{T}$, such that the parameter-dependent LMIs (2.12) hold for all $\alpha \in \mathcal{T}$, $t \in \mathbb{T}$. Then, there exists a parameter-dependent matrix $M(\alpha) \succ 0$, for $\alpha \in \mathcal{T}$, such that

$$Q(\delta\alpha) \succ A(\alpha)Q(\alpha)A(\alpha)' + B(\alpha)B(\alpha)' + M(\alpha) \qquad (A.3)$$

for all $\alpha \in \mathcal{T}$. Consequently, combining (A.2) and (A.3) implies that $Q(\alpha) \succ \bar{Q}(\alpha)$ for all $\alpha \in \mathcal{T}$. In turn, (2.12b) gives

$$W(\alpha) \succ C(\alpha)Q(\alpha)C(\alpha)' \succ C(\alpha)\bar{Q}(\alpha)C(\alpha)', \quad \forall \alpha \in \mathcal{T},$$

proving that the inequality (2.13) holds. $\qquad\qquad\qquad \square$

A.5 Proof of Theorem 5

For technical reasons, a separate proof is provided for the continuous-time, respectively, the discrete-time case.

Continuous-time case: Suppose that there exist bounded matrices $P(\alpha(t)) \in \mathbb{S}_+^{n_x}$ and $W(\alpha(t)) \in \mathbb{S}_+^{n_z}$ for $\alpha \in \mathcal{T}$, $t \in \mathbb{T}$, such that the LMIs (2.14) are feasible for all $\alpha \in \mathcal{T}$, $t \in \mathbb{T}$. In continuous time, the parameter-dependent LMI (2.14a) is explicitly given by

$$\begin{bmatrix} P(\alpha)A(\alpha) + A(\alpha)'P(\alpha) + \delta P(\alpha) & P(\alpha)B(\alpha) \\ B(\alpha)'P(\alpha) & -I \end{bmatrix} \prec 0,$$

which, using the Schur complement (see Appendix B.1), is equivalent to

$$P(\alpha)A(\alpha) + A(\alpha)'P(\alpha) + \delta P(\alpha) + P(\alpha)B(\alpha)B(\alpha)'P(\alpha) \prec 0. \tag{A.4}$$

Now define $Q(\alpha) := P(\alpha)^{-1}$, such that $\delta Q(\alpha) = -P(\alpha)^{-1}\delta P(\alpha)P(\alpha)^{-1}$. Hence, pre- and postmultiplying (A.4) by $Q(\alpha) := P(\alpha)^{-1}$ results in the equivalent condition (2.12a), where we use the fact that $P(\alpha)^{-1}$ exists, since $P(\alpha(t))$ is positive definite for all $\alpha \in \mathcal{T}$, $t \in \mathbb{T}$. Furthermore, pre- and postmultiplying the parameter-dependent LMI (2.14b) by

$$\begin{bmatrix} I & 0 \\ 0 & Q(\alpha) \end{bmatrix},$$

the following equivalent LMI in terms of $Q(\alpha)$ is obtained:

$$\begin{bmatrix} W(\alpha) & C(\alpha)Q(\alpha) \\ Q(\alpha)C(\alpha)' & Q(\alpha) \end{bmatrix}. \tag{A.5}$$

Applying the Schur complement on (A.5) results in the equivalent condition (2.12b). Therefore, the conditions of Theorem 4 (see page 14) are fulfilled for all $\alpha \in \mathcal{T}$, $t \in \mathbb{T}$, finishing the proof. $\qquad\square$

Discrete-time case: Assume that there exist bounded matrices $P(\alpha(t)) \in \mathbb{S}_+^{n_x}$ and $W(\alpha(t)) \in \mathbb{S}_+^{n_z}$ for $\alpha \in \mathcal{T}$, $t \in \mathbb{T}$, such that the LMIs (2.14) are feasible for all $\alpha \in \mathcal{T}$, $t \in \mathbb{T}$. In discrete time, the parameter-dependent LMI (2.14a) equals

$$\begin{bmatrix} A(\alpha)'P(\delta\alpha)A(\alpha) - P(\alpha) & A(\alpha)'P(\delta\alpha)B(\alpha) \\ B(\alpha)'P(\delta\alpha)A(\alpha) & B(\alpha)'P(\delta\alpha)B(\alpha) - I \end{bmatrix} \prec 0,$$

which is, using the Schur complement (see Appendix B.1), equivalent to

$$\begin{bmatrix} P(\delta\alpha) & P(\delta\alpha)A(\alpha) & P(\delta\alpha)B(\alpha) \\ A(\alpha)'P(\delta\alpha) & P(\alpha) & 0 \\ B(\alpha)'P(\delta\alpha) & 0 & I \end{bmatrix} \succ 0.$$

Applying the Schur complement again gives the equivalent condition

$$\begin{bmatrix} P(\delta\alpha) - P(\delta\alpha)B(\alpha)B(\alpha)'P(\delta\alpha) & P(\delta\alpha)A(\alpha) \\ A(\alpha)'P(\delta\alpha) & P(\alpha) \end{bmatrix} \succ 0. \qquad (A.6)$$

Defining $Q(\alpha) := P(\alpha)^{-1}$, such that $Q(\delta\alpha) = P(\delta\alpha)^{-1}$, pre- and postmultiplication of (A.6) by

$$\begin{bmatrix} Q(\delta\alpha) & 0 \\ 0 & Q(\alpha) \end{bmatrix}$$

yields the following equivalent LMI in terms of $Q(\alpha)$:

$$\begin{bmatrix} Q(\delta\alpha) - B(\alpha)B(\alpha)' & A(\alpha)Q(\delta\alpha) \\ Q(\delta\alpha)A(\alpha)' & Q(\alpha) \end{bmatrix} \succ 0. \qquad (A.7)$$

Note that $P(\alpha)^{-1}$ exists, since $P(\alpha(t))$ is positive definite for all $\alpha \in \mathcal{T}$, $t \in \mathbb{T}$. A third application of the Schur complement reveals that (A.7) is equivalent to the parameter-dependent LMI (2.12a). The fact that the LMIs (2.14b) and (2.12b) are equivalent, as is shown in the proof corresponding to the continuous-time case, implies that the conditions of Theorem 4 (see page 14) are fulfilled for all $\alpha \in \mathcal{T}$, $t \in \mathbb{T}$, finishing the proof. $\qquad\square$

A.6 Proof of Theorem 6

Suppose that there exist bounded matrices $P(\alpha(t)) \in \mathbb{S}_+^{2n_x}$, $X_1(\alpha(t)) \in \mathbb{R}^{2n_x \times (n_x+n_u)}$, $X_2(\alpha(t)) \in \mathbb{R}^{n_w \times (n_x+n_u)}$, and $X_3(\alpha(t)) \in \mathbb{R}^{(n_x+n_u) \times (n_x+n_u)}$, and a bounded scalar $\gamma > 0$ such that the parameter-dependent LMI (3.9) is feasible for all $\alpha \in \mathcal{T}$, $t \in \mathbb{T}$. Then, deriving the matrix

$$\begin{bmatrix} \Upsilon(\alpha)\tilde{C}_y(\alpha) & \Upsilon(\alpha)\tilde{D}_{yw}(\alpha) & -I \end{bmatrix}_\perp = \begin{bmatrix} I & 0 \\ 0 & I \\ \Upsilon(\alpha)\tilde{C}_y(\alpha) & \Upsilon(\alpha)\tilde{D}_{yw}(\alpha) \end{bmatrix}, \qquad (A.8)$$

noting that (3.8) implies

$$Q_{\Psi,\infty}(\alpha) \begin{bmatrix} I & 0 \\ 0 & I \\ \Upsilon(\alpha)\tilde{C}_y(\alpha) & \Upsilon(\alpha)\tilde{D}_{yw}(\alpha) \end{bmatrix} = \begin{bmatrix} I & 0 \\ \mathcal{A}_{\Theta_a}(\alpha) & \mathcal{B}_{\Theta_a}(\alpha) \\ 0 & I \\ \mathcal{C}_{\Theta_a}(\alpha) & \mathcal{D}_{\Theta_a}(\alpha) \end{bmatrix},$$

and applying the projection lemma (see Appendix B.2) on the parameter-dependent LMI (3.9), the following equivalent condition is obtained:

$$
\begin{bmatrix} I & 0 \\ \mathcal{A}_{\Theta_a}(\alpha(t)) & \mathcal{B}_{\Theta_a}(\alpha(t)) \\ 0 & I \\ \mathcal{C}_{\Theta_a}(\alpha(t)) & \mathcal{D}_{\Theta_a}(\alpha(t)) \end{bmatrix}'
\begin{bmatrix} \Phi(\alpha(t)) & 0 & 0 \\ 0 & -\gamma I & 0 \\ 0 & 0 & I \end{bmatrix}
\begin{bmatrix} I & 0 \\ \mathcal{A}_{\Theta_a}(\alpha(t)) & \mathcal{B}_{\Theta_a}(\alpha(t)) \\ 0 & I \\ \mathcal{C}_{\Theta_a}(\alpha(t)) & \mathcal{D}_{\Theta_a}(\alpha(t)) \end{bmatrix} \prec 0
$$

(A.9)

for all $\alpha \in \mathcal{T}$, $t \in \mathbb{T}$. Since $P(\alpha(t)) \succ 0$ for all $\alpha \in \mathcal{T}$, $t \in \mathbb{T}$, Theorem 3 (see page 13) implies that H_{Θ_a} is exponentially stable and satisfies the $\mathcal{H}_\infty$ performance bound $\|H_{\Theta_a}\|_\infty < \sqrt{\gamma}$. Observing that $\Theta(\alpha)$ has the same stability and performance properties as $\Theta_a(\alpha)$, it is clear that H_Θ is exponentially stable and $\|H_\Theta\|_\infty < \sqrt{\gamma}$, finishing the proof. $\square$

A.7 Proof of Theorem 7

Suppose that there exist bounded matrices $P(\alpha(t)) \in \mathbb{S}_+^{2n_x}$, $W(\alpha(t)) \in \mathbb{S}_+^{n_z}$, $X_1(\alpha(t)) \in \mathbb{R}^{2n_x \times (n_x+n_u)}$, $X_2(\alpha(t)) \in \mathbb{R}^{n_w \times (n_x+n_u)}$, $X_3(\alpha(t)) \in \mathbb{R}^{(n_x+n_u) \times (n_x+n_u)}$, $X_4(\alpha(t)) \in \mathbb{R}^{n_z \times (n_x+n_u)}$, $X_5(\alpha(t)) \in \mathbb{R}^{2n_x \times (n_x+n_u)}$, and $X_6(\alpha(t)) \in \mathbb{R}^{n_w \times (n_x+n_u)}$, such that the parameter-dependent LMIs (3.11) are feasible for all $\alpha \in \mathcal{T}$, $t \in \mathbb{T}$. Then, since (A.8) implies that

$$
Q_{\Psi,2}(\alpha) \begin{bmatrix} I & 0 \\ 0 & I \\ \Upsilon(\alpha)\tilde{C}_y(\alpha) & \Upsilon(\alpha)\tilde{D}_{yw}(\alpha) \end{bmatrix} = \begin{bmatrix} I & 0 \\ \mathcal{A}_{\Theta_a}(\alpha) & \mathcal{B}_{\Theta_a}(\alpha) \\ 0 & I \end{bmatrix},
$$

application of the projection lemma results in the equivalent condition

$$
\begin{bmatrix} I & 0 \\ \mathcal{A}_{\Theta_a}(\alpha(t)) & \mathcal{B}_{\Theta_a}(\alpha(t)) \\ 0 & I \end{bmatrix}'
\begin{bmatrix} \Phi(\alpha(t)) & 0 \\ 0 & -I \end{bmatrix}
\begin{bmatrix} I & 0 \\ \mathcal{A}_{\Theta_a}(\alpha(t)) & \mathcal{B}_{\Theta_a}(\alpha(t)) \\ 0 & I \end{bmatrix} \prec 0
$$

for all $\alpha \in \mathcal{T}$, $t \in \mathbb{T}$. Furthermore, deriving the matrix

$$
\begin{bmatrix} 0 & \Upsilon(\alpha)\tilde{C}_y(\alpha) & -I \end{bmatrix}_\perp = \begin{bmatrix} I & 0 \\ 0 & I \\ 0 & \Upsilon(\alpha)\tilde{C}_y(\alpha) \end{bmatrix},
$$

and noting that (3.8) implies

$$
\begin{bmatrix} W(\alpha) & \mathcal{C}_\Psi(\alpha) & \tilde{D}_{zu}(\alpha) \end{bmatrix}
\begin{bmatrix} I & 0 \\ 0 & I \\ 0 & \Upsilon(\alpha)\tilde{C}_y(\alpha) \end{bmatrix} = \begin{bmatrix} W(\alpha) & \mathcal{C}_{\Theta_a}(\alpha) \end{bmatrix},
$$

application of the projection lemma shows the equivalence between (3.11b) and

$$
\begin{bmatrix} W(\alpha(t)) & \mathcal{C}_{\Theta_{\mathrm{a}}}(\alpha(t)) \\ \mathcal{C}_{\Theta_{\mathrm{a}}}(\alpha(t))' & P(\alpha(t)) \end{bmatrix} \succ 0,
$$

for all $\alpha \in \mathcal{T}$, $t \in \mathbb{T}$. Therefore, Theorem 5 (see page 14) implies that $H_{\Theta_{\mathrm{a}}}$ is exponentially stable and satisfies the $\mathcal{H}_2$ performance bound (3.10). Observing that $\Theta(\alpha)$ has the same stability and performance properties as $\Theta_{\mathrm{a}}(\alpha)$, it is clear that H_{Θ} is exponentially stable and satisfies (3.10), finishing the proof. $\qquad\square$

A.8 Proof of Theorem 8

Suppose that, for a given stabilizing controller $\Psi(\alpha(t)) \in \mathbb{R}^{(n_x+n_u)\times(n_x+n_y)}$ (defined as in (3.2)), a prefixed controller order q ($0 \leq q \leq n_x$), and a given bounded matrix $A_{22}(\alpha(t)) \in \mathbb{R}^{(n_x-q)\times(n_x-q)}$ corresponding to exponentially stable dynamics, there exist bounded matrices $P(\alpha(t)) \in \mathbb{S}_+^{2n_x}$, $\bar{\Theta}(\alpha(t)) \in \mathbb{R}^{(q+n_u)\times(n_x+n_y)}$ as in (3.12), and $Y(\alpha(t)) \in \mathbb{R}^{(n_x+n_u)\times(n_x+n_u)}$ as in (3.13), and a bounded scalar $\gamma > 0$ such that the parameter-dependent LMI (3.14) is feasible for all $\alpha \in \mathcal{T}$, $t \in \mathbb{T}$. According to the parameterizations (3.3) and (3.12), the nonlinear transformation (3.16) yields the following structure for $\bar{\Theta}(\alpha)$:

$$
\bar{\Theta}(\alpha) = \begin{bmatrix} Y_{11}(\alpha) & Y_{13}(\alpha) \\ Y_{31}(\alpha) & Y_{33}(\alpha) \end{bmatrix} \begin{bmatrix} A_c(\alpha) & A_{12}(\alpha) & B_c(\alpha) \\ C_c(\alpha) & C_2(\alpha) & D_c(\alpha) \end{bmatrix}. \tag{A.10}
$$

Note that the nonlinear transformation (3.16) is well-defined, since feasibility of (3.14) implies that the inverse

$$
\begin{bmatrix} Y_{11}(\alpha) & Y_{13}(\alpha) \\ Y_{31}(\alpha) & Y_{33}(\alpha) \end{bmatrix}^{-1}
$$

exists for all $\alpha \in \mathcal{T}$. Combining (A.10) and (3.15), and using the specific structure (3.7) of the lifted controller $\Theta_{\mathrm{a}}(\alpha)$, we obtain

$$
Z(\alpha) = Y(\alpha)(\Theta_{\mathrm{a}}(\alpha) - \Psi(\alpha)) = Y(\alpha)\Upsilon(\alpha). \tag{A.11}
$$

Substituting (A.11) in the parameter-dependent LMI (3.14) reveals that the conditions (3.9) subject to the structural constraints

$$
X_1(\alpha) = 0, \qquad X_2(\alpha) = 0, \qquad X_3(\alpha) = Y(\alpha)
$$

are feasible for all $\alpha \in \mathcal{T}$, $t \in \mathbb{T}$. Therefore, applying Theorem 6 (see page 33) finishes the proof. $\qquad\square$

A.9   Proof of Theorem 9

Suppose that, for a given stabilizing controller $\Psi(\alpha(t)) \in \mathbb{R}^{(n_x+n_u) \times (n_x+n_y)}$ (defined as in (3.2)), a prefixed controller order q ($0 \leq q \leq n_x$), and a given bounded matrix $A_{22}(\alpha(t)) \in \mathbb{R}^{(n_x-q) \times (n_x-q)}$ corresponding to exponentially stable dynamics, there exist bounded matrices $P(\alpha(t)) \in \mathbb{S}_+^{2n_x}$, $\bar{\Theta}(\alpha(t)) \in \mathbb{R}^{(q+n_u) \times (n_x+n_y)}$ as in (3.12), and $Y(\alpha(t)) \in \mathbb{R}^{(n_x+n_u) \times (n_x+n_u)}$ as in (3.13), such that the parameter-dependent LMIs (3.17) are feasible for all $\alpha \in \mathcal{T}$, $t \in \mathbb{T}$. Then, by following the steps of the proof presented in Appendix A.8 and using relation (A.11), it is clear that the matrix inequalities (3.17) subject to the structural constraints

$$X_1(\alpha) = 0, \qquad X_2(\alpha) = 0, \qquad X_3(\alpha) = Y(\alpha),$$

$$X_4(\alpha) = 0, \qquad X_5(\alpha) = 0, \qquad X_6(\alpha) = -Y(\alpha),$$

are feasible for all $\alpha \in \mathcal{T}$, $t \in \mathbb{T}$. Consequently, application of Theorem 7 (see page 34) finishes the proof. $\qquad\square$

Appendix B

Mathematical tools

> Two very useful tools which are used troughout this thesis, namely the Schur complement [18, 19] and the projection lemma [41], are included for the sake of completeness.

B.1 Schur complement

Let $Q \in \mathbb{S}^m$, $S \in \mathbb{S}^n$ and $R \in \mathbb{R}^{m \times n}$. Then, the nonlinear matrix inequality

$$Q \prec 0, \quad S - R'Q^{-1}R \prec 0$$

holds if, and only if, the LMI

$$\begin{bmatrix} S & R' \\ R & Q \end{bmatrix} \prec 0$$

is feasible.

B.2 Projection lemma

Given a matrix $Z \in \mathbb{S}^n$ and two matrices U and V of column dimension n, the following are equivalent:

- There exists an unstructured matrix X such that

$$U'XV + V'X'U + Z \prec 0.$$

- The projection inequalities with respect to X hold:

$$U'_\perp Z U_\perp \prec 0,$$

$$V'_\perp Z V_\perp \prec 0,$$

where $U_\perp$ and $V_\perp$ are arbitrary matrices whose columns form a basis for the null space of U and V, respectively.

Appendix C

Model order reduction for LTD systems

| This appendix presents a technical addenda to the model order reduction approach of Chapter 7.

C.1   Sparse system representation

If the grid points in the spectral discretization of (7.6) are chosen as (7.14), then we can express the transfer function (7.11) as

$$\Gamma_x^N(s) = F_N \left(sG_N - I\right)^{-1} H_N + \mathbf{D},$$

where

$$F_N = \begin{bmatrix} CR_0 & CR_1 & \cdots & CR_{N-1} \end{bmatrix},$$

$$G_N = \Sigma_N^{-1}\Pi_N,$$

and

$$H_N = \begin{bmatrix} R_0^{-1}\left(I - \frac{\tau_{\max}}{2}R_1\right)R_0^{-1}\mathbf{B} \\ \frac{\tau_{\max}}{2}R_0^{-1}\mathbf{B} \\ 0 \\ \vdots \\ 0 \end{bmatrix}$$

with Σ_N and Π_N defined by

$$
\Sigma_N = \begin{bmatrix} R_0 & R_1 & \cdots & R_{N-1} \\ & I_{n_x} & & \\ & & \ddots & \\ & & & I_{n_x} \end{bmatrix},
$$

and

$$
\Pi_N = \frac{\tau_{\max}}{4} \begin{bmatrix}
\frac{4}{\tau_{\max}} & \frac{4}{\tau_{\max}} & \frac{4}{\tau_{\max}} & \cdots & & \cdots & \frac{4}{\tau_{\max}} \\
2 & 0 & -1 & & & & \\
& \frac{1}{2} & 0 & -\frac{1}{2} & & & \\
& & \frac{1}{3} & 0 & \ddots & & \\
& & & \frac{1}{4} & \ddots & -\frac{1}{N-3} & \\
& & & & \ddots & 0 & -\frac{1}{N-2} \\
& & & & & \frac{1}{N-1} & 0
\end{bmatrix} \otimes I
$$

with

$$
R_i = A_0 T_i(1) + \sum_{k=1}^{m_x} A_k T_i\left(-2\frac{\tau_k}{\tau_{\max}} + 1\right), \quad i = 0, \ldots, N-1.
$$

C.2 Adaptive construction

Assume that $N_1, N_2 \in \mathbb{N}$ with $N_1 < N_2$. Then the matrices $\Sigma_{N_1}, \Pi_{N_1}, F_{N_1}, H_{N_1}$, as in Appendix C.1, are submatrices of $\Sigma_{N_2}, \Pi_{N_2}, F_{N_2}, H_{N_2}$.

C.3 Dynamic construction of a Krylov space

Fix an integer k, assume that $1 \le k \le N$, and consider the Krylov space

$$
\mathcal{K}_k(G_N, b) := \operatorname{span}\{b, G_N b, \ldots, G_N^{k-1} b\}, \tag{C.1}
$$

where b is a block vector of size $Nn_x \times n_u$. The block Arnoldi algorithm builds the Krylov sequence, block vector by block vector, while the vectors are additionally orthogonalized. Assuming that the block vector b in (C.1) has the special structure

$$
b = \begin{bmatrix} x_0' & 0 & \cdots & 0 \end{bmatrix}', \quad x_0 \in \mathbb{R}^{n_x \times n_u}, \tag{C.2}
$$

only the first $2n_x, 3n_x, \ldots, kn_x$ block rows of the block vectors $G_N b, \ldots, G_N^{k-1} b$ are nonzero. Moreover, computation of the matrix vector products only requires sub-matrices of G_N. Hence, in the computation of the Krylov space, we can restrict to storing only the nonzero part of the block vectors and using the relevant part of G_N. Incorporating this in the block Arnoldi algorithm, we arrive at Algorithm 1. In the description we use notation common for Arnoldi iterations: we let $\underline{\mathcal{H}}_i \in \mathbb{R}^{(i+1)n_u \times i n_u}$ denote the dynamically constructed rectangular block Hessenberg matrix and $\mathcal{H}_i \in \mathbb{R}^{i n_u \times i n_u}$ the corresponding $i \times i$ upper blocks. To simplify the notation, the Krylov space (C.1) with starting vector (C.2) is denoted by $\mathcal{K}_k(G_N, x_0)$.

Algorithm 1 (Dynamic construction of a Krylov space).

Require: $x_0 \in \mathbb{R}^{n_x \times n_u}$.

1: *Let $x_0 = Q_0 R_0$ be the reduced QR factorization of x_0. Set $V_1 = Q_0$ and let $\underline{\mathcal{H}}_0$ be the empty matrix.*

2: **for** $i = 1, 2, \ldots, k$ **do**

3:     *Let $W_i = G_{i+1} \begin{bmatrix} Q_{i-1} \\ 0 \end{bmatrix}$.*

4:     *Orthogonalization: compute $H_i = \begin{bmatrix} V_i' & 0 \end{bmatrix} W_i$ and $\hat{W}_i = W_i - \begin{bmatrix} V_i \\ 0 \end{bmatrix} H_i$.*

5:     *Normalization: compute the reduced QR factorization $\hat{W}_i = Q_i R_i$ of $\hat{W}_i$.*

6:     *Let $\underline{\mathcal{H}}_i = \begin{bmatrix} \underline{\mathcal{H}}_{i-1} & H_i \\ 0 & R_i \end{bmatrix} \in \mathbb{R}^{(i+1)n_u \times i n_u}$.*

7:     *Expand V_i into $V_{i+1} = \begin{bmatrix} V_i \\ 0 \end{bmatrix} \Big| \, Q_i \end{bmatrix}$.*

8: **end for**

Output: *V_k, $\mathcal{H}_k$ and $\underline{\mathcal{H}}_k$, where the columns of V_k form an orthogonal basis for $\mathcal{K}_k(G_k, x_0)$, and $\mathcal{H}_k = V_k' G_k V_k$.*

Note that, due to the special structure of the starting block vector and matrix G_N,
$$\begin{bmatrix} V_k' & 0 & \cdots & 0 \end{bmatrix}' \in \mathbb{R}^{N n_x \times n_u}$$
is a basis for $\mathcal{K}_k(G_N, x_0)$ for any $N \geq k$ and, correspondingly,
$$\mathcal{H}_k = \begin{bmatrix} V_k' & 0 & \cdots & 0 \end{bmatrix} G_N \begin{bmatrix} V_k \\ 0 \\ \vdots \\ 0 \end{bmatrix}.$$

That is, $\mathcal{H}_k$ can be considered as an orthogonal projection of G_N on a Krylov subspace, for *any* $N \geq k$.

C.4   Proof of Theorem 11

The proof is obtained by adapting the corresponding result in [79] to the MIMO setting.

Take any $N \geq k$. By Theorem 10, Γ_x and Γ_x^N match (at least) $k-1$ moments at zero and 2 moments at infinity. Hence, it remains to show that Γ_x^N and $\Gamma_x^{(k)}$ satisfy this moment matching property.

We know that $\begin{bmatrix} V_k' & 0 & \cdots & 0 \end{bmatrix}'$ is a basis for $\mathcal{K}_k(G_N, R_0^{-1}\mathbf{B})$, and that $\Gamma_x^{(k)}$ is obtained from Γ_x^N by projecting on this space. A simple computation shows that

$$H_N = G_N \begin{bmatrix} R_0^{-1}\mathbf{B} \\ 0 \\ \vdots \\ 0 \end{bmatrix}.$$

Therefore, we have

$$\mathcal{K}_k(G_N, R_0^{-1}\mathbf{B}) = \operatorname{span}\left\{ G_N^{-1}H_N, H_N, G_N H_N, \ldots, G_N^{k-2}H_N \right\}.$$

This is what we need to have $k-1$ moments at zero and 2 at infinity carried over in the projection [4]. $\qquad\square$

C.5   Construction of a reduced delay-free model

Algorithm 2 (Construction of a reduced delay-free model)**.**

1: Apply Algorithm 1 with $x_0 = R_0^{-1}\mathbf{B}$ and construct $G^{(k)} = \mathcal{H}_k$.

2: At the same time dynamically construct $F^{(k)}$ and $H^{(k)}$, defined in (7.17).

Output: *Matrices $F^{(k)}$, $G^{(k)}$ and $H^{(k)}$ of the reduced model of order kn_u, and the corresponding transfer function $\Gamma_x^{(k)}(s) = F^{(k)}(sG^{(k)} - I)^{-1}H^{(k)} + \mathbf{D}$.*

Bibliography

[1] C. M. Agulhari, R. C. L. F. Oliveira, and P. L. D. Peres. Robust $\mathcal{H}_\infty$ static output-feedback design for time-invariant discrete-time polytopic systems from parameter-dependent state-feedback gains. In *Proceedings of the 2010 American Control Conference*, pages 4677–4682, Baltimore, MD, USA, July 2010.

[2] C. M. Agulhari, R. C. L. F. Oliveira, and P. L. D. Peres. Static output feedback control of polytopic systems using polynomial Lyapunov functions. In *Proceedings of the 49th IEEE Conference on Decision and Control*, pages 6894–6901, December 2010.

[3] C. M. Agulhari, R. C. L. F. Oliveira, and P. L. D. Peres. LMI relaxations for reduced-order robust $\mathcal{H}_\infty$ control of continuous-time uncertain linear systems. *IEEE Transactions on Automatic Control*, 57(6):1532–1537, 2012.

[4] A. C. Antoulas. *Approximation of large-scale dynamical systems*. Advances in Design and Control 12. SIAM Publications, Philadelphia, 2005.

[5] P. Apkarian and R. J. Adams. Advanced gain-scheduling techniques for uncertain systems. *IEEE Transactions on Control System Technology*, 6:21–32, 1998.

[6] P. Apkarian and D. Noll. Nonsmooth $\mathcal{H}_\infty$ synthesis. *IEEE Transactions on Automatic Control*, 51(1):71–86, January 2006.

[7] P. Apkarian, P. C. Pellanda, and H. D. Tuan. Mixed $\mathcal{H}_2/\mathcal{H}_\infty$ multi-channel linear parameter-varying control in discrete time. *Systems & Control Letters*, 41(5):333–346, 2000.

[8] D. Arzelier, G. Deaconu, S. Gumussoy, and D. Henrion. $\mathcal{H}_2$ for HIFOO. In *International Conference on Control and Optimization with Industrial Applications*, Bilkent University, Ankara, Turkey, August 2011.

[9] T. Asai and S. Hara. Convex parametrization of reduced order controllers for a class of problems under partial state measurements. In *Proceedings of the 36th Conference on Decision and Control*, pages 189–190, San Diego, California, USA, December 1997.

[10] T. Asai and S. Hara. A unified approach to LMI-based reduced order self-scheduling control synthesis. *Systems & Control Letters*, 36(1):75–86, 1999.

[11] Z. Bai and R. W. Freund. A partial Padé-via-Lanczos method for reduced-order modeling. *Linear Algebra and its Applications*, 332-334:139–164, 2001.

[12] Z. Bai and Y. Su. Dimension reduction of second-order dynamical systems via a second-order Arnoldi method. *SIAM Journal on Matrix Analysis and Applications*, 26(5):1692–1709, 2005.

[13] P. Ballesteros, X. Shu, W. Heins, and C. Bohn. *Advances on Analysis and Control of Vibrations*, chapter LPV gain-scheduled output feedback for active control of harmonic disturbances with time-varying frequencies. InTech, Croatia, 2012.

[14] K. A. Barbosa, C. E. De Souza, and A. Trofino. Robust $\mathcal{H}_2$ filtering for discrete-time uncertain linear systems using parameter-dependent Lyapunov functions. In *Proceedings of the 2002 American Control Conference*, pages 3224–3229, Anchorage, AK, USA, May 2002.

[15] G. Becker and A. Packard. Robust performance of linear parametrically varying systems using parametrically-dependent linear feedback. *Systems & Control Letters*, 23(3):205 – 215, 1994.

[16] V. D. Blondel and J. N. Tsitsiklis. A survey of computational complexity results in systems and control. *Automatica*, 36(9):1249–1274, 2000.

[17] S. Boyd and C. Barratt. *Linear Controller Design: Limits of Performance*. Prentice-Hall, 1991.

[18] S. Boyd, L. El Ghaoui, E. Feron, and V. Balakrishnan. *Linear Matrix Inequalities in System and Control Theory*, volume 15 of *Studies in Applied Mathematics*. SIAM, Philadelphia, 1994.

[19] S. Boyd and L. Vandenberghe. *Convex Optimization*. Cambridge University Press, Cambridge, 2004.

[20] D. Breda, S. Maset, and R. Vermiglio. Pseudospectral differencing methods for characteristic roots of delay differential equations. *SIAM Journal on Scientific Computing*, 27(2):482–495, 2005.

[21] J. F. Camino, M. C. de Oliveira, and R. E. Skelton. "Convexifying" linear matrix inequality methods for integrating structure and control design. *Journal of Structural Engineering*, 129:978–988, 2003.

[22] M. Corno, M. Tanelli, S. M. Savaresi, and L. Fabbri. Design and validation of a gain-scheduled controller for the electronic throttle body in ride-by-wire racing motorcycles. *IEEE Transactions on Control Systems Technology*, 19(1):18–30, January 2011.

[23] C. A. R. Crusius and A. Trofino. Sufficient LMI conditions for output feedback control problems. *IEEE Transactions on Automatic Control*, 44(5):1053–1057, May 1999.

[24] R. F. Curtain and H. Zwart. *An introduction to infinite-dimensional linear systems theory.* Springer-Verlag, 1995.

[25] C. de Boor. *A Practical Guide to Splines*, volume 27 of *Applied Mathematical Sciences.* Springer-Verlag, 2001.

[26] J. De Caigny. *Contributions to the modeling and control of Linear Parameter-Varying systems.* PhD thesis, KU Leuven, December 2009.

[27] J. De Caigny, J. F. Camino, R. C. L. F. Oliveira, P. L. D. Peres, and J. Swevers. Gain-scheduled $\mathcal{H}_2$ and $\mathcal{H}_\infty$ control of discrete-time polytopic time-varying systems. *IET Control Theory and Applications*, 4(3):362–380, March 2010.

[28] J. De Caigny, J. F. Camino, R. C. L. F. Oliveira, P. L. D. Peres, and J. Swevers. Gain-scheduled dynamic output feedback for discrete-time LPV systems. *International Journal of Robust and Nonlinear Control*, 22(5):535–558, 2011.

[29] J. De Caigny, J. F. Camino, and J. Swevers. Interpolation-based modeling of MIMO LPV systems. *IEEE Transactions on Control Systems Technology*, 19(1):46–63, 2011.

[30] J. A. de Loera and F. Santos. An effective version of Pólya's theorem on positive definite forms. *Journal of Pure and Applied Algebra*, 108(3):231–240, 1996.

[31] M. C. de Oliveira, J. Bernussou, and J. C. Geromel. A new discrete-time robust stability condition. *Systems & Control Letters*, 37:261–265, 1999.

[32] M. C. de Oliveira, J. C. Geromel, and J. Bernussou. Extended $\mathcal{H}_2$ and $\mathcal{H}_\infty$ norm characterizations and controller parametrizations for discrete-time systems. *International Journal of Control*, 75(9):666–679, 2002.

[33] M. Dettori and C. W. Scherer. LPV design for a CD player: an experimental evaluation of performance. In *Proceedings of the 40th IEEE Conference on Decision and Control*, pages 4711–4716, Orlando, Florida, USA, 2001.

[34] A. L. Do, C. Spelta, S. Savaresi, O. Sename, L. Dugard, and D. Delvecchio. An LPV control approach for comfort and suspension travel improvements of semi-active suspension systems. In *Proceedings of the 49th IEEE Conference on Decision and Control*, pages 5560–5565, Atlanta, Georgia, USA, December 2010.

[35] J. Dong and G.-H. Yang. Robust static output feedback control for linear discrete-time systems with time-varying uncertainties. *Systems & Control Letters*, 57:123–131, 2008.

[36] X. Du and G.-H. Yang. LMI conditions for $\mathcal{H}_\infty$ static output feedback control of discrete-time systems. In *Proceedings of the 47th IEEE Conference on Decision and Control*, pages 5450–5455, Cancun, Mexico, December 2008.

[37] Z. Emedi and A. Karimi. Robust fixed-order discrete-time LPV controller design. In *Preprints of the 19th World Congress, IFAC*, pages 6914–6919, Cape Town, South Africa, August 2014.

[38] P. Feldman and R. W. Freund. Efficient linear circuit analysis by Padé approximation via the Lanczos process. *IEEE Transactions on Computer-Aided Design*, 14:639–649, 1995.

[39] R. W. Freund. Subspaces associated with higher-order linear dynamical systems. *BIT*, 45:495–516, 2005.

[40] M. Fu and Z. Luo. Computational complexity of a problem arising in fixed order output feedback design. *Systems & Control Letters*, 30(5):209–215, 1997.

[41] P. Gahinet and P. Apkarian. A linear matrix inequality approach to $\mathcal{H}_\infty$ control. *International Journal of Robust and Nonlinear Control*, 4(4):421–448, 1994.

[42] K. Gallivan, E. Grimme, and P. Van Dooren. A rational Lanczos algorithm for model reduction. *Numerical Algorithms*, 12:33–63, 1996.

[43] M. Green and D. J. Limebeer. *Linear Robust Control*. Prentice-Hall, 1995.

[44] K. M. Grigoriadis and R. E. Skelton. Low-order control design for LMI problems using alternating projection methods. *Automatica*, 32:1117–1125, 1996.

[45] K. M. Grigoriadis and F. Wu. Integrated $\mathcal{H}_\infty$ plant/controller design via linear matrix inequalities. In *Proceedings of the 36th IEEE Conference on Decision and Control*, pages 789–790, San Diego, California, USA, December 1997.

[46] E. Grimme, D. Sorensen, and P. Van Dooren. Model reduction of state space systems via an implicitly restarted Lanczos method. *Numerical Algorithms*, 12:1–31, 1996.

[47] S. Gumussoy, D. Henrion, M. Millstone, and M. L. Overton. Multiobjective robust control with HIFOO 2.0. In *Proceedings of the 6th IFAC Symposium on Robust Control Design*, pages 144–149, Haifa, Israel, June 2009.

[48] W. M. Haddad and V. Chellaboina. *Nonlinear Dynamical Systems and Control*. Princeton University Press, 2008.

[49] G. H. Hardy, J. E. Littlewood, and G. Pólya. *Inequalities*. Cambridge University Press, Cambridge, UK, 2 edition, 1952.

[50] D. Henrion and M. Šebek. Overcoming non-convexity in polynomial robust control design. In *Proceedings of the Symposium of Mathematical Theory of Networks and Systems (MTNS)*, Leuven, Belgium, 2004.

[51] D. Henrion, M. Šebek, and V. Kučera. Positive polynomials and robust stabilization with fixed-order controllers. *IEEE Transactions on Automatic Control*, 48(7):1178–1186, 2003.

[52] G. Hilhorst, G. Pipeleers, W. Michiels, R. C. L. F. Oliveira, P. L. D. Peres, and J. Swevers. Reduced-order $\mathcal{H}_2/\mathcal{H}_\infty$ control of discrete-time LPV systems with experimental validation on an overhead crane test setup. In *Proceedings of the 2015 American Control Conference*, pages 125–130, Chicago, IL, USA, July 2015.

[53] G. Hilhorst, G. Pipeleers, W. Michiels, R. C. L. F. Oliveira, P. L. D. Peres, and J. Swevers. An iterative convex approach for fixed-order robust $\mathcal{H}_2/\mathcal{H}_\infty$ control of discrete-time linear systems with parametric uncertainty. In 54th *Conference on Decision and Control*, Osaka, Japan, December 2015 (accepted).

[54] G. Hilhorst, G. Pipeleers, W. Michiels, and J. Swevers. Sufficient LMI conditions for reduced-order multi-objective $\mathcal{H}_2/\mathcal{H}_\infty$ control of LTI systems. *European Journal of Control*, 23:17–25, May 2015.

[55] C. Hoffmann and H. Werner. A survey of linear parameter-varying control applications validated by experiments or high-fidelity simulations. *IEEE Transactions on Control Systems Technology*, 23(2):416–433, March 2015.

[56] C. W. J. Hol and C. W. Scherer. Sum of squares relaxations for polynomial semidefinite programming. In *Proc. Symp. on Mathematical Theory of Networks and Systems (MTNS), Leuven, Belgium*, 2004.

[57] G. W. Housner, L. A. Bergman, T. K. Caughey, A. G. Chassiakos, R. O. Claus, S. F. Masri, R. E. Skelton, T. T. Soong, B. F. Spencer, and J. T. P. Yao. Structural control: Past, present and future. *Journal of Engineering Mechanics*, 123(9):897–971, 1997.

[58] T. Iwasaki and R. E. Skelton. All controllers for the general $\mathcal{H}_\infty$ control problem: LMI existence conditions and state space formulas. *Automatica*, 30(8):1307–1317, 1994.

[59] E. Jarlebring, K. Meerbergen, and W. Michiels. A Krylov method for the delay eigenvalue problem. *SIAM Journal on Scientific Computing*, 32(6):3278–3300, 2010.

[60] I. M. Jin and A. E. Sepulveda. Structural/control system optimization with variable actuator masses. *AIAA Journal*, 33(9):1709–1714, 1995.

[61] H. K. Khalil. *Nonlinear Systems*. Prentice Hall, 2002.

[62] P. P. Khargonekar and M. A. Rotea. Mixed $\mathcal{H}_2/\mathcal{H}_\infty$ control: a convex optimization approach. *IEEE Transactions on Automatic Control*, 36:824–837, 1991.

[63] H. Köroğlu. $\mathcal{H}_\infty$ synthesis with unstable weighting filters: An LMI solution. In *Proceedings of the 52nd IEEE Conference on Decision and Control*, pages 2429–2434, Firenze, Italy, December 2013.

[64] H. Köroğlu and P. Falcone. New LMI conditions for static output feedback synthesis with multiple performance objectives. In *Proceedings of the 53rd IEEE Conference on Decision and Control*, pages 866–871, Los Angeles, CA, USA, December 2014.

[65] H. Kwakernaak. Robust control and $\mathcal{H}_\infty$-optimization – tutorial paper. *Automatica*, 29:255–273, 1993.

[66] J. B. Lasserre. *Moments, positive polynomials and their applications*, volume 1. World Scientific, 2009.

[67] L. H. Lee. Reduced-order solutions to $\mathcal{H}_\infty$ and LPV control problems involving partial-state feedback. In *Proceedings of the 1997 American Control Conference*, pages 1762–1765, Albuquerque, New Mexico, USA, June 1997.

[68] F. Leibfritz. COMPl$_e$ib: COnstrained Matrix-optimization Problem library - a collection of test examples for nonlinear semidefinite programs, control system design and related problems. Technical report, 2004.

[69] F. Leibfritz and W. Lipinski. Description of the benchmark examples in COMPl$_e$ib 1.0. Technical report, 2003.

[70] D. J. Leith and W. E. Leithead. Comments on the prevalence of linear parameter varying systems. Technical report, Dept. Electron. Elect. Eng., Univ. Strathclyde, Glasgow, UK, 1999.

[71] D. J. Leith and W. E. Leithead. Survey of gain-scheduling analysis and design. *International Journal of Control*, 73(11):1001–1025, 2000.

[72] J. Löfberg. Yalmip : A toolbox for modeling and optimization in MATLAB. In *Proceedings of the CACSD Conference*, pages 284–289, Taipei, Taiwan, 2004.

[73] J. Lu and R. E. Skelton. Integrating structure and control design to achieve mixed $\mathcal{H}_2/\mathcal{H}_\infty$ performance. *International Journal of Control*, 73(16):1449–1462, 2000.

[74] A. M. Lyapunov. *The general problem of the stability of motion.* PhD thesis, Kharkov Mathematical Society, 1892.

[75] A. M. Lyapunov. The general problem of the stability of motion. *International Journal of Control*, 55:531–773, 1992. (This is the English translation of the Russian original published in 1892).

[76] I. Masubuchi, A. Ohara, and N. Suda. LMI-based controller synthesis: a unified formulation and solution. *International Journal of Robust and Nonlinear Control*, 8:669–686, 1998.

[77] M. Mattei. Sufficient conditions for the synthesis of $\mathcal{H}_\infty$ fixed-order controllers. *International Journal of Robust and Nonlinear Control*, 10:1237–1248, 2000.

[78] K. Meerbergen. The quadratic Arnoldi method for the solution of the quadratic eigenvalue problem. *SIAM Journal on Matrix Analysis and Applications*, 30(4):1463–1482, 2008.

[79] W. Michiels, E. Jarlebring, and K. Meerbergen. Krylov based model order reduction of time-delay systems. *SIAM Journal on Matrix Analysis and Applications*, 32(4):1399–1421, 2011.

[80] W. Michiels and S.-I. Niculescu. *Stability and Stabilization of Time-Delay Systems: An Eigenvalue-Based Approach.* Advances in Design and Control 12, SIAM Publications, Philadelphia, 2007.

[81] W. Michiels, T. Vyhlídal, and P. Zítek. Control design for time-delay systems based on quasi-direct pole placement. *Journal of Process Control*, 20:337–343, 2010.

[82] J. Mohammadpour and C. W. Scherer, editors. *Control of Linear Parameter Varying Systems with Applications*. Springer, New York, 2012.

[83] C. F. Morais, M. F. Braga, R. C. L. F. Oliveira, and P. L. D. Peres. Robust state feedback control for discrete-time linear systems via LMIs with a scalar parameter. In *Proceedings of the 2013 American Control Conference*, pages 3870–3875, Washington, DC, USA, June 2013.

[84] MOSEK ApS. *The MOSEK optimization toolbox for MATLAB manual. Version 7.1 (Revision 32).*, 2015. http://docs.mosek.com/7.1/toolbox.pdf.

[85] R. A. Nichols, R. T. Reichert, and W. J. Rugh. Gain scheduling for $\mathcal{H}_\infty$ controllers: a flight control example. *IEEE Transactions on Control System Technology*, 1(2):69–79, 1993.

[86] R. C. L. F. Oliveira, P. Bliman, and P. L. D. Peres. Robust LMIs with parameters in multi-simplex: Existence of solutions and applications. In *Proceedings of the 47th IEEE Conference on Decision and Control*, pages 2226–2231, December 2008.

[87] R. C. L. F. Oliveira and P. L. D. Peres. Parameter-dependent LMIs in robust analysis: Characterization of homogeneous polynomially parameter-dependent solutions via LMI relaxations. *IEEE Transactions on Automatic Control*, 52:1334–1340, 2007.

[88] R. C. L. F. Oliveira and P. L. D. Peres. Time-varying discrete-time linear systems with bounded rates of variation: Stability analysis and control design. *Automatica*, 45(11):2620–2626, 2009.

[89] R. Orsi, U. Helmke, and J. B. Moore. A Newton-like method for solving rank constrained linear matrix inequalities. *Automatica*, 42(11):1875–1882, 2006.

[90] B. Paijmans, W. Symens, H. Van Brussel, and J. Swevers. Gain-scheduling control for mechatronic systems with position dependent dynamics. In *Proceedings of the International Conference on Noise and Vibration Engineering (ISMA)*, Leuven, Belgium, 2006.

[91] J. Partington. *Unsolved Problems in Mathematical Systems and Control Theory*, chapter Model reduction of delay systems, pages 29–32. Princeton University Press, 2004.

[92] D. Peaucelle and D. Arzelier. An efficient numerical solution for $\mathcal{H}_2$ static output feedback synthesis. In *Proceedings of the 2001 European Control Conference*, pages 3800–3805, Porto, Portugal, September 2001.

[93] D. Peaucelle, D. Arzelier, O. Bachelier, and J. Bernussou. A new robust D-stability condition for real convex polytopic uncertainty. *Systems & Control Letters*, 40(1):21–30, 2000.

[94] G. Pipeleers, B. Demeulenaere, J. Swevers, and L. Vandenberghe. Extended LMI characterizations for stability and performance of linear systems. *Systems & Control Letters*, 58:510–518, 2009.

[95] W. J. Rugh and J. S. Shamma. Research on gain scheduling. *Automatica*, 36:1401–1425, 2000.

[96] M. S. Sadabadi and A. Karimi. An LMI formulation of fixed-order $\mathcal{H}_\infty$ and $\mathcal{H}_2$ controller design for discrete-time systems with polytopic uncertainty. In *Proceedings of the 52nd IEEE Conference on Decision and Control*, pages 2453–2458, Firenze, Italy, December 2013.

[97] M. G. Safonov, K. C. Goh, and J. H. Ly. Control system synthesis via bilinear matrix inequalities. In *Proceedings of the 1994 American Control Conference*, pages 45–49, Baltimore, MD, USA, 1994.

[98] S. Sastry. *Nonlinear systems : analysis, stability, and control*. Interdisciplinary applied mathematics. Springer, New York, 1999.

[99] M. Sato. Gain-scheduled output-feedback controllers depending solely on scheduling parameters via parameter-dependent Lyapunov functions. *Automatica*, 47(12):2786–2790, 2011.

[100] C. W. Scherer. LPV control and full block multipliers. *Automatica*, 37(3):361–375, 2001.

[101] C. W. Scherer. Relaxations for robust linear matrix inequality problems with verifications for exactness. *SIAM Journal on Matrix Analysis and Applications*, 27(2):365–395, June 2005.

[102] C. W. Scherer. LMI relaxations in robust control. *European Journal of Control*, 12(1):3–29, 2006.

[103] C. W. Scherer, P. Gahinet, and M. Chilali. Multiobjective output-feedback control via LMI optimization. *IEEE Transactions on Automatic Control*, 42(7):896–911, 1997.

[104] C. W. Scherer and C. W. J. Hol. Matrix sum-of-squares relaxations for robust semi-definite programs. *Mathematical Programming*, 107:189–211, 2006.

[105] C. W. Scherer and S. Weiland. *Linear Matrix Inequalities in Control*. 2004. Lecture Notes for a course of the Dutch Institute of Systems and Control.

[106] L. L. Schumaker. *Spline Functions: Basic Theory*. Cambridge University Press, 2007.

[107] U. Shaked. A LPV approach to robust $\mathcal{H}_2$ and $\mathcal{H}_\infty$ static output-feedback design. In *Proceedings of the 41st IEEE Conference on Decision and Control*, pages 3476–3481, Las Vegas, Nevada, USA, December 2002.

[108] J. S. Shamma. *Control of Linear and Parameter Varying Systems with Applications*, chapter An overview of LPV systems. Springer-Verlag, 2012.

[109] R. E. Skelton, B. R. Hanks, and M. Smith. Structure redesign for improved dynamic response. *Journal of Guidance, Control, and Dynamics*, 15(5):1272–1278, 1992.

[110] R. E. Skelton, T. Iwasaki, and K. M. Grigoriadis. *A unified approach to control design*. Taylor and Francis, London, 1998.

[111] S. Skogestad and I. Postlethwaite. *Multivariable Feedback Control: Analysis and Design*. John Wiley & Sons, 2005.

[112] A. A. Stoorvogel. The robust $\mathcal{H}_2$ control problem: a worst-case design. *IEEE Transactions on Automatic Control*, 38(9):1358–1370, 1993.

[113] J. F. Sturm. Using SeDuMi 1.02, a MATLAB toolbox for optimization over symmetric cones. *Optimization Methods and Software*, 11–12:625–653, 1999.

[114] V. L. Syrmos, C. T. Abdallah, P. Dorato, and K. Grogoriadis. Static output feedback – a survey. *Automatica*, 23(2):125–137, 1997.

[115] K. C. Toh, M.J. Todd, and R. H. Tutuncu. SDPT3 – a MATLAB software package for semidefinite programming. *Optimization Methods and Software*, 11:545–581, 1999.

[116] Q. Tran Dinh, S. Gumussoy, W. Michiels, and M. Diehl. Combining convex-concave decompositions and linearization approaches for solving BMIs, with application to static output feedback. *IEEE Transactions on Automatic Control*, 57(6):1377–1390, 2011.

[117] L. N. Trefethen. *Spectral Methods in MATLAB*. SIAM Publications, Philadelphia, 2000.

[118] A. Trofino. Sufficient LMI conditions for the design of static and reduced order controllers. In *Proceedings of the 48th IEEE Conference on Decision and Control*, pages 6668–6673, Shanghai, China, December 2009.

[119] M. C. Tsai, E. J. M. Geddes, and I. Postlethwaite. Pole-zero cancellations and closed-loop properties of an $\mathcal{H}_\infty$ mixed sensitivity design problem. *Automatica*, 28(3):519–530, 1992.

[120] T. Vyhlídal, P. Zítek, and K. Paulů. *Topics in Time Delay Systems, Analysis, Algorithms and Control*, chapter Design, Modelling and Control of the Experimental Heat Transfer Set-Up, pages 303–313. Berlin: Springer, 2009.

[121] M. Groot Wassink, M. van de Wal, C. W. Scherer, and O. Bosgra. LPV control for a wafer stage: Beyond the theoretical solution. *Control Engineering Practice*, 13:231–245, February 2005.

[122] F. Wijnheijmer, G. Naus, W. Post, M. Steinbuch, and P. Teerhuis. Modelling and LPV control of an electro-hydraulic servo system. In *Proceedings of the 2006 IEEE International Conference on Control Applications*, pages 3116–3121, Munich, Germany, October 2006.

[123] J. C. Willems. Dissipative dynamical systems. *European Journal of Control*, 13:134–151, 2007.

[124] J. C. Willems and J. W. Polderman. *Introduction to mathematical systems theory: a behavioral approach*, volume 26. Springer Science & Business Media, 2013.

[125] Y.-P. Yang and Y.-A. Chen. Multiobjective optimization of hard disk suspension assemblies. II: Integrated structure and control design. *Computers & Structures*, 59(4):771–782, 1996.

[126] K. Zavari, G. Pipeleers, and J. Swevers. Multi-$\mathcal{H}_\infty$ controller design and illustration on an overhead crane. In *IEEE Multi-Conference on Systems and Control*, pages 670–674, Dubrovnik, Croatia, October 2012.

[127] K. Zavari, G. Pipeleers, and J. Swevers. Gain-scheduled controller design: illustration on an overhead crane. *IEEE Transactions on Industrial Electronics*, 61:3713–3718, 2014.

Curriculum Vitae

Personal information

Gijs Hilhorst, male
27 December 1986, Naarden, The Netherlands
gijs_hilhorst@hotmail.com

Education

2011-2015   PhD researcher at the Department of Mechanical Engineering, KU Leuven, Heverlee, Belgium. Funded by the Research Foundation-Flanders (FWO-Vlaanderen), research project G0.0712.11: "Fixed-order controller design for linear infinite-dimensional and parameter-varying systems, optimizing stability and $\mathcal{H}_2/\mathcal{H}_\infty$ criteria". Supervisors: prof. Goele Pipeleers, prof. Jan Swevers and prof. Wim Michiels.

2013 June-October   Research visit to prof. Pedro L. D. Peres and prof. Ricardo C. L. F. Oliveira at the School of Electrical and Computer Engineering, University of Campinas - UNICAMP, Campinas, São Paulo, Brazil.

2008-2011   Master degree in Applied Mathematics, Systems and Control track, University of Twente, Enschede, The Netherlands. Master thesis title: "Stabilisation of linear time-invariant systems subject to output saturation". Supervisor: prof. Anton A. Stoorvogel.

2010 April-August Traineeship at the Centre for Complex Dynamic Systems and Control, University of Newcastle, Newcastle, New South Wales, Australia. Research topic: "Control of marine vessels using the port-Hamiltonian framework". Supervisors: prof. Tristan Perez and dr. Alejandro Donaire.

2005-2008 Bachelor degree in Applied Mathematics, University of Twente, Enschede, The Netherlands. Bachelor thesis title: "Meten van waterstanden in de Westerschelde". Supervisor: prof. Anton A. Stoorvogel. Minor in Psychology.

1999-2005 Secondary school (VWO, natuur & techniek), partly bilingual education: Laar & Berg, Laren (Noord-Holland), The Netherlands.

Skills

Languages Dutch (native proficiency), English (full professional proficiency), French (limited working proficiency), Portuguese (limited working proficiency), German (limited working proficiency), Indonesian (elementary proficiency).

Mobility Driving license.

List of publications

Articles in internationally reviewed academic journals

[1] G. Hilhorst, G. Pipeleers, W. Michiels, R. C. L. F. Oliveira, P. L. D. Peres, and J. Swevers. Fixed-order linear parameter-varying feedback control of a lab-scale overhead crane. *IEEE Transactions on Control Systems Technology*, (under revision).

[2] G. Hilhorst, G. Pipeleers, W. Michiels, and J. Swevers. Sufficient LMI conditions for reduced-order multi-objective $\mathcal{H}_2/\mathcal{H}_\infty$ control of LTI systems. *European Journal of Control*, 23:17–25, May 2015.

[3] W. Michiels, G. Hilhorst, T. Vihlídal, G. Pipeleers, and J. Swevers. Reduced modeling and control of delay systems, with application to a heat exchanger. *Journal of Process Control*, (in preparation for submission).

Article in internationally recognized academic book

[1] W. Michiels, G. Hilhorst, G. Pipeleers, and J. Swevers. *Recent results on time-delay systems: analysis and control*, chapter Model order reduction for time-delay systems, with application to fixed-order $\mathcal{H}_2$ optimal controller design. Advances in Delays and Dynamics. Springer, (to appear).

Papers in international conference proceedings

[1] G. Hilhorst, G. Pipeleers, W. Michiels, R. C. L. F. Oliveira, P. L. D. Peres, and J. Swevers. Reduced-order $\mathcal{H}_2/\mathcal{H}_\infty$ control of discrete-time LPV systems with experimental validation on an overhead crane test setup. In *Proceedings*

of the 2015 American Control Conference, pages 125–130, Chicago, IL, USA, July 2015.

[2] G. Hilhorst, G. Pipeleers, W. Michiels, R. C. L. F. Oliveira, P. L. D. Peres, and J. Swevers. An iterative convex approach for fixed-order robust $\mathcal{H}_2/\mathcal{H}_\infty$ control of discrete-time linear systems with parametric uncertainty. In 54th *Conference on Decision and Control*, Osaka, Japan, December 2015 (accepted).

[3] G. Hilhorst, G. Pipeleers, R. C. L. F. Oliveira, P. L. D. Peres, and J. Swevers. On extended LMI conditions for $\mathcal{H}_2/\mathcal{H}_\infty$ control of discrete-time linear systems. In *Proceedings of the* 19th *IFAC world congress*, pages 9307–9312, Cape Town, South Africa, August 2014.

[4] G. Hilhorst, G. Pipeleers, and J. Swevers. An LMI approach for reduced-order $\mathcal{H}_2$ LTI controller synthesis. In *Proceedings of the 2013 American Control Conference*, pages 2392–2396, Washington, DC, USA, June 2013.

[5] G. Hilhorst, G. Pipeleers, and J. Swevers. Reduced-order multi-objective $\mathcal{H}_\infty$ control of an overhead crane test setup. In *Proceedings of the* 52nd *Conference on Decision and Control*, pages 770–775, Firenze, Italy, December 2013.

Abstracts in international conference proceedings

[1] G. Hilhorst, G. Pipeleers, and J. Swevers. Optimal design of reduced-order LPV controllers. In *Book of Abstracts of the* 31st *Benelux Meeting on Systems and Control*, page 129, Heijen/Nijmegen, The Netherlands, 27-29 March 2012.

[2] G. Hilhorst, G. Pipeleers, and J. Swevers. Multiobjective $\mathcal{H}_2/\mathcal{H}_\infty$ controller design for LTI systems. In *Book of Abstracts of the* 32nd *Benelux Meeting on Systems and Control*, page 41, Houffalize, Belgium, 26-28 March 2013.

[3] G. Hilhorst, G. Pipeleers, and J. Swevers. Control design for discrete-time linear systems using extended LMIs with scalar parameters. In *Book of Abstracts of the* 34nd *Benelux Meeting on Systems and Control*, page 57, Heijen/Nijmegen, The Netherlands, 25-27 March 2014.

FACULTY OF ENGINEERING SCIENCE
DEPARTMENT OF MECHANICAL ENGINEERING
MOTION ESTIMATION, CONTROL AND OPTIMIZATION (MECO) RESEARCH GROUP
Celestijnenlaan 300B, B-3001 Heverlee, België
https://www.mech.kuleuven.be/en/pma/research/meco